REPORT DOCUMENTATION PAGE

Form Approved OMB NO. 0704-0188

1. REPORT DATE (DD-MM-YYYY)	2. REPORT TYPE	3. DATES COVERED (From - To)
31-05-2010	Final Report	1-Aug-2006 - 31-Jan-2010

4. TITLE AND SUBTITLE

Injection Laser Using Rare Earth Doped GaN Thin Films for Visible and Infrared Applications

5a. CONTRACT NUMBER
W911NF-06-1-0296

5b. GRANT NUMBER

5c. PROGRAM ELEMENT NUMBER
611102

6. AUTHORS

Andrew Steckl

5d. PROJECT NUMBER

5e. TASK NUMBER

5f. WORK UNIT NUMBER

7. PERFORMING ORGANIZATION NAMES AND ADDRESSES

University of Cincinnati
Office of Sponsored Programs
Suite 7148, Edwards One
Cincinnati, OH 45221 -0627

8. PERFORMING ORGANIZATION REPORT NUMBER

9. SPONSORING/MONITORING AGENCY NAME(S) AND ADDRESS(ES)

U.S. Army Research Office
P.O. Box 12211
Research Triangle Park, NC 27709-2211

10. SPONSOR/MONITOR'S ACRONYM(S)
ARO

11. SPONSOR/MONITOR'S REPORT NUMBER(S)
49718-EL.1

12. DISTRIBUTION AVAILIBILITY STATEMENT

Approved for Public Release; Distribution Unlimited

13. SUPPLEMENTARY NOTES

The views, opinions and/or findings contained in this report are those of the author(s) and should not contrued as an official Department of the Army position, policy or decision, unless so designated by other documentation.

14. ABSTRACT

This is a proposal to develop an injection laser on Si using rare-earth doped GaN heteroepitaxially grown on Si substrates. The success of this approach will result in the availability of a laser light sources directly built on Si and operating at wavelengths throughout the visible and near-IR range. We have demonstrated the first ever visible lasing on Si using GaN:Eu grown on Si (with unique AlGaN transition layers) by optical pumping. The preliminary results are very encouraging: stimulated emission threshold of only ~110kW/cm2, optical gain of ~ 100/cm and loss

15. SUBJECT TERMS

GaN, rare earths, molecular beam epitaxy, photoluminescence

16. SECURITY CLASSIFICATION OF:			17. LIMITATION OF ABSTRACT	15. NUMBER OF PAGES	19a. NAME OF RESPONSIBLE PERSON
a. REPORT	b. ABSTRACT	c. THIS PAGE			Andrew Steckl
UU	UU	UU	UU		19b. TELEPHONE NUMBER: 513-556-4777

Report Title

Injection Laser Using Rare Earth Doped GaN Thin Films for Visible and Infrared Applications

ABSTRACT

This is a proposal to develop an injection laser on Si using rare-earth doped GaN heteroepitaxially grown on Si substrates. The success of this approach will result in the availability of a laser light sources directly built on Si and operating at wavelengths throughout the visible and near-IR range. We have demonstrated the first ever visible lasing on Si using GaN:Eu grown on Si (with unique AlGaN transition layers) by optical pumping. The preliminary results are very encouraging: stimulated emission threshold of only ~110kW/cm2, optical gain of ~ 100/cm and loss of ~ 45/cm. The proposed program will develop an injection laser based on AlGaN-GaN:RE-AlGaN double heterojunction structures built on Si substrates.

List of papers submitted or published that acknowledge ARO support during this reporting period. List the papers, including journal references, in the following categories:

(a) Papers published in peer-reviewed journals (N/A for none)

1. J. Hite, G. T. Thaler, R. Khanna, C .R. Abernathy, S. J. Pearton, J. H. Park, A. J. Steckl, and J. M. Zavada, "Optical and Magnetic Properties of Eu-Doped GaN", Appl. Phys. Lett. 89, pp. 132119, Oct. 2006.
2. A. J. Steckl, J. H. Park, and J. M. Zavada, Invited Paper, "Prospects for Rare Earth Doped GaN Lasers on Si", Materials Today, 10, pp. 20-27, July 2007.
3. H. Y. Peng, C-W. Lee, H. O. Everitt, C. Munasinghe, D. S. Lee and A. J. Steckl, "Spectroscopic and energy transfer studies of Eu3+ centers in GaN", Journal of Applied Physics, Vol. 102, pp. 073520-1 to -9, Oct. 2007.
4. N. Nepal, S. M. Bedair, N. A. El-Masry, D. S. Lee, A. J. Steckl, J. M. Zavada, "Correlation between compositional fluctuation and magnetic properties of Tm-doped AlGaN alloys" Appl. Phys. Lett., 91, pp. 22503/1-3, Nov. 2007.
5. J. H. Park and A. J. Steckl, "Effect of process conditions on gain and loss in GaN:Eu cavities on different substrates", Physica Status Solidi A 205, pp. 26-29, Jan. 2008.
6. V. Mahalingam, V. Sudarsan, P. Munusamy, F. C. J. M. van Veggel, R. Wang, A. J. Steckl, "Mg2+-doped GaN nanoparticles as blue emitters; a method to avoid sintering at high temperatures", Small 4, pp. 105-110, Jan. 2008.
7. N. Nepal, J. M. Zavada, D. S. Lee and A. J. Steckl, "Dynamics of ultraviolet emissions in Tm-doped AlN using above band gap excitation" Appl. Phys. Lett. 93, 061110, Aug. 2008.
8. R. Wang, A. J. Steckl, E. E. Brown, U. Hommerich, and J. M. Zavada, "Effect of Si co-doping on Eu3+ luminescence in GaN", J. Appl. Phys. 105, 04310715, Feb. 2009.
9. N. Nepal, J. M. Zavada, D. S. Lee and A. J. Steckl, A. Sedhain, J. Y. Lin, and H. X. Jiang "Deep ultraviolet photoluminescence excitation of Tm-doped AlGaN alloys", Appl. Phys. Lett. 94, 111103, 16 Mar. 2009.
10. V. Mahalingam, E. Bovero, P. Munusamy, A. G. Brolo, F. C. J. M. van Veggel, R. Wang, and A. J. Steckl, "Optical and Structural Characterization of the blue-emitting Mg2+- and Zn2+-doped GaN Nanoparticles", RSC J. Mat. Chem. 19, 3889-3894, April 2009.
11. Y. D. Glinka, H. O. Everitt, D. S. Lee and A. J. Steckl "Direct and Indirect Photoluminescence Excitation and UV emission from Tm-doped AlxGa1-xN", J. Appl. Phys. 105, 083509, 15 Apr. 2009.
12. Z. Fleischman, C. Munasinghe, A. Steckl, A. Wakahara, J. Zavada, V. Dierolf, "Site-Selective Spectroscopy and Excitation Pathways of Eu ions in GaN", Appl. Phys. B, 97, 607-618, Nov. 2009.
13. R. Wang, A. J. Steckl, N. Nepal, J. M. Zavada, "GaN:Eu+Si Magnetic and Electronic Properties", J. Appl. Phys. 107, 013901, 05 Jan 2010.
14. R. Wang and A. J. Steckl, "Effect of Growth Conditions on Eu3+ Luminescence in GaN", J Crystal Growth, 312 (5), 680-684, 15 Feb 2010.

Number of Papers published in peer-reviewed journals: 14.00

(b) Papers published in non-peer-reviewed journals or in conference proceedings (N/A for none)

Number of Papers published in non peer-reviewed journals: 0.00

(c) Presentations

1. L. Bodiou, A. Braud, J-L. Doualan, R. Moncorgé, K. Lorenz, E. Alves, J. H. Park, and A. J. Steckl, "Optical properties of Eu, Er implanted and Eu in-situ doped GaN", 6th International Conference on f-elements, Sept. 2006, Wroclaw, Poland.
2. A. J. Steckl, Invited Presentation, "Visible Lasing on Si Using Rare Earth Doped GaN", LEOS Group IV Photonics, Ottawa Canada, Sept. 2006.
3. A. J. Steckl, Invited Presentation, "The Quest for Rare Earth Lasing in Gallium Nitride – Current Status and Future Prospects", Int'l. Workshop on Impurity-based Electroluminscent Devices and Materials, Wakashima Japan, Oct. 2006.
4. A. J. Steckl and J. H. Park, "Stimulated Emission at Visible Wavelengths from Europium Doped GaN", International Wide Bandgap Nitrides Conference, Kyoto Japan, Oct. 2006.
5. R. Wang and A. J. Steckl, "Effect of Si and Er co-doping on Electrical Properties and Electroluminescence from GaN:Er LEDs on Si substrate", MRS Spring Meeting, San Francisco, March 2008.
6. N. Nepal, J. M. Zavada, E. Brown, U. Hommerich, D. S. Lee and A. J. Steckl, "Ultraviolet Luminescence from Thullium-doped Aluminum Gallium Nitride Epilayers ", Mat. Res. Soc. Conference, Boston, Dec. 2008.
7. N. Nepal, J. M. Zavada, R. Wang and A. J. Steckl, "Enhanced Ferromagnetism in Eu-Si co-doped GaN Thin Films", Mat. Res. Soc. Conference, San Francisco, Apr. 2009.

Number of Presentations: 7.00

Non Peer-Reviewed Conference Proceeding publications (other than abstracts):

Number of Non Peer-Reviewed Conference Proceeding publications (other than abstracts): 0

Peer-Reviewed Conference Proceeding publications (other than abstracts):

R. Wang and A. J. Steckl, "Effect of Si and Er co-doping on Green Electroluminescence from GaN:Er LEDs on Si Substrate", Proc. Mat. Res. Soc. 1068, C05-03, May 2008.

Number of Peer-Reviewed Conference Proceeding publications (other than abstracts): 1

(d) Manuscripts

Number of Manuscripts: 0.00

Patents Submitted

Patents Awarded

Graduate Students

NAME	PERCENT_SUPPORTED
Rui Wang	0.50
Mingyu Zhong	0.50
FTE Equivalent:	**1.00**
Total Number:	**2**

Names of Post Doctorates

NAME	PERCENT_SUPPORTED
FTE Equivalent:	
Total Number:	

Names of Faculty Supported

NAME	PERCENT_SUPPORTED	National Academy Member
Andrew Steckl	0.06	No
FTE Equivalent:	**0.06**	
Total Number:	**1**	

Names of Under Graduate students supported

NAME	PERCENT_SUPPORTED
FTE Equivalent:	
Total Number:	

Student Metrics

This section only applies to graduating undergraduates supported by this agreement in this reporting period

The number of undergraduates funded by this agreement who graduated during this period:	0.00
The number of undergraduates funded by this agreement who graduated during this period with a degree in science, mathematics, engineering, or technology fields:	0.00
The number of undergraduates funded by your agreement who graduated during this period and will continue to pursue a graduate or Ph.D. degree in science, mathematics, engineering, or technology fields:	0.00
Number of graduating undergraduates who achieved a 3.5 GPA to 4.0 (4.0 max scale):	0.00
Number of graduating undergraduates funded by a DoD funded Center of Excellence grant for Education, Research and Engineering:	0.00
The number of undergraduates funded by your agreement who graduated during this period and intend to work for the Department of Defense	0.00
The number of undergraduates funded by your agreement who graduated during this period and will receive scholarships or fellowships for further studies in science, mathematics, engineering or technology fields:	0.00

Names of Personnel receiving masters degrees

NAME
Total Number:

Names of personnel receiving PHDs

NAME
Rui Wang
Total Number: 1

Names of other research staff

NAME	PERCENT_SUPPORTED
FTE Equivalent:	
Total Number:	

Sub Contractors (DD882)

Inventions (DD882)

Final Report – US Army Research Office

Injection Laser Using Rare Earth Doped GaN Thin Films for Visible and Infrared Applications

Andrew J. Steckl (PI), Rui (Ray) Wang and Mingyu (Jimmy) Zhong

May 2010

Summary

Rare Earth (RE) doped III-nitrides are being investigated for potential applications in optical communication and displays, due to the wide and direct energy bandgap of GaN resulting in low thermal quenching of RE^{3+} ion sharp emission from ultraviolet (UV) through visible to infrared (IR) region. The UC Nanolab has been at the forefront of RE doped GaN research and has achieved many advances in areas ranging from material growth to device fabrication.

This project studied RE^{3+} emission in GaN material, focusing on the effects of electronic impurity (Si) co-doping on RE^{3+} luminescence. Advanced RE doped GaN electroluminescent devices (ELDs) were also designed and fabricated. Detailed device characterization was carried out and the effect of co-dopant was investigated.

Eu-doped GaN thin films were grown on sapphire wafers by molecular beam epitaxy (MBE) technique and the growth conditions were optimized for the strongest Eu^{3+} luminescence. It was found that GaN thin film quality and Eu doping concentration mutually affected Eu^{3+} luminescence. High quality GaN:Eu thin films were grown under Ga rich condition (III/V>1), but the strongest Eu^{3+} luminescence was obtained under

slightly N rich condition (III/V<1). The optimum Eu doping concentration is ~0.1-1.0at.%, depending on the GaN:Eu thin film quality. Higher growth temperature (>750ºC) was also found to enhance Eu^{3+} luminescence (~10×) and efficiency (~30×).

The effect of Si co-doping in GaN:RE thin films was investigated. Eu^{3+} photoluminescence (PL) was enhanced ~5-10× by moderate Si co-doping (~0.05at. %) mostly due to the increase of Eu^{3+} PL lifetime, but decreased very fast at high Si co-doping concentration (>0.08at.%). The increase of Eu^{3+} PL lifetime is possibly due to the incorporation of Si uniformly distributing Eu^{3+} ions and shielding Eu-Eu interactions. Combined with the increase in excitation cross section and carrier flux, there is a significant enhancement on Eu^{3+} PL intensity. The electrical properties of GaN:RE thin films were changed from high resistive to weakly n-type due to increased electron concentration introduced by Si co-doping.

GaN:RE ELDs were fabricated and the electrical and optical properties were studied by I-V and electroluminescence (EL) measurements. A hetero-junction PIN structure was designed on n-GaN:Si/GaN:RE/p-Si, employing p-Si substrates as p-type conductive layer. RE^{3+} ions EL emission was found to be much stronger under forward bias than under reverse bias. The Si co-doping was also studied in GaN:RE ELDs. It was found that Er^{3+} EL had strong visible & IR emission under forward bias, while there is little or no emission under reverse bias. A p-n^- hetero-junction structure formed between p-Si and n^--GaN:(Si, Er) layers was proposed to be responsible for the emission control. GaN:(Si, Eu) AC thin film ELDs were also fabricated and it was demonstrated that the Si co-doping increased the Eu^{3+} ions emission intensity and efficiency.

List of Tables and Figures

1. Introduction

1.1. Properties of III-Nitride Semiconductors

III-nitride semiconductors are very attractive to optoelectronics and photonics research area because they have wide and direct energy bandgap, which is clearly shown in Fig 1.1 (bandgap energy and lattice constant of semiconductors). For example, the bandgap energy of GaN is 3.4eV, which is much higher than Si (1.14eV) and GaAs (1.42ev). The properties of III-nitride semiconductors are given in Table 1.1[1]. Si and GaAs are also listed for comparison.

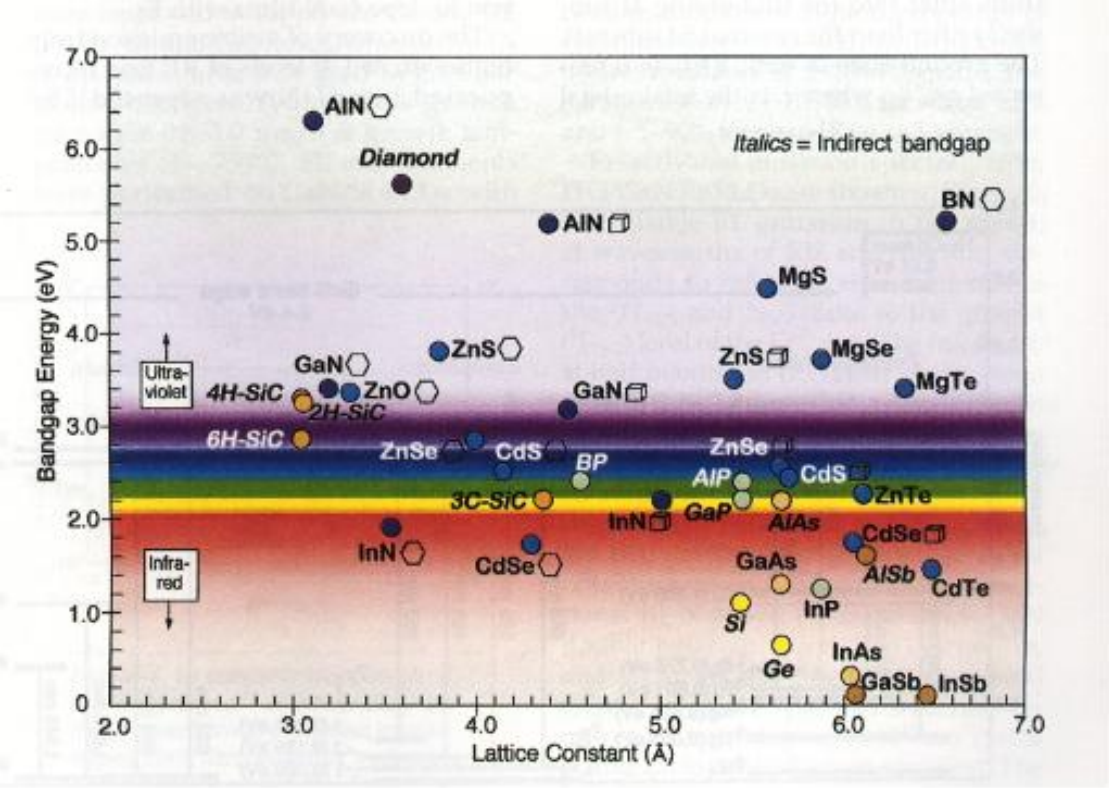

Fig 1.1 Bandgap energy and lattice constant of common semiconductors.

Table 1.1 Properties of Si, GaAs and III-nitride semiconductors.[1]

Basic Parameters		Si	GaAs	GaN		AlN	InN
Crystal structure		Diamond	Zinc Blende	Wurtzite	Zinc Blende	Wurtzite	Wurtzite
Lattice constant (Å)	a	5.431	5.65325	3.189	4.52	3.11	3.5446
	c	-	-	5.186	-	4.98	5.7034
Group of symmetry		O^7_h-Fd3m	T^2_d-F43m	C^4_{6v}-$P6_3mc$	T^2_d-F43m	C^4_{6v}-$P6_3mc$	C^4_{6v}-$P6_3mc$
Atomic Desity (cm^{-3})		5×10^{22}	4.4×10^{22}	8.9×10^{22}		9.6×10^{22}	6.4×10^{22}
Energy Bandgap (eV)		1.12(I*)	1.42(D*)	3.39(D)	3.2(D)	6.2(D)	0.7(D)
Refractive Index		3.42	3.3	2.29	2.3	2.0	2.9
Optical phonon energy (meV)		63	35	91.2	87.3	99.2	73
Intrinsic Carrier Concentration (cm^{-3})		1×10^{10}	2.1×10^{6}	-	-	-	-
Dielectric constant		11.7	12.9	8.9	9.7	9.14	15.3
Intrinsic resistivity (Ω·cm)		3.2×10^{5}	3.3×10^{8}	-	-	-	-
Effective conduction band density of states (cm^{-3})		3.2×10^{19}	4.7×10^{17}	2.3×10^{18}	1.2×10^{18}	6.3×10^{18}	9×10^{17}
Effective valence band density of states (cm^{-3})		1.8×10^{19}	9.0×10^{-18}	4.6×10^{19}	4.1×10^{19}	4.8×10^{20}	5.3×10^{19}
Electron affinity (eV)		4.05	4.07	4.1	4.1	0.6	-
Breakdown field (V/cm)		3×10^{5}	4×10^{5}	5×10^{6}		1.8×10^{6}	-
Mobility electrons ($cm^2\ V^{-1}s^{-1}$)		≤1400	≤8500	≤1000		300	≤3200
Mobility holes ($cm^2\ V^{-1}s^{-1}$)		≤450	≤400	≤200	≤ 350	14	<80
Electron thermal velocity (m/s)		2.3×10^{5}	4.4×10^{5}	-	-	1.85×10^{5}	3.4×10^{5}
Hole thermal velocity (m/s)		1.65×10^{5}	1.8×10^{5}	-	-	0.41×10^{5}	9.0×10^{4}
Melting point (°C)		1412	1240	2500		3000	1100
Thermal conductivity ($W\ cm^{-1}\ °C^{-1}$)		1.3	0.55	1.3		1.47	0.45
Thermal diffusivity (cm^2s^{-1})		0.8	0.31	0.43		2.85	0.2
Density (g/cm^{-3})		2.329	5.317	6.15		3.255	6.81

* I=Indirect, D=Direct

As shown in the table, the bandgap energy of III-nitride semiconductors is 6.2eV for AlN, 3.4eV for GaN and 0.7eV for InN. Combined with their ternary and quaternary alloys such AlGaN, InGaN and AlGaInN, III-nitride semiconductors can provide bandgap emissions from ultraviolet to infrared wavelength (200nm to 1770nm), which is very promising for application of short wavelength (high frequency) light emitting devices and Lasers and photovoltaic devices (solar cell).

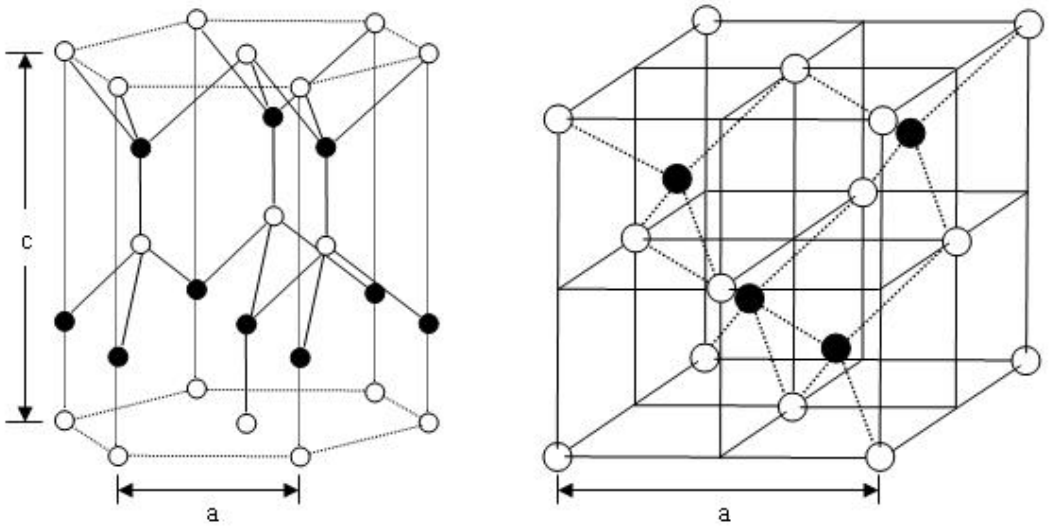

(a) (b)

Fig 1.2 Unit cell of (a) wurtzite and (b) zinc blende structure.

The stable crystal structure of III-nitrides is wurtzite structure, shown in Fig 1.2a. The unit cell is hexagon, which has two lattice constants, ***a*** and ***c***. The symmetry group of wurtzite structures is C^4_{6v}-$P6_3mc$. A wurtzite crystal is composed of two independent hexagonal closed packed sublattices, displaced by 5/8 on the c(0001) axis. Another crystal structure is zinc blende (cubic) structure, also shown in Fig 1.2b. Zinc blende structure has

a cubic unit cell with one lattice constant ***a***, while the atoms inside the cell are located in the same positions of diamond crystal structure. The space group of zincblende structure is T^2_d-*F43m*. The unit cell of wurtzite and zinc blende crystal structure seems very different. However, the environment of all atoms in the structure is pretty similar. Each atom can be viewed as the center of a tetrahedron, while four nearest neighbor atoms sitting at the corners.

The chemical bonding of III-nitride semiconductors is covalent with partially ionic. This strong chemical bonding provides very good thermal and mechanical properties, which are suitable for high temperature device application and also helpful for high temperature thin film deposition process. Moreover, high breakdown voltage provides III-nitride semiconductors useful for high power electronics application.

1.2. Development of III-Nitride Semiconductor Research

III-Nitride semiconductors have been studied for more than one hundred year. AlN was first synthesized in 1907[2] and GaN was firstly synthesized in 1937[3, 4]. In 1959 small GaN crystals was synthesized by hot gallium metals in ammonia gas ambient condition.[5] GaN thin film was firstly grown[6] on sapphire substrates with vapor deposition method by Maruska and Tietjen in 1969. Such GaN thin films had bandgap energy of 3.39eV and electron concentration above $10^{19}cm^{-3}$.

In 1971, Manasevit[7] utilized metal-organic chemical vapor deposition (MOCVD) to grow GaN and AlN thin films on sapphire and silicon carbide (SiC) substrates. The methyl derivatives of the elements, namely trimethylgallium (TMGa) and trimethylaluminum (TMAl), were mixed with ammonia (NH_3) and hydrogen (H_2) gas and decomposed on the

substrate with very high temperature. But GaN thin films were not of good quality and exhibited high unintentional n-type conductivity.

In 1983 Yoshida[8] used AlN-coated sapphire substrates (an AlN intermediate layer grown on sapphire at high temperature) to grow GaN thin films with improved electrical and optical properties. Good quality of GaN thin films were obtained in 1986 by Amano and Akasaki[9] with the optimized "two-step growth" method in metal-organic vapor phase epitaxy (MOVPE) technique. A thin AlN buffer layer was firstly grown on nitridated sapphire wafers at low temperature, followed by GaN layer growth at a much higher temperature. The AlN buffer layer provides high density nucleation center and promotes the lateral growth of main layer, resulting in great enhancement on the quality of GaN thin films. In 1991 Nakamura[10] used a low temperature GaN buffer layer and a "two-flow" method to grow a better quality of GaN layer with electron concentration of 8×10^{15} cm^{-3} and mobility of 1500 $cm^2/V\bullet s$. In this "two-flow" method, a top N_2 and H_2 mixture subflow will help reactant gas of main flow to reach the surface and promote 2D growth but suppress 3D growth. The effect of AlN and GaN buffer layer growth condition including the growth temperature and thickness was studied[10-14] by several groups. The MOCVD/VPE technique has been widely used for III-nitride growth today.

Molecular beam epitaxy (MBE) technique had been difficult for the growth of III-nitride semiconductors because the commonly used nitrogen source — NH_3 is stable at low growth temperature. The gas-phase reactions do not occur in MBE, so that the growth rate is very small. The efficiency of ammonia incorporation in GaN MBE growth was studied[15] to reveal two regimes: NH_3 flux region and Ga flux region. Reactive species of N_2 obtained by electron cyclotron resonance (ECR)[16] or radio frequency (RF) plasma[17]

appeared as a good substitute for NH_3 gas. The group III elements are introduced by heating high purity elements in Knudsen or effusion cells. The growth temperature, group III flux and group V source are so adjusted that the incorporation of both elements is in a 1:1 ratio. “Two-step method” with low temperature buffer layer was also used[16] in MBE technique to grow high quality GaN thin film.

Generally, undoped GaN is unintentionally n-type conductive with electron concentration higher than $10^{17}cm^{-3}$. It was believed that the nitrogen vacancy (N_v) acts as a donor and accounts for such n-type conductivity.[18] N-type GaN was easily obtained by Si doping.[19, 20] However, it took long time to get p-type GaN thin films until Amano[21] used low-energy electron beam irradiation (LEEBI) treatment on Mg doped GaN layers. It was found[22] that Mg:H complexes were formed in as-deposited GaN:Mg layer and hydrogen passivates Mg acceptors. The electron beam irradiation treatment can dissociate Mg:H complexes and remove hydrogen. In 1992 Nakamura[23] found that thermal annealing above 700ºC could also activate Mg acceptor in GaN thin films. However, the hole mobility and concentration could be[24] up to $30cm^2/V\cdot s$ and $3\times10^{18}cm^{-3}$ because of high Mg ionization energy and self compensation effect[25].

First GaN p-n junction light emitting diodes (LEDs)[21] were fabricated with LEEBI treated p-type GaN:Mg layer. Later, blue/ultraviolet LEDs were realized based on hetero-structure technology such as InGaN/GaN[26] and InGaN/AlGaN[27]. These achievements brought blue III-Nitride LEDs commercially available. Stimulated emissions was demonstrated[28] from GaN thin films and blue/ultraviolet laser diodes were also realized[29-31]. Meantime, III-nitride based electronic devices were also widely researched. The first metal semiconductor field effect transistor (MESFET)[32] based on

GaN and high electron mobility transistor (HEMT)[33] based on GaN/AlGaN heterojunction were demonstrated by Khan in 1993. In 2006, GaN/InGaN bipolar light emitting transistors[34] (LET) was firstly reported by Chu-Kung.

1.3. Rare Earth Elements: Mysterious Lighting Sources

Rare earth (RE) elements, also called Lanthanides, include fifteen elements from Lanthanum to Lutetium. The electron configurations of Lanthanide elements and ions are shown in the following:

La	Ce	Pr	Nd	Pm	Sm	Eu	Gd	Tb	Dy	Ho	Er	Tm	Yb	Lu
57	58	59	60	61	62	63	64	65	66	67	68	69	70	71

$$RE: 1s^2 2s^2 2p^6 3s^2 3p^6 3d^{10} 4s^2 4p^6 4d^{10} 4f^m 5s^2 5p^6 (5d^1) 6s^2$$

$$RE^{3+}: 1s^2 2s^2 2p^6 3s^2 3p^6 3d^{10} 4s^2 4p^6 4d^{10} \boxed{4f^n} 5s^2 5p^6$$

RE elements typically have a partly filled $4f^m$ orbital (La, Gd and Lu also has partly filled $5s^1$ orbital), which is surrounded by completely filled $5s^2$, $5p^6$ and $6s^2$ orbital. Generally when RE atoms were ionized, they became trivalent RE^{3+} ions by the lost of two electrons in $6s^2$ orbital and one electron in $4f^n$ or $5s^1$ orbital. Because of the special electron configuration (partly filled $4f^n$ ($0 \le n \le 14$) orbital shielded by fully filled $5s^2$ and $5p^6$ orbital), RE^{3+} ions have sharp optical absorption and emission spectra, which are widely used in optoelectronics and photonics. The emissions are from radiative transitions between the inner $4f$ electrons. The fully filled $5s^2$ and $5p^6$ orbitals provide the shielding on $4f^{n-1}$ electrons transitions and prevent the influence from the effect of host materials so that the absorption and emission lines are independent of the host materials.

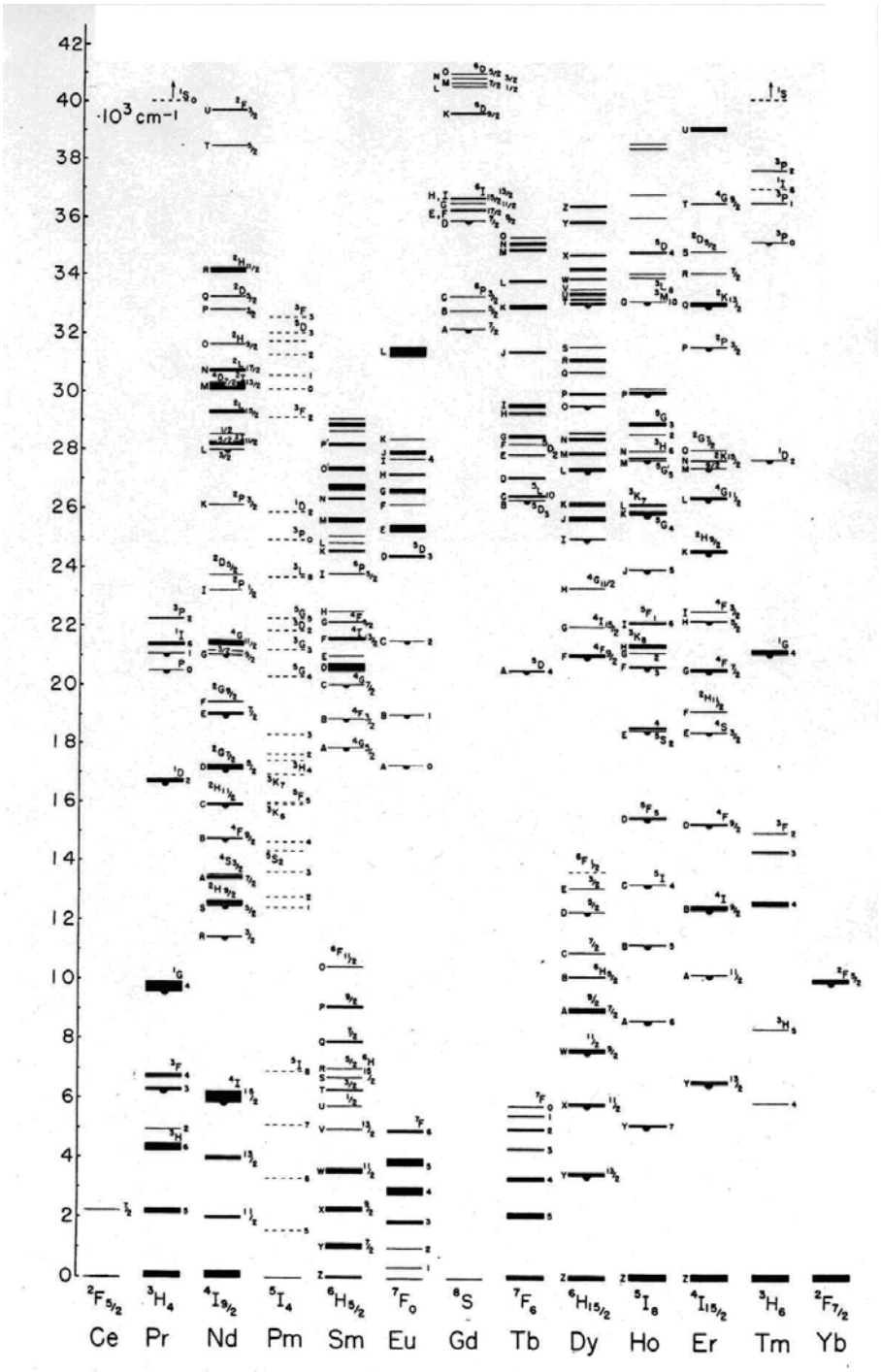

Fig 1.3 Dieke diagram: energy levels of the 4f configurations of RE^{3+} ions.[35]

Based on explanation of RE ions optical spectra from Judd[36] and Ofelt[37], 4*f*-4*f* electrons transitions are forbidden in free ions and could only occur when RE ions were in the noncenntrosymmetric field, that is in a site without inversion symmetry. Such odd-parity crystal field could allow the mixture of states from opposite-parity configuration like 5*d* into the 4*f* electrons wavefunctions so that forced electrical dipole transitions became allowed. Radiative transitions of electrical dipole in 4*f* shell yield sharp emission spectra of RE ions. The full energy levels of the 4*f* configurations of the trivalent RE ions can be found in "Dieke Diagram"[35], shown in Fig 1.3. The width of the bars shows the order of magnitude of the crystal filed splitting.

There are two major types of emission mechanisms for RE ions in semiconductor hosts, shown in Fig 1.4a[38]. One is called impact excitation. Hot carriers such as high energy electrons were injected into the hosts in cathodoluminescence and electroluminescence, directly collided with RE^{3+} ions and transferred the energy to 4*f* shells of RE^{3+} ions. Radiative transitions occurred and photons were emitted out. Impurity states around RE^{3+} ions deep level centers could also be involved to provide energy transferring channels. The other one is called electron-hole recombination. The electron-hole pairs were generated by the absorption of incident photons in photoluminescence or injected electrons and holes in electroluminescence. With the recombination of electron-hole pairs, the energy was transferred to RE ions so that radiative relaxation occurred in 4*f* electron levels. Not all energy transitions from the excited state to the ground state can result in photo emissions. There are several energy nonradiative relaxation processes such as multiphonon emission or Auger de-excitation, also shown in Fig 1.4a. Therefore, it is vital to improve radiative

transition probability and suppress the nonradiative transition processes. Additionally, structural and chemical defects were found to mediate RE emission in GaN. As shown in Fig. 1.4b[39], a broad defect/trap level just below GaN conduction band (~290meV) plays an important role in energy transferring from GaN host to Eu^{3+} ion energy levels.

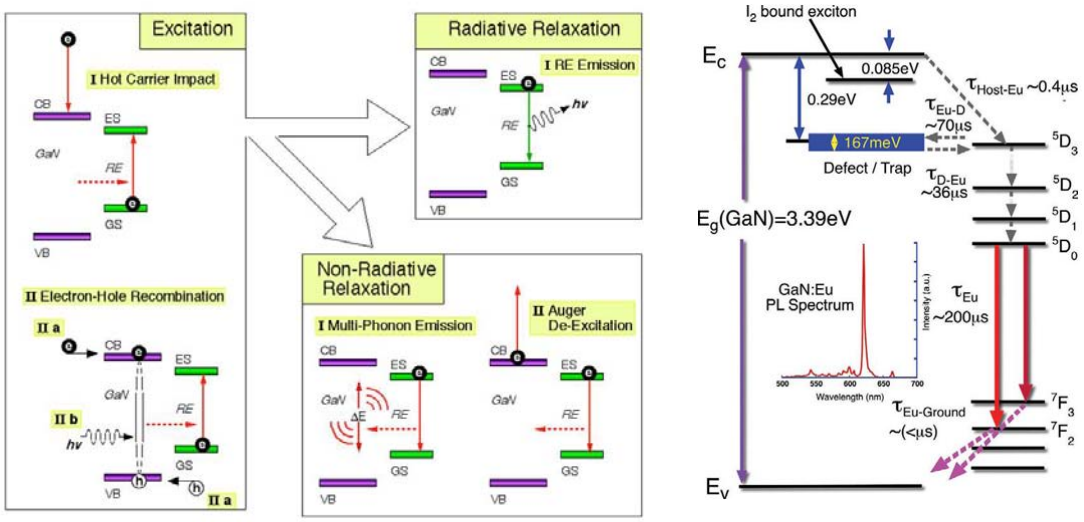

Fig 1.4 (a) Major emission mechanisms of RE^{3+} ions in GaN[38];

(b) Defect-mediated RE emission mechanism in GaN[39].

Two quenching effects on RE ions emission exist: thermal quenching and concentration quenching. When the energy difference between the excited states and the ground states decreased to less than 4-5 times as the vibration frequencies of the surroundings, a few high energy vibrations occurred and phonons were emitted out. Such nonradiative process is called “multi-phonon emission”. Concentration quenching occurred when two identical ions were close enough at high concentration levels (a few atomic percent) so that the nonradiative processes such as energy migration or cross relaxation happened.

References

[1] "New Semiconductor Materials: Characteristics and Properties.," Ioffe Physico-Technical Institute.

[2] F. R. Fichter, "Uber Aluminiumnitrid," *Z. Anorg. Chem.* , vol. 54, p. 322, 1907.

[3] J. V. Lirmann and H. S. Schdanov, "The crystalline structure of GaN," *Acta Physicochim. URSS,* vol. 6, p. 306, 1937.

[4] R. Juza and H. Hahn, "Über die Kristallstrukturen von Cu3N, GaN und InN Metallamide und Metallnitride," *Z. Anorg. Allg. Chem.*, vol. 234, p. 282, 1938.

[5] H. Grimmeiss and Z. H- Koelmans, *Nature(London),* vol. 14a, 1959.

[6] H. P. Maruska and J. J. Tietjen, "The preparation and properties of vapor-deposited single-crystal-line GaN," *Appl. Phys. Lett.,* vol. 15, p. 327, 2003.

[7] H. M. Manasevit, F. M. Erdmann, and W. I. Simpson, "The use of metalorganics in the preparation of semiconductor materials. IV. The nitrides of aluminum and gallium," *J. Electrochem. Soc.* , vol. 118, pp. 1864-1868, 1971.

[8] S. Yoshida, S. Misawa, and S. Gonda, "Improvements on the electrical and luminescent properties of reactive molecular beam epitaxially grown GaN films by using AlN-coated sapphire substrates," *Appl. Phys. Lett.*, vol. 42, p. 427, 1983.

[9] H. Amano, N. Sawaki, I. Akasaki, and Y. Toyoda, "Metalorganic vapor phase epitaxial growth of a high quality GaN film using an AlN buffer layer," *Appl. Phys. Lett.*, vol. 48, p. 353, 1986.

[10] S. Nakamura, "GaN growth using GaN buffer layer," *Jpn. J. Appl. Phy.*, vol. 30, pp. L1705-1707, 1991.

[11] N. Grandjean, M. Leroux, M. Lat, and J. Massies, "Gas source molecular beam epitaxy of wurtzite GaN on sapphire substrates using GaN buffer layers," *Appl. Phys. Lett.*, vol. 71, p. 240, 1997.

[12] K. S. Kim, C. S. Oh, K. J. Lee, G. M. Yang, C. H. Hong, K. Y. Lim, H. J. Lee, and A. Yoshikawa, "Effects of growth rate of a GaN buffer layer on the properties of GaN on a sapphire substrate," *Appl. Phys. Lett.*, vol. 85, p. 8441, 1999.

[13] T. Ito, K. Ohtsuka, K. Kuwahara, M. Sumiya, Y. Takano, and S. Fuke, "Effect of AlN buffer layer deposition conditions on the properties of GaN layer," *J. Cry. Grow.*, vol. 205, pp. 20-24, 1999.

[14] K. Uchida, K. Nishida, M. Kondo, and H. Munekata, "Epitaxial growth of GaN layers with double-buffer layers," *J. Cry. Grow.*, vol. 189, pp. 270-274, 1998.

[15] M. Mesrine, N. Grandjean, and J. Massies, "Efficiency of NH_3 as nitrogen source for GaN molecular beam epitaxy," *Applied Physics Letters*, vol. 72, pp. 350-352, 1998.

[16] T. D. Moustakas, T. Lei, and R. J. Molnar, "Growth of GaN by ECR-assisted MBE," *Physica B: Condensed Matter*, vol. 185, pp. 36-49, 1993.

[17] W. E. Hoke, P. J. Lemonias, and D. G. Weir, "Evaluation of a new plasma source for molecular beam epitaxial growth of InN and GaN films," *J. Cry. Growth*, vol. 111, pp. 1024-1028, 1991.

[18] D. W. Jenkins and J. D. Dow, "Electronic structures and doping of InN, $In_xGa_{1-x}N$, and $In_xAl_{1-x}N$," *Phys. Rev. B*, vol. 39, pp. 3317-3329, 1989.

[19] H. Murakami, T. Asahi, H. Amano, K. Hiramatsu, N. Sawaki, and I. Akasaki, "Growth of Si-doped $Al_xGa_{1-x}N$ on(0001) sapphire substrate by metalorganic vapor phase epitaxy," *J. Cry. Grow.*, vol. 115, pp. 648-651, 1991.

[20] J. G. Kim, A. C. Frenkel, H. Liu, and R. M. Park, "Growth by molecular beam epitaxy and electrical characterization of Si-doped zinc blende GaN films deposited on ?SiC coated (001) Si substrates," *Appl. Phys. Lett.*, vol. 65, p. 91, 1994.

[21] H. Amano, M. Kito, K. Hiramatsu, and I. Akasaki, "P-type conduction in Mg-doped GaN treated with low-energy electron beam irradiation (LEEBI)," *Jpn. J. Appl. Phy.*, vol. 28, pp. L2112-2114, 1989.

[22] J. A. V. Vechten, J. D. Zook, R. D. Horning, and B. Goldenberg, "Defeating Compensation in Wide Gap Semiconductors by Growing in H that is Removed by Low Temperature De-Ionizing Radiation," *Jpn. J. Appl. Phys.,* vol. 31, pp. 3662-3663, 1992.

[23] S. Nakamura, T. Mukai, M. Senoh, and N. Iwasa, "Thermal annealing effects on p-type Mg-doped GaN films," *Jpn. J. Appl. Phy.*, vol. 31, pp. L139-L142, 1992.

[24] A. Bhattacharyya, W. Li, J. Cabalu, T. D. Moustakas, D. J. Smith, and R. L. Hervig, "Efficient p-type doping of GaN films by plasma-assisted molecular beam epitaxy," *Appl. Phys. Lett.*, vol. 85, p. 4956, 2004.

[25] H. Obloh, K. H. Bachem, U. Kaufmann, M. Kunzer, M. Maier, A. Ramakrishnan, and P. Schlotter, "Self-compensation in Mg doped p-type GaN grown by MOCVD," *J. Cry. Grow.*, vol. 195, pp. 270-273, 1998.

[26] S. Nakamura, M. Senoh, and T. Mukai, "P-GaN/N-InGaN/N-GaN Double-Heterostructure Blue-Light-Emitting Diodes," *Jpn. J. Appl. Phy.*, vol. 32, pp. L8-L11, 1993.

[27] S. Nakamura, T. Mukai, and M. Senoh, "Candela-class high-brightness InGaN/AlGaN double-heterostructure blue-light-emitting diodes," *Appl. Phys. Lett.*, vol. 64, p. 1687, 1994.

[28] H. Amano, T. Asahi, and I. Akasaki, "Stimulated Emission Near Ultraviolet at Room Temperature from a GaN Film Grown on Sapphire by MOVPE Using an AlN Buffer Layer," *Jpn. J. Appl. Phy.*, vol. 29, p. L205, 1990.

[29] I. Akasaki, S. Sota, H. Sakai, T. Tanaka, M. Koike, and H. Amano, "Shortest wavelength semiconductor laser diode," *Electonic Lett.*, vol. 32, pp. 1105-1106, 1996.

[30] K. Itaya, M. Onomura, J. Nishio, L. Sugiura, S. Saito, M. Suzuki, J. Rennie, S. Nunoue, M. Yamamoto, and H. Fujimoto, "Room temperature pulsed operation of nitride based multi-quantum-well laser diodes with cleaved facets on conventional C-face sapphire substrates," *Jpn. J. Appl. Phy.*, vol. 35, pp. L1315-L1317, 1996.

[31] S. Nakamura, M. Senoh, S. Nagahama, N. Iwasa, T. Yamada, T. Matsushita, H. Kiyoku, and Y. Sugimoto, "InGaN Multi-Quantum-Well-Structure Laser Diodes with Cleaved Mirror Cavity Facets," *Jpn. J. Appl. Phy.*, vol. 35, p. 15, 1996.

[32] M. A. Khan, J. N. Kuznia, A. R. Bhattarai, and D. T. Olson, "Metal semiconductor field effect transistor based on single crystal GaN," *Appl. Phys. Lett.*, vol. 62, p. 1786, 1993.

[33] M. A. Khan, A. Bhattarai, J. N. Kuznia, and D. T. Olson, "High electron mobility transistor based on a GaN-AlGaN heterojunction," *Appl. Phys. Lett.*, vol. 63, p. 1214, 1993.

[34] B. F. Chu-Kung, M. Feng, G. Walter, N. Holonyak Jr, T. Chung, J. H. Ryou, J. Limb, D. Yoo, S. C. Shen, and R. D. Dupuis, "Graded-base InGaN/ GaN heterojunction bipolar light-emitting transistors," *Appl. Phys. Lett.*, vol. 89, p. 082108, 2006.

[35] G. H. Dieke and H. M. Crosswhite, "The spectra of the doubly and triply ionized rare earths," *Appl. Opt.*, vol. 2, pp. 675-686, 1963.

[36] B. R. Judd, "Optical Absorption Intensities of Rare-Earth Ions," *Phys. Rev.* , vol. 127, pp. 750-761, 1962.

[37] G. S. Ofelt, "Intensities of Crystal Spectra of Rare-Earth Ions," *Appl. Phys. Lett.*, vol. 37, p. 511, 2004.

[38] A. J. Steckl, J. Heikenfeld, M. Garter, R. Birkhahn, and D. S. Lee, "Rare Earth Doped Gallium Nitride - Light Emission From Ultraviolet to Infrared," *Compound Semiconductor*, vol. 6, pp. 48-52, 2000.

[39] A. J. Steckl, J. H. Park, and J. M. Zavada, "Prospects for rare earth doped GaN lasers on Si," *Materials Today*, vol. 10, pp. 20-27, 2007.

2. Rare Earth Doped Gallium Nitride Research in UC Nanola

2.1. Motivation of Rare Earth Doped GaN Research

Although RE^{3+} ions emission wavelengths are independent of the host materials, the emission intensity and efficiency are highly dependent on the host due to the strong effect of the host on the radiative transition probability. Many host materials such as fluoride glasses[1, 2], sol-gels[3], ceramics[4] and semiconductors have been researched. Si[5, 6] were used as the host for Er, which can enable Er^{3+} ions to emit the infrared emission (1.54μm). However, it suffers the low RE density and severe temperature quenching. Such temperature quenching has been demonstrated to be inversely proportional to the host material's energy bandgap[7]. Wide bandgap II-VI semiconductors[8-10] were utilized as host materials, but limited by the weakly bonded lattice and the defects due to additional charges by substitutional location of the RE^{3+} ions on the II^{2+} element cation site. Therefore, people are attracted to the III-nitride Semiconductors. III-nitride semiconductors such as GaN have great qualities as the host materials, including: direct energy bandgap which is necessary in optical application, wide energy bandgap resulting in low thermal quenching on RE luminescence, strong chemical bonded lattice which allows a high RE doping concentrations, charge neutrality with trivalent RE^{3+} ions substitutionally replacing trivalent III^{3+} element ions in the lattice, thermal and chemical robustness.

According to "Dieke Diagram"[11], 4*f* electrons energy levels from several RE^{3+} (Eu, Er & Tm) ions in GaN energy bandgap are shown in Fig 2.1. Visible and infrared emissions can be obtained with the radative transitions between some energy levels. For example, 4*f* electrons in Eu^{3+} ions can have radiative relaxation from ^5D_i to ^7F_j energy levels, resulting in yellow/red emissions at 543nm, 600nm, 621nm and 632nm.

Table 2.1 Development of GaN:RE research in UC Nanolab.

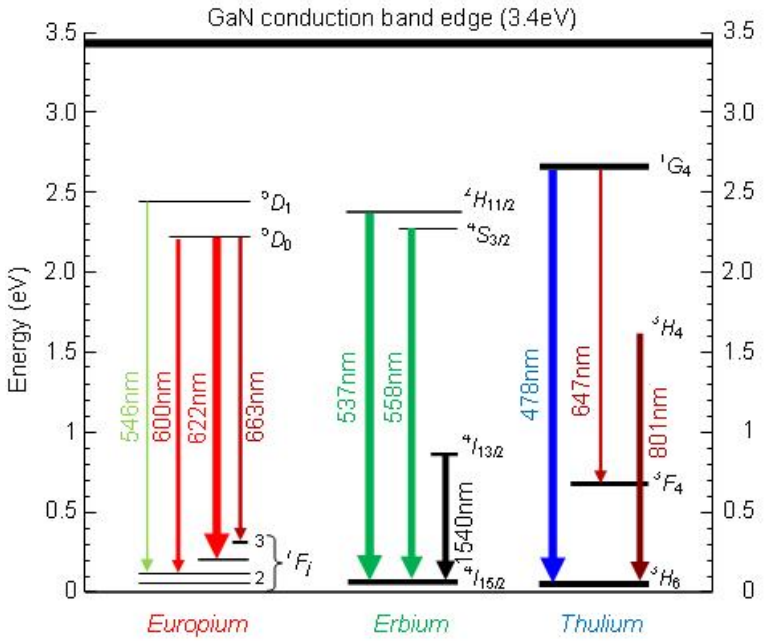

Fig 2.1 4f energy levels from selected rare earth ions in GaN bandgap.

2.2. Previous Achievements in UC Nanolab

RE doped GaN and other III-nitride semiconductors have been studied in Nanoelectronics Labortory in University of Cincinnati since 1997. There are many achievements not only in RE doped GaN thin film growth and characterization, but also in RE doped GaN electroluminescent device application. The summary of GaN:RE research in Nanolab was shown in Table 2.1.

Year	Results	Reference
1998	First visible emission from GaN:Er/sapphire	[12]
	Green emission from GaN:Er/Si	[13]
	Green electroluminescence from GaN:Er schottky barrier diodes	[14]
1999	Visible and IR electroluminescence from GaN:Er/Si schottky diodes	[15]
	Red luminescence from GaN:Pr/Si	[16]
	Red luminescence from GaN:Eu/Si	[17]
	Blue luminescence from GaN:Tm/Si	[18]
	RGB colors display from GaN:RE	[19]
	Turquoise emission from GaN:(Er+Tm)	[19]
2000	Yellow or orange emission from GaN:(Eu+Er)	[20]
	Low voltage GaN:Er electroluminescent devices	[21]
2001	Multiple color capability from GaN:RE	[19, 22, 23]
	Electroluminescence from GaN:Er under AC bias	[24]
	Room-temperature-grown GaN:RE	[25]
2002	Switchable color GaN:RE electroluminescent devices	[26]
	GaN:RE phosphor thick film dielectric electroluminescent device	[27-29]
	Optimization of GaN:Er growth condition	[30-32]
	Lateral color integration of GaN:RE	[33]
2003	Three-color integration of GaN:RE	[34]
	Enhanced blue emission from $Al_xGa_{1-x}N$:Tm	[35]
2004	Stimulated emission from GaN:Eu	[36]
	Enhanced red emission from GaN:Eu by interrupted growth epitaxy	[37]
2005	Visible laser from GaN:Eu/Si	[38]
2007	Prospects of GaN:RE/Si lasers research	[39]
2008	GaN:RE ELDs emission mechanism controlled by Si co-doping	[40]
2009	Enhanced Eu red emission in GaN:Eu by Si co-doping	[41]
	Optimization of GaN:Eu growth condition	[42]
	Enhanced Eu ferromagnetism from GaN:Eu by Si co-doping	[43]
	Enhanced Eu red emission from $Al_xGa_{1-x}N$:Eu	[44]

(1) First visible emission from RE doped GaN

Green visible emission from Er doped GaN on sapphire substrate was firstly reported[12] by Nanolab in 1998. The emission spectrum consists of two narrow green lines at 537 and 558 nm and a broad peak at light blue wavelengths (480–510 nm). The narrow lines have been identified as Er transitions from the $^2H_{11/2}$ and $^4S_{3/2}$ levels to the $^4I_{15/2}$ ground state, shown in Fig 2.1. Er doped GaN on Si substrates also showed[13] similar green emission spectrum. Later, visible and IR electroluminescence (EL) from GaN:Er on sapphire and Si substrates was demonstrated[14, 15].

(2) RGB color achievement by different RE doping

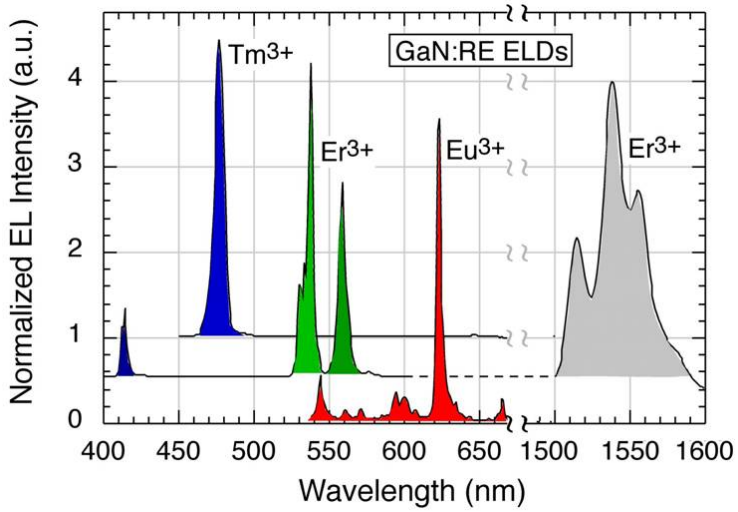

Fig 2.2 Emission spectra from Eu, Er, Tm doped GaN.[45]

Primary three RGB colors were achieved[19] by different RE doping in GaN host: red light from Pr[16], Eu[17]; green light from Er[12-15]; blue light from Tm[18]. The emission spectra from several RE doped GaN were shown in Fig 2.2[45]. As clearly seen in the spectra, red emission at ~622nm is from $^5D_0 \rightarrow {}^7F_2$ transitions in Eu^{3+} ions, green emissions at 537nm & 558nm and IR emission at 1540nm are from $^2H_{11/2} \rightarrow {}^4I_{15/2}$, $^4S_{3/2} \rightarrow {}^4I_{15/2}$, $^4I_{13/2} \rightarrow {}^4I_{15/2}$ in Er^{3+} ions, blue emission at 477nm is from $^1G_4 \rightarrow {}^3H_6$ in Tm^{3+} ions.

(3) Multiple color capability

Co-doping of different RE elements was made to realize intermediate colors, such as turquoise[19] from Er and Tm co-doped GaN, orange or yellow[20] from Er and Eu co-doped GaN. Therefore, multiple color capability [19, 22, 23] of GaN:RE thin films was realized and the results are shown in Fig 2.3[19, 23]. Lateral integration[34] of RGB colors from GaN:RE thin film was also accomplished.

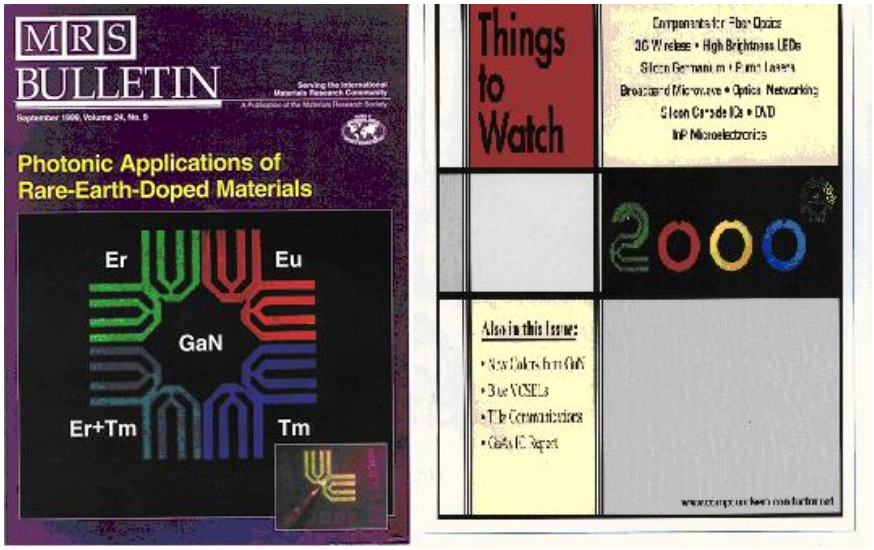

Fig 2.3 Multiple color capability from RE doped GaN shown in [19, 23].

(4) DC and AC devices

RE doped GaN DC electroluminescent devices (ELDs) were successfully fabricated[14] based on a simple schottky diode structure. Patterned ITO thin films were directly deposited on GaN:RE layer grown on Si or sapphire wafers. When the external voltage was biased between inner and outer ITO electrodes, the RE ions EL was emitted out from the inner electrode.

EL from GaN:RE phosphors was also researched under AC bias[24] condition. Thick dielectric electroluminescent (TDEL) devices[27-29] based on GaN:RE were fabricated and optimized. Such devices are very attractive to the flat panel displays (FPD) area because of multiple color capability and good thermal stability.

(5) Optimization of GaN:RE thin film growth

The growth conditions including Er cell temperature[30], growth temperature[31] and Ga cell temperature[32] were optimized for the goal of strongest Er^{3+} ions luminescence. It was found that the optimum growth conditions is slight N-rich condition (III/V<1) at 600ºC, resulting in ~1.0at.% Er doping concentration. Low temperature even room temperature RE doped GaN thin films were also successfully grown[25] and EL emissions were observed from as-grown and enhanced by post-annealing.

(6) Lasing from RE^{3+} ions

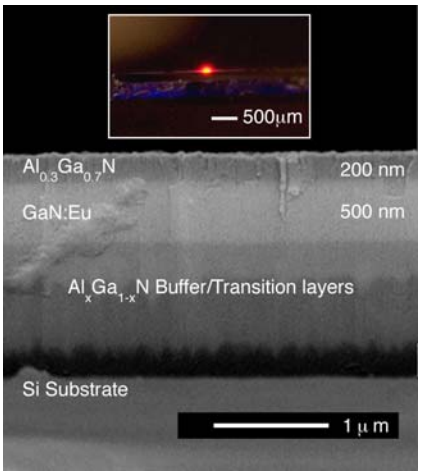

Fig 2.4 Lasing emission from Eu^{3+} ions in GaN:Eu grown on Si wafers.[38]

Demonstration of room temperature stimulated emissions from GaN:Eu thin films was first reported[36] by Nanolab in 2004. A modal gain of ~43cm^{-1} and a modal loss of

~20cm^{-1} were obtained. The first visible laser[38] for RE doped GaN on Si substrate, shown in Fig 2.4, was successfully fabricated by GaN:Eu growth on AlGaN buffer layer coated p-Si(111) substrates.

2.3. Goals of Research

RE doped GaN research in the Nanolab has resulted in many achievements in thin film growth and characterizations. Simple DC and AC GaN:RE ELDs were also fabricated and tested. However, there are still many questions in RE^{3+} ions emission mechanism in GaN, such as the effect of structural and chemical defects. Therefore, the main goal of this research was to study RE emission in GaN materials and devices, focusing on the effect of *co-doping of rare earth luminescent impurities and electronic impurities*. The following tasks were pursued:

(1) Optimization of RE doped GaN growth

The growth conditions have been demonstrated[30-32] to have great effect on GaN:Er thin film quality and Er^{3+} ions luminescence. Therefore, it is important and necessary to continue optimize the growth conditions for other RE doped GaN such as Eu. So my first work is to study the effect of growth conditions such as III/V ratio, growth temperature and Eu cell temperature on Eu^{3+} luminescence. Meantime, some other factors such as the substrates and different nitrides hosts can be also researched.

(2) Effect of co-dopant (Si) on RE^{3+} luminescence

It was found[46-48] that the structural or chemical defects introduced during the growth process play an important role in the energy transfer process to RE sites. On this basis, we proposed that the co-dopants in GaN:RE thin films could also mediate the RE^{3+} emission

process in GaN. Therefore, my second work is to study the effect of co-dopants in RE doped GaN. Si was chosen to be the co-dopant because Si is available in our MBE system and easily to *in situ* co-doped in GaN:RE thin films. The effect of Si co-doping on optical an electrical properties of GaN:RE will be studied.

(3) Design and fabrication of RE doped GaN ELDs

Simple DC and AC GaN:RE devices showed the RE^{3+} ions EL spectra, but could not give detailed information in device application of RE doped GaN. Therefore, advanced GaN:RE ELDs, especially homo-junction and hetero-junction p-type-intrinsic-n type (PIN) LEDs, needed be designed and fabricated. The initial device structure and fabrication processes were subsequently optimized. The dominant RE^{3+} EL emission mechanism was investigated. Moreover, the effect of Si co-doping in GaN:RE ELDs was studied.

References

[1] M. D. Shinn, W. A. Sibley, M. G. Drexhage, and R. N. Brown, "Optical transitions of Er3+ ions in fluorozirconate glass," *Phys. Rev. B*, vol. 27, p. 6635, 1983.

[2] M. Dejneka, E. Snitzer, and R. E. Riman, "Blue, green and red fluorescence and energy transfer of Eu^{3+} in fluoride glasses," *J. Lumin.*, vol. 65, pp. 227-245, 1995.

[3] X. Fan, M. Wang, and G. Xiong, "Spectroscopic studies of rare earth ions in silica glasses prepared by the sol-gel process " *Materials Letters*, vol. 27, pp. 177-181, 1996.

[4] S. Bachir, C. Sandouly, J. Kossanyi, and J. C. Ronfard-Haret, "Rare earth-doped polycrystalline zinc oxide electroluminescent ceramics," *J. Phys. Chem. Solids*, vol. 57, pp. 1869-1879, 1996.

[5] G. Franzo, S. Coffa, F. Priolo, and C. Spinella, "Mechanism and performance of forward and reverse bias electroluminescence at 1.54 mu m from Er-doped Si diodes," *J. Appl. Phys.*, vol. 81, pp. 2784-2793, 1997.

[6] W. Jantsch, S. Lanzerstorfer, L. Palmetshofer, M. Stepikhova, and H. Preier, "Different Er centres in Si and their use for electroluminescent devices," *J. Lumin.*, vol. 80, pp. 9-17, 1998.

[7] P. N. Favennec, H. L'Haridon, M. Salvi, D. Moutonnet, and Y. Le Guillou, "Luminescence of erbium implanted in various semiconductors: IV, III-V and II-VI materials," *Electonic Lett.*, vol. 25, p. 718, 1989.

[8] S. Bachir, K. Azuma, J. Kossanyi, P. Valat, and J. C. Ronfard-Haret, "Photoluminescence of polycrystalline zinc oxide co-activated with trivalent rare earth ions and lithium. Insertion of rare-earth ions into zinc oxide," *J. Lumin.*, vol. 75, pp. 35-49, 1997.

[9] D. Kahng, "Electroluminescence of Rare-Earth and Transition Metal Molecules in II-VI Compounds via Impact Excitation," *Appl. Phys. Lett.*, vol. 13, pp. 210-212, 1968.

[10] R. Boyn, "4f-4f Luminescence of Rare-Earth Centers in II-VI Compounds," *Phys. Stat. Sol. (b)*, vol. 148, pp. 11-47, 1988.

[11] G. H. Dieke and H. M. Crosswhite, "The spectra of the doubly and triply ionized rare earths," *Appl. Opt.*, vol. 2, pp. 675-686, 1963.

[12] A. J. Steckl and R. Birkhahn, "Visible emission from Er-doped GaN grown by solid source molecular beam epitaxy," *Appl. Phys. Lett.*, vol. 73, p. 1700, 1998.

[13] R. Birkhahn and A. J. Steckl, "Green emission from Er-doped GaN grown by molecular beam epitaxy on Si substrates," *Appl. Phys. Lett.*, vol. 73, p. 2143, 1998.

[14] A. J. Steckl, M. Garter, R. Birkhahn, and J. Scofield, "Green electroluminescence from Er-doped GaN Schottky barrier diodes," *Appl. Phys. Lett.*, vol. 73, p. 2450, 1998.

[15] M. Garter, J. Scofield, R. Birkhahn, and A. J. Steckl, "Visible and infrared rare-earth-activated electroluminescence from indium tin oxide Schottky diodes to GaN: Er on Si," *Appl. Phys. Lett.*, vol. 74, p. 182, 1999.

[16] R. Birkhahn, M. Garter, and A. J. Steckl, "Red light emission by photoluminescence and electroluminescence from Pr-doped GaN on Si substrates," *Appl. Phys. Lett.*, vol. 74, p. 2161, 1999.

[17] J. Heikenfeld, M. Garter, D. S. Lee, R. Birkhahn, and A. J. Steckl, "Red light emission by photoluminescence and electroluminescence from Eu-doped GaN," *Appl. Phys. Lett.*, vol. 75, p. 1189, 1999.

[18] A. J. Steckl, M. Garter, D. S. Lee, J. Heikenfeld, and R. Birkhahn, "Blue emission from Tm-doped GaN electroluminescent devices," *Appl. Phys. Lett.*, vol. 75, p. 2184, 1999.

[19] A. J. Steckl and J. M. Zavada, "Photonic applications of rare-earth-doped materials," *Mat. Res. Soc. Bulletin*, vol. 24, pp. 16-17, 1999.

[20] D. S. Lee, J. Heikenfeld, R. Birkhahn, M. Garter, B. K. Lee, and A. J. Steckl, "Voltage-controlled yellow or orange emission from GaN codoped with Er and Eu," *Appl. Phys. Lett.*, vol. 76, p. 1525, 2000.

[21] J. Heikenfeld, D. S. Lee, M. Garter, R. Birkhahn, and A. J. Steckl, "Low-voltage GaN: Er green electroluminescent devices," *Appl. Phys. Lett.*, vol. 76, p. 1365, 2000.

[22] A. J. Steckl, J. Heikenfeld, D. S. Lee, and M. Garter, "Multiple color capability from rare earth-doped gallium nitride," *Mat. Sci. & Eng. B*, vol. 81, pp. 97-101, 2001.

[23] A. J. Steckl, J. Heikenfeld, M. Garter, R. Birkhahn, and D. S. Lee, "Rare Earth Doped Gallium Nitride - Light Emission From Ultraviolet to Infrared," *Compound Semiconductor*, vol. 6, pp. 48-52, 2000.

[24] J. Heikenfeld and A. Steckl, "Alternating current thin-film electroluminescence of GaN: Er," *Appl. Phys. Lett.*, vol. 77, p. 3520, 2000.

[25] D. S. Lee and A. J. Steckl, "Room-temperature-grown rare-earth-doped GaN luminescent thin films," *Appl. Phys. Lett.*, vol. 79, p. 1962, 2001.

[26] J. Heikenfeld and A. J. Steckl, "Rare-earth-doped GaN switchable color electroluminescent devices," *IEEE Trans. Electron Devices*, vol. 49, pp. 1545-1551, 2002.

[27] J. Heikenfeld and A. J. Steckl, "Electroluminescent devices using a high-temperature stableGaN-based phosphor and thick-film dielectric layer," *IEEE Trans. Electron Devices*, vol. 49, pp. 557-563, 2002.

[28] J. Heikenfeld and A. J. Steckl, "Contrast-enhancement in black dielectric electroluminescent devices," *IEEE Trans. Electron Devices*, vol. 49, pp. 1348-1352, 2002.

[29] C. Munasinghe, J. Heikenfeld, R. Dorey, R. Whatmore, J. P. Bender, J. F. Wager, and A. J. Steckl, "High brightness ZnS and GaN electroluminescent devices using PZT thick dielectric layers," *IEEE Trans. Electron Devices*, vol. 52, pp. 194-203, 2005.

[30] D. S. Lee, J. Heikenfeld, and A. J. Steckl, "Optimum Er concentration for in situ doped GaN visible and infrared luminescence," *Appl. Phys. Lett.*, vol. 79, p. 719, 2001.

[31] D. S. Lee, J. Heikenfeld, and A. J. Steckl, "Growth-temperature dependence of Er-doped GaN luminescent thin films," *Appl. Phys. Lett.*, vol. 80, p. 344, 2002.

[32] D. S. Lee and A. J. Steckl, "Ga flux dependence of Er-doped GaN luminescent thin films," *Appl. Phys. Lett.*, vol. 80, p. 728, 2002.

[33] D. S. Lee and A. J. Steckl, "Lateral color integration on rare-earth-doped GaN electroluminescent thin films," *Appl. Phys. Lett.*, vol. 80, p. 1888, 2002.

[34] Y. Q. Wang and A. J. Steckl, "Three-color integration on rare-earth-doped GaN electroluminescent thin films," *Appl. Phys. Lett.*, vol. 82, p. 502, 2003.

[35] D. S. Lee and A. J. Steckl, "Enhanced blue emission from Tm-doped Al x Ga 1-x N electroluminescent thin films," *Appl. Phys. Lett.*, vol. 83, pp. 2094-2096, 2003.

[36] J. H. Park and A. J. Steckl, "Laser action in Eu-doped GaN thin-film cavity at room temperature," *Appl. Phys. Lett.*, vol. 85, p. 4588, 2004.

[37] C. Munasinghe and A. J. Steckl, "GaN: Eu electroluminescent devices grown by interrupted growth epitaxy," *Mat. Res. Soc. Symp. Proc.*, vol. 496, pp. 636-642, 2006.

[38] J. H. Park and A. J. Steckl, "Demonstration of a visible laser on silicon using Eu-doped GaN thin films," *Appl. Phys. Lett.*, vol. 98, p. 056108, 2005.

[39] A. J. Steckl, J. H. Park, and J. M. Zavada, "Prospects for rare earth doped GaN lasers on Si," *Materials Today*, vol. 10, pp. 20-27, 2007.

[40] R. Wang and A. Steckl, "Effect of Si and Er Co-doping on Green Electroluminescence from GaN:Er LEDs," in *Mat. Res. Soc. Symp. Proc.*, San Francisco, CA, 2008, pp. C05-03.

[41] R. Wang, A. J. Steckl, E. E. Brown, U. Hommerich, and J. M. Zavada, "Effect of Si co-doping on Eu^{3+} luminescence in GaN," *J. Appl. Phys.*, vol. 105, p. 043107, 2009.

[42] R. Wang and A. J. Steckl, "Effect of Growth Condition on Eu^{3+} Luminescence from GaN:Eu Thin Films Grown by RF plasma Molecular Beam Epitaxy," *In preparation*, 2009.

[43] N. Nepal, J. M. Zavada, R. Wang, and A. J. Steckl, "Electrical and Magnetic Properties of GaN Co-doped with Si and Eu," *In preparation*, 2009.

[44] R. Wang and A. J. Steckl, "Luminescence Properties of Eu doped $Al_xGa_{1-x}N$," *In preparation*, 2009.

[45] A. J. Steckl, J. C. Heikenfeld, L. Dong-Seon, M. J. Garter, C. C. Baker, W. Yongqiang, and R. Jones, "Rare-earth-doped GaN: growth, properties, and fabrication of electroluminescent devices," *IEEE J. Selected Topics in Quantum Electronics*, , vol. 8, pp. 749-766, 2002.

[46] E. E. Nyein, U. Hommerich, J. Heikenfeld, D. S. Lee, A. J. Steckl, and J. M. Zavada, "Spectral and time-resolved photoluminescence studies of Eu-doped GaN," *Appl. Phys. Lett.*, vol. 82, pp. 1655-1657, 2003.

[47] H. Y. Peng, C. W. Lee, H. O. Everitt, D. S. Lee, A. J. Steckl, and J. M. Zavada, "Effect of optical excitation energy on the red luminescence of Eu^{3+} in GaN," *Appl. Phys. Lett.*, vol. 86, p. 051110, 2005.

[48] Z. Li, H. Bang, G. Piao, J. Sawahata, and K. Akimoto, "Growth of Eu-doped GaN by gas source molecular beam epitaxy and its optical properties," *J. Crystal Growth*, vol. 240, pp. 382-388, 2002.

3. Material Growth of Gallium Nitride

3.1. Growth Technique

GaN and other III-nitride semiconductors in NanoLab are grown by RF plasma assisted solid source molecular beam epitaxy (SSMBE) technique. Ultra pure elements (metals and semiconductors) are heated and evaporated in Knudsen effusion sources. The evaporated atoms have long mean free path in ultra high vacuum (10^{-10}~10^{-11}Torr) so that they form a molecular beam and do not interact with each other until they reach the wafer. The deposition rate of MBE technique is very slow (usually few hundred nanometers per hour), which allows the film grow epitaxially (layer by layer). Fig 3.1 shows an overview of Riber 32 MBE system in Nanolab.

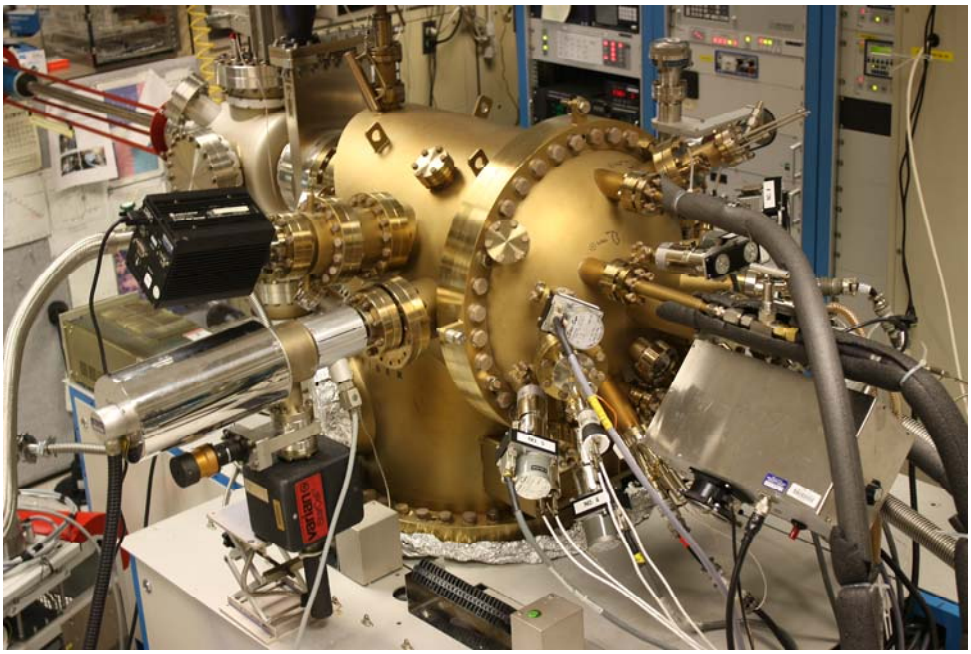

Fig 3.1 Overview of Riber 32 molecular beam epitaxy (MBE) system.

Riber 32 MBE system in Nanolab is a two-chamber system, consisting of growth chamber, load lock chamber, vacuum pumps, effusion sources and control cabinets. Crystal V7, OEM control software from Riber, is used to control the equipments, monitor the systems, perform the growth and record the data. Fig 3.2 shows a picture of software control panel.

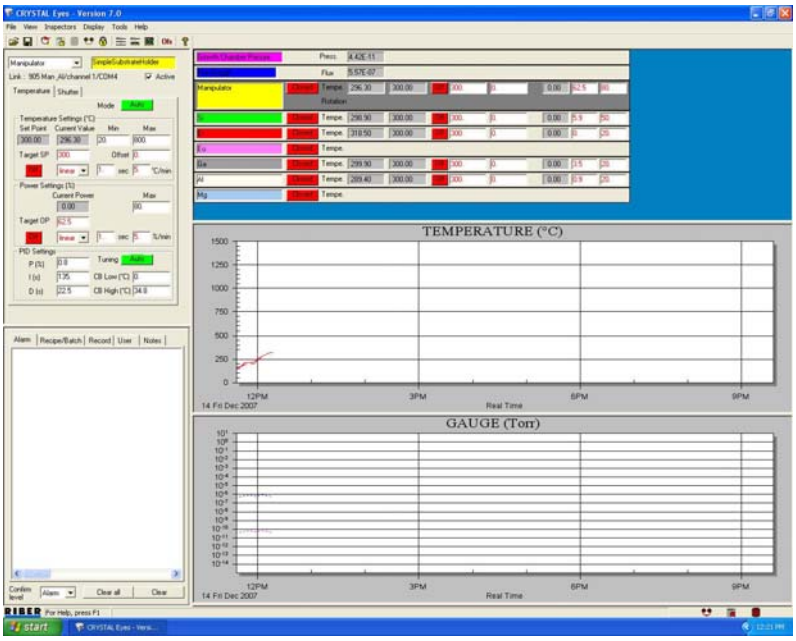

Fig 3.2 MBE control software: Crystal V7.

A CTI on-board cryopump with water cooling compressor maintains the vacuum of growth chamber at low 10^{-10}Torr. During the growth process, the chamber can be cooled down by liquid nitrogen with pressure at low 10^{-11}Torr. A standard ion pump provides load lock pressure as low as ~10^{-9}Torr for wafers outgassing and transferring. There are also titanium sublimator pumps (TSP) in growth chamber and load lock.

Six solid effusion sources are installed in the system, also shown in Fig 3.1. III element sources are available with 6N Ga and Al metals filled in 200g Veeco SUMO cells. N-type

and p-type dopant sources for GaN are introduced by 6N Si and 5N Mg metals in Veeco dopant cells. RE elements are evaporated from 3N metals in Veeco SUMO cells (Er, Tm) and Riber ABN cell (Eu). All effusion sources are controlled by Eurotherm temperature controller.

Nitrogen gas is provided by ultra high purity (UHP) nitrogen gas cylinder and the flow is controlled by a mass flow controller (MFC) installed in the gas line. The plasma was generated into a discharge chamber filled nitrogen gas by inductively coupled RF energy at a frequency of 13.56MHz, which is composed of approximately ~5% nitrogen ions and ~95% nitrogen molecules. An advanced energy RF power supply can provide up to 600W power and a plasma matching box can be manually adjusted to get the minimum reflected power. A typical gas flow of 1.8sccm and 400W RF power could have the base system pressure ~5.5×10^{-5}Torr.

Several ion gauges are installed in the system, one for load lock and the other two for growth chamber. One of them in growth chamber is close to the cyropump and interlocked with the cryopump gate. Once the ion gauge were off or the pressure were above 10^{-3}Torr or the cyropump was dead, the cyopump gate would be automatically closed to separate the chamber from the cryopump. The other one on the manipulator is used for the element flux measurements. The measured value is called beam epitaxy pressure (BEP), exponentially proportional to the effusion source temperature.

A Leybold transpector gas analysis system is installed in the growth chamber as residual gas analyzer (RGA), detecting leaks and contaminants. It consists of the ion source, the quadrupole mass filter and the ion detector. By ionizing the gas molecules, separating them by mass and measuring the quantity, it can indicate the partial pressure of gases

characteristic of processes occurring within a vacuum, and therefore can be used to investigate the nature of a process or to monitor process conditions. Fig 3.3 shows the typical mass spectrum in our MBE system.

Fig 3.3 Spectrum of residual gas analyzer (RGA).

3.2. Characterization Measurements

The characterizations of GaN thin films were studied by various semiconductor analysis equipments, including the crystal quality of GaN thin film checked by reflection high energy electron diffraction (RHEED) and X-ray diffraction (XRD), the thin film topology measured by scanning electron microscopy (SEM) and atomic force microscopy (AFM), the optical properties studied by photoluminescence (PL), the electrical properties measured by Hall effect measurements, the RE doping profile and concentration investigated by secondary ion mass spectroscopy (SIMS), etc.

(1) Reflection High Energy Electron Diffraction

RHEED tool is widely used to *in situ* monitor the crystal growth in MBE technique. High energy electron beams are generated by electron gun and incident on the sample surface at a very small angle. The electrons diffracted by the atoms on the surface interfere constructively at specific angles and form regular patterns on the detector. The position of atoms on the sample surface affects the electron diffraction so that the pattern at the detector is a function of the sample surface. So it is very useful to "real time" monitor the atomic layer growth.

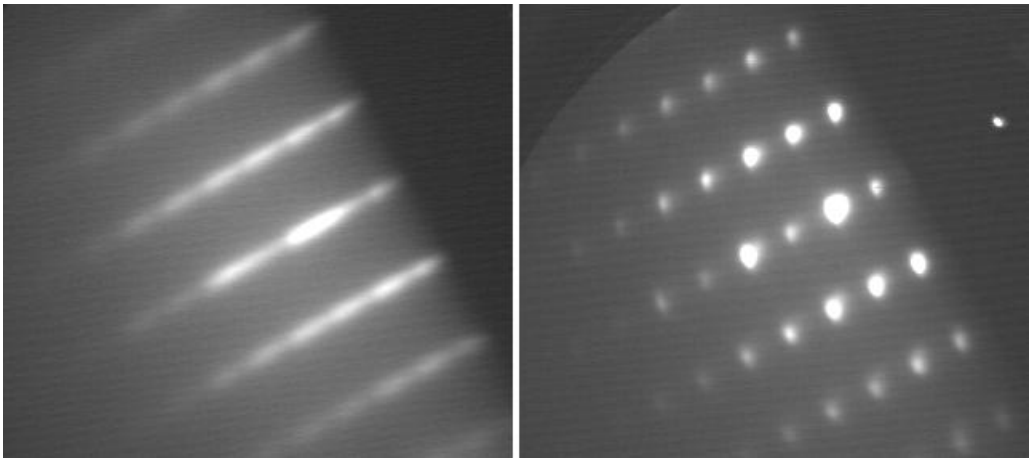

(a) (b)

Fig 3.4 RHEED pattern on (a) 2d and (b) 3d GaN thin film growth.[1]

A STAIB instrument electron gun is installed in our MBE system with a high voltage supply. The diffracted pattern on the photoluminescent detector is captured by a CCD camera. A typical RHEED picture for 2-dimensional wurtzite GaN growth is a streaky pattern, shown in Fig 3.4a[1]. Such 2-dimesnial growth means layer-by-layer growth, which is desirable for thin film growth. A spotty pattern would appear for a 3-dimensional wurtzite GaN growth or Cubic GaN growth, shown in Fig 3.4b.

(2) X-Ray Diffraction

The crystallographic structure of thin films can be checked by XRD measurements. The incident X-ray waves strike the atoms and electrons, causing the secondary spherical waves emanating from the electrons. If atoms are arranged symmetrically, these waves will add constructively at only a few specific directions, determined by the Bragg's Law: $2d\sin(2\theta) = n\lambda$, where d is the space between atomic layers, θ is the incident angle, n is an integer and λ is the wavelength.

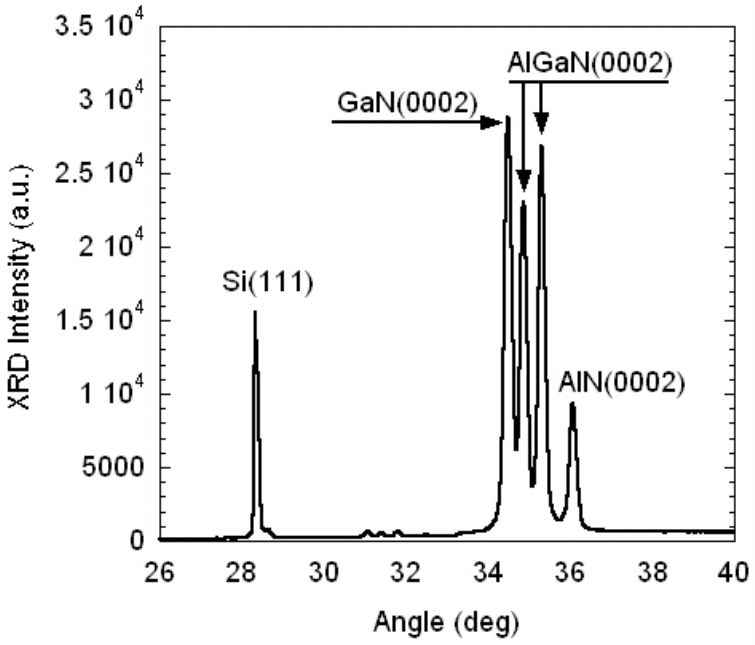

Fig 3.5 XRD measurement spectrum on GaN/AlGaN/AlN on Si wafers.

Nanolab's XRD system is Rigaku MiniFlex with a Cu Kα X-ray gun at 1.542Å. The distance of wurtzite Hexagonal GaN is ~5.186Å, so the angle 2θ is around 34.5º. Similarly, for wurtzite AlN, the angle is around 36º. A typical XRD spectrum for GaN/AlGaN/AlN layers on Si substrates is shown in Fig 3.5. The peaks between GaN peak (34.5º) and AlN

peak (36º) in the figure are from ternary alloy $Al_xGa_{1-x}N$. High intensity and narrow linewidth (FWHM) of XRD peaks show the good crystal quality of thin films.

(3) Secondary ion mass spectroscopy

Fig 3.6 Overview of PHI D-SIMS(secondary ions mass spectroscopy) system.

The chemical composition and the dopant depth profile were checked by SIMS measurements. SIMS is the most sensitive surface analysis technique, being able to detect elements present in the parts per billion range. A focused primary ion beam is sputtered on the sample surface and ejected out the secondary ions, which are collected by the detector with a mass analyzer to determine the elemental, isotopic, or molecular composition.

Fig 3.6 shows the picture of PHI D-SIMS 6600 system in Nanolab. Two focused primary ion beam, O_2 and Ce, can be used to eject the secondary ions with positive or negative

charges. There is also one electron gun to provide electron beam for TV imaging and neutralization. A quadrupole mass analyzer separates the masses by resonant electric fields, where only masses of choice are able to pass and be detected by the detector. The chamber was kept in the vacuum of low 10^{-10}Torr by a standard ion pump. A typical SIMS spectrum from GaN:Eu/Sapphire sample was shown in Fig 3.7. The Eu atomic concentration can be calculated from the reference samples.

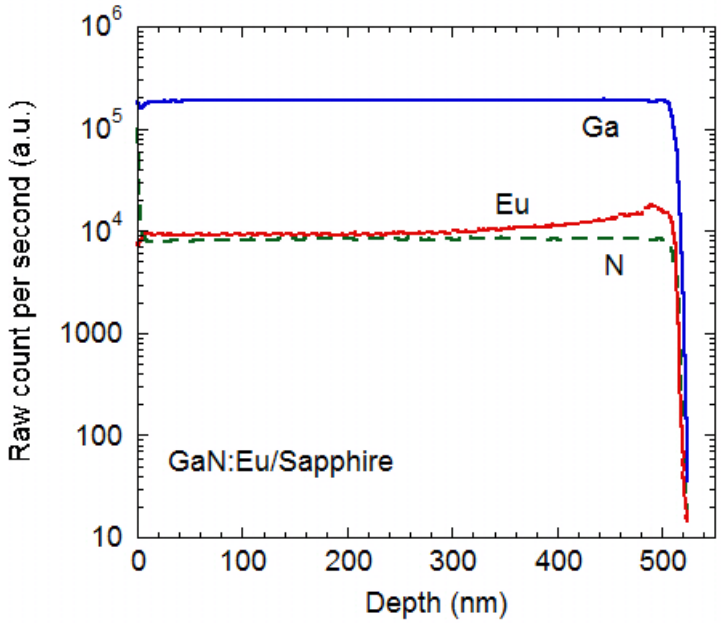

Fig 3.7 SIMS measurement spectrum on GaN:Eu/Al_2O_3 samples.

(4) Photoluminescence

The optical properties of GaN thin films and RE dopants were studied by "above-bandgap" PL measurement. The mechanism of RE^{3+} PL emission incorporates the following steps: (1) absorption of excitation photons by GaN bandgap and electron-hole pair generation; (2) electron-hole recombination with energy transfer to RE^{3+} sites; (3) radiative relaxation of excited RE^{3+} sites with 4*f* level emission.

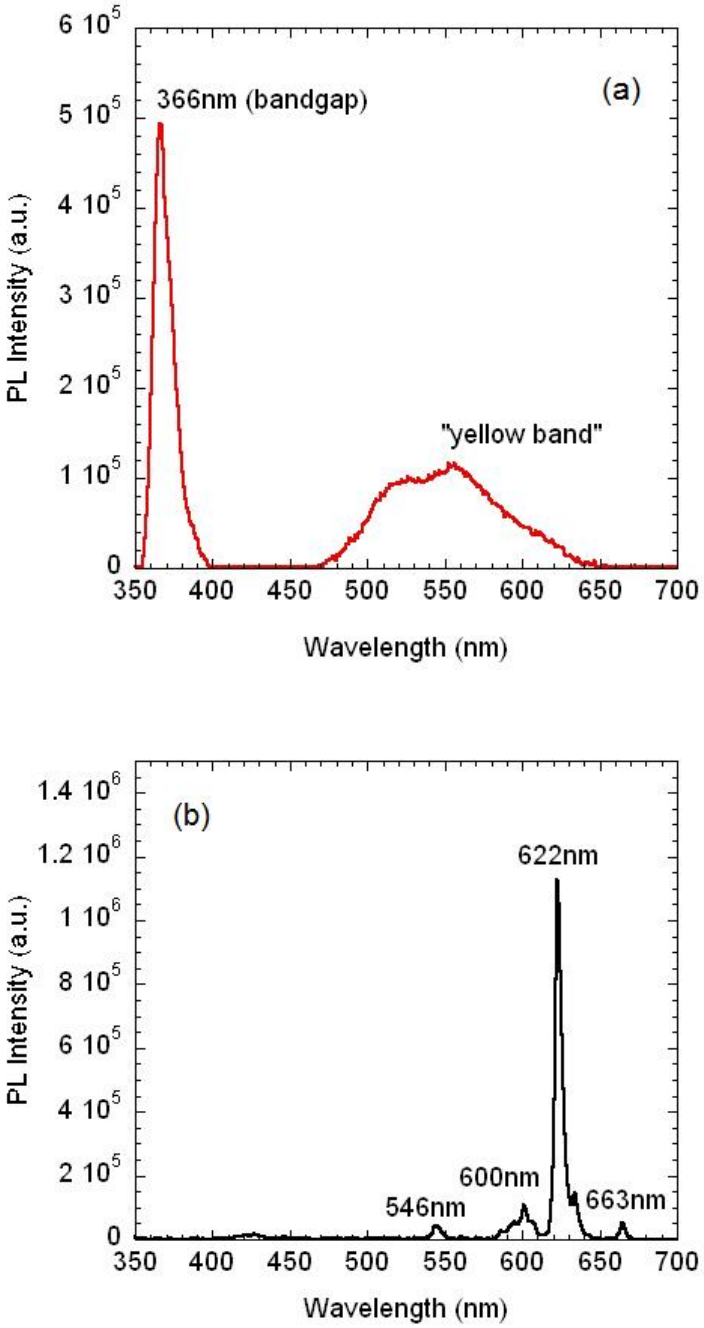

Fig 3.8 PL spectra from (a) undoped GaNand (b) GaN:Eu thin films.

Room temperature PL measurements in Nanolab were “above-bandgap” excited by an Omnichrome series 74 He-Cd laser at 325nm. PL spectra were acquired by a Princeton Instruments/Acton Research SP2550i spectrometer system equipped with a photon

multiplier tube (PMT) detector for visible emission and an InGaAs detector for IR emission. Fig 3.8 shows typical PL spectra from undoped GaN and Eu doped GaN thin films. The peak at 366nm in undoped GaN is from free exciton bandgap radiative relaxation. The broad band around 500-600nm in undoped GaN PL spectrum is attributed to the donor acceptor pairs (DAP). In Eu doped GaN PL spectrum, the bandgap and "yellow band" disappeared, but Eu^{3+} related emission lines appeared. The main peak is at ~622nm from the radiative transition $^5D_0$-$^7F_2$. Some weaker emission lines at ~600nm ($^5D_0$-$^7F_1$), ~663nm ($^5D_0$-$^7F_3$) and ~546nm ($^5D_1$-$^7F_1$) were also present in the spectrum.

(5) Scanning Electron Microscopy

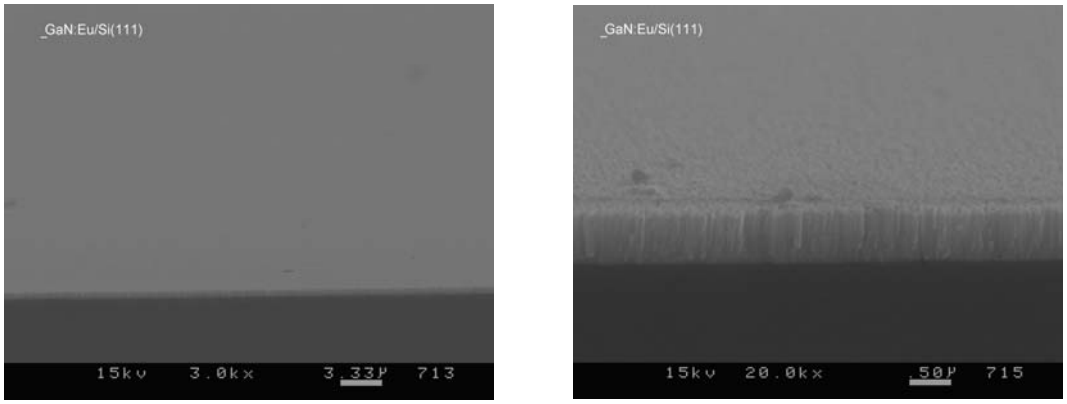

(a) (b)

Fig 3.9 SEM image on the (a) surface and (b) cross section of GaN:Eu/Si samples.

Because of the limitations of optical microscope, it is important and necessary to use some other tools such as SEM to study the topography and interface of nanometer range thin films. A high energy electron beam is incident on the samples and interact the surface atoms. The secondary electrons and backscattered electrons, etc, are detected by the

detector and converted into high resolution image of sample surface. The magnification of SEM can be reached as high as 100k×.

Nanolab has a conventional SEM system from International Science Instruments. The maximum magnification can be ~30k×. Fig 3.9 shows a SEM image on the surface and cross section of GaN:Eu thin films grown on Si substrate. The surface is smooth and clean. 2-dimensional column growth was clearly seen in the picture. The thickness of thin films was estimated as ~0.6μm.

(6) Hall Effect Measurement

The conductivity of GaN thin films was measured by Hall effect measurement. When the current is flowed through the semiconductor layer in a magnetic field, the electrons or holes experience the Lorentz force in a direction perpendicular to the magnetic field and current. The movement of the electrons created a voltage, called Hall effect voltage V_H, given by the following formula: $V_H = \frac{-IB}{dne}$, where I is the current flow, B is magnetic flux density, d is thickness of conductive semiconductor, n is the carrier concentration and e is electron charge. The sign of Hall effect voltage decides if the conductivity type is p-type (holes) or n-type (electrons). The carrier concentration and the mobility can be calculated.

A MMR Hall effect measurement system is used to measure the conductivity of GaN thin films in Nanolab. Undoped GaN thin films are usually n-type conductive with the electron concentration ~10^{17}/cm^3. Si doped n-type GaN thin films can reach the electron concentration up to ~10^{20}/cm^3 with the electron mobility ~20cm^2/V·s.

(7) Four Point Probe Measurement

Four point probe measurement was also used to check the sheet resistance and resistivity of thin films. A fixed current was flowed through the film through two outer probes and the

voltage was measured between two inner probes. If the space between the probes is much smaller than the sample size, but much larger than the thin film thickness, the resistivity and sheet resistance of the thin film can be calculated by $\rho = (\pi t/\ln 2)V/I$ and $R_s = \rho/t = 4.53V/I$.

3.3. Growth Process of GaN Thin Films

Growth of GaN and other III-nitrides by MBE technique in Nanolab includes the following steps:

(1) Substrates cleaning and outgassing

Sapphire is the most common used substrates for undoped GaN growth because of large availability, low cost and stable thermal properties. The crystal orientations of *c*-plane (0001) sapphire and GaN are parallel, while the unit cell of GaN rotated by 30º about the *c* axis from sapphire. However, the lattice constant of sapphire is 4.578Å, so there is big lattice mismatch from wurtzite GaN (3.189Å) and AlN (3.11Å). *6H*-SiC are also extensively used for III-nitride growth because of closer lattice constant (3.073Å), resulting much less lattice mismatch (1~4%). Si substrates are also attractive to nitride growth because of easy integration with Si photonics and microelectronics.

Most of GaN thin films were grown on Si(111) and sapphire wafers in Nanolab and further electrical device were fabricated on these samples. Some GaN templates were also used for the growth, including GaN grown on sapphire from TDI corporation, AlGaN/AlN grown on p-Si(111) from Nitronex company.

The substrates were wet chemically cleaned before loading in the MBE system. A standard RCA clean procedure was used for Si substrates cleaning. Sapphire wafers were

cleaned by a mixture of H_2SO_4 and H_3PO_4, while GaN templates were cleaned by a mixture[2] of H_2SO_4 and H_2O_2. After wet cleaning, the substrates were loaded in loadlock and outgassed for a few hours at ~300ºC to heat out the water vapor. Then the substrates were transferred to growth chamber and stayed at 500ºC under ultra high vacuum. Every time just before the growth, the substrates were degassed at 850ºC for 10mins.

(2) Surface nitridation

The sapphire substrates were generally exposed only in the nitrogen plasma at high temperature prior to the nitride growth, which is so called “nitridation” process. It is reported[3] that nitrogen atoms would adsorbed on the surface and a very thin AlN_x relax layer would be formed. Such AlN relax layer minimized the lattice mismatch and promote GaN nucleation. A typical nitridation process in Nanolab is ~10mins at substrate temperature of 850ºC. However, no nitridation process was performed on Si substrates. Instead, several Al atomic layers (~10secs deposition) were deposited on Si wafers, followed by ~10sec nitridation to form AlN layer. Although it was reported[4] that SiN_x layer could improve GaN thin film growth quality, the nitridation on Si wafers didn’t help but hurt on GaN quality in our lab.

(3) Buffer Layer

Buffer layer has been the key to grow high quality GaN thin films because of large lattice mismatch between substrates and GaN. Since Amano and Akasaki introduced a “two-step growth method”[5] in MOVPE system, a low temperature buffer layer was widely used in the growth of GaN and other III-nitrides. Such buffer layer can form the nucleation of AlN/GaN and accommodate the relaxation of misfit dislocations caused by lattice mismatch.

In Nanolab, an AlN or GaN buffer layer was usually grown at 500ºC for ~2-5mins, having the thickness of ~20-50nm. However, GaN was not used for buffer layer on Si substrates because of Si migration and formation of $SiGaN_x$ layer. A low temperature AlN buffer layer followed by a high temperature AlN buffer layer was grown to prevent this Si migration problem.

(4) Main Layer

After buffer layer growth, undoped or doped GaN thin films were grown at high temperature. The quality of GaN thin films was affected by many factors, such as Ga and Al cell temperature, nitrogen plasma, dopants cell temperature and growth temperature. The optimization of the growth condition is necessary and important to the properties of GaN thin films and RE ions luminescence. It will be discussed in Chapter 4.

3.4. Si doped N-type GaN Growth

To fabricate electroluminescent devices, it is necessary to grow conductively doped GaN thin films. Si doped GaN thin films were grown on sapphire substrates by MBE system and growth condition was optimized. The electrical properties such electron mobility and carrier concentration were investigated by Hall Effect measurement.

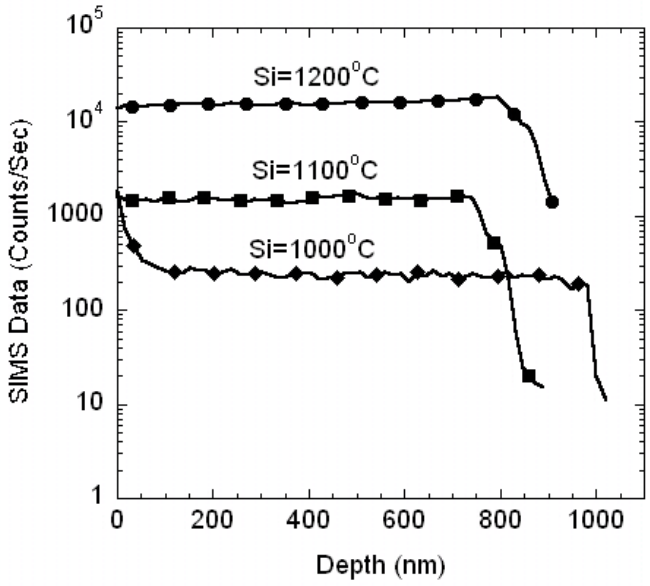

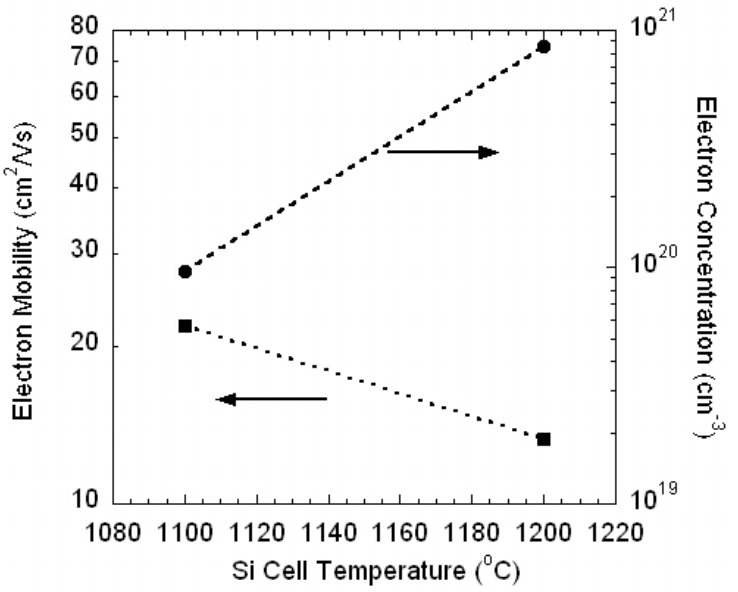

Fig 3.10 (a) Si doping profile in GaN thin films measured by SIMS;

(b)Electron concentration and mobility of GaN:Si thin films vs Si temperature.

Different Si concentration doped GaN thin films were grown on sapphire wafers. Si doping profile by SIMS measurement is plotted in Fig 3.10a. The growth temperature and Ga cell temperature were kept 800ºC and 885ºC (III/V≥1). As Si temperature increased, more Si atoms were incorporated into GaN thin films and the Si concentration increased. The results from Hall effect measurements are plotted in Fig 3.10b. The electron concentration increased with Si concentration increasing, while the electron mobility decreased.

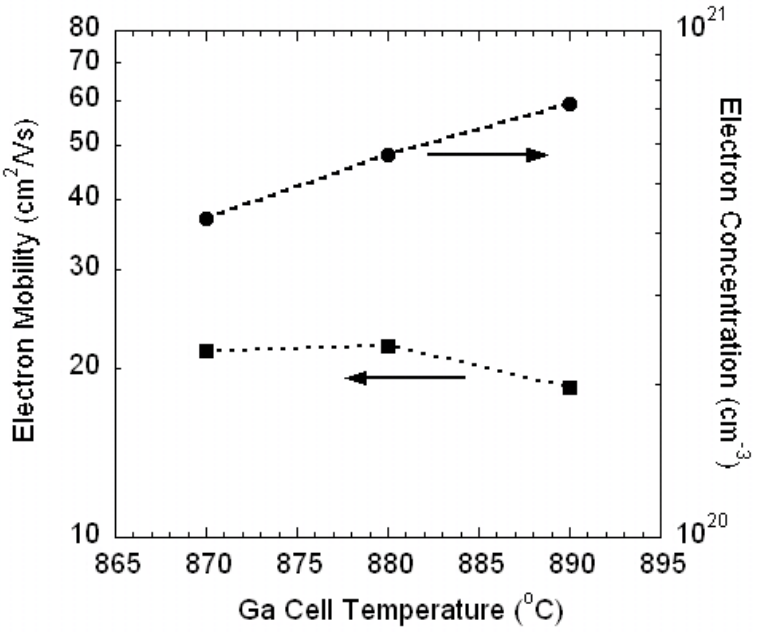

Fig 3.11 Electron concentration and mobility of GaN:Si thin films vs Ga temperature.

The effect of Ga cell temperature on the conductivity of GaN:Si thin films was shown in Fig. 3.11. As seen from the figure, high Ga cell temperature will enhance the electron concentration, but the mobility decreased a little. It was thought that most of Si atoms would replace Ga sites in the lattice and the incorporation of Ga and Si atoms is competitive so that high Ga cell temperature possibly caused Si doping concentration decrease a little. However, the increase of electron concentration could be explained by the improved ionization efficiency, enhanced by better thin film quality grown on higher III/V ratio condition.

3.5. Mg Doped P-type GaN Growth

P-type GaN growth is always difficult because of large background electrons carriers in undoped GaN thin films and high activation energy of acceptors. So far Mg is the most

promising acceptor for GaN, whose activation energy is ~160meV. P-type GaN:Mg thin film was sucessfully grown by MOCVD[6] with postgrowth annealing and MBE technique[7]. The hole concentration is up to $10^{18}/cm^3$ but the hole mobility can only be a few cm^2/Vs. High p-type conductivity is difficult to obtain due to high ionization voltage and self compensation effect[8].

Mg doped p-type GaN thin films were also grown on sapphire substrates by MBE technique in Nanolab. The effect of Mg and Ga cell temperature and growth temperature were studied. The results from SIMS measurements were shown in Fig. 3.12. The Mg doping concentration increases with Mg cell temperature, but decreases with Ga cell temperature and growth temperature. Fig 3.13 shows PL measurement results from GaN:Mg samples. The broad PL peak around ~430nm is from Mg acceptor energy levels in GaN bandgap. However, all Mg doped GaN thin films are high resistive, which shows that most of Mg atoms in GaN lattice are not ionized so that the hole concentration is very low. It is pointed out[9] that the polarity of surface (Ga-polar growth) is the key to grow p-type conductive GaN:Mg.

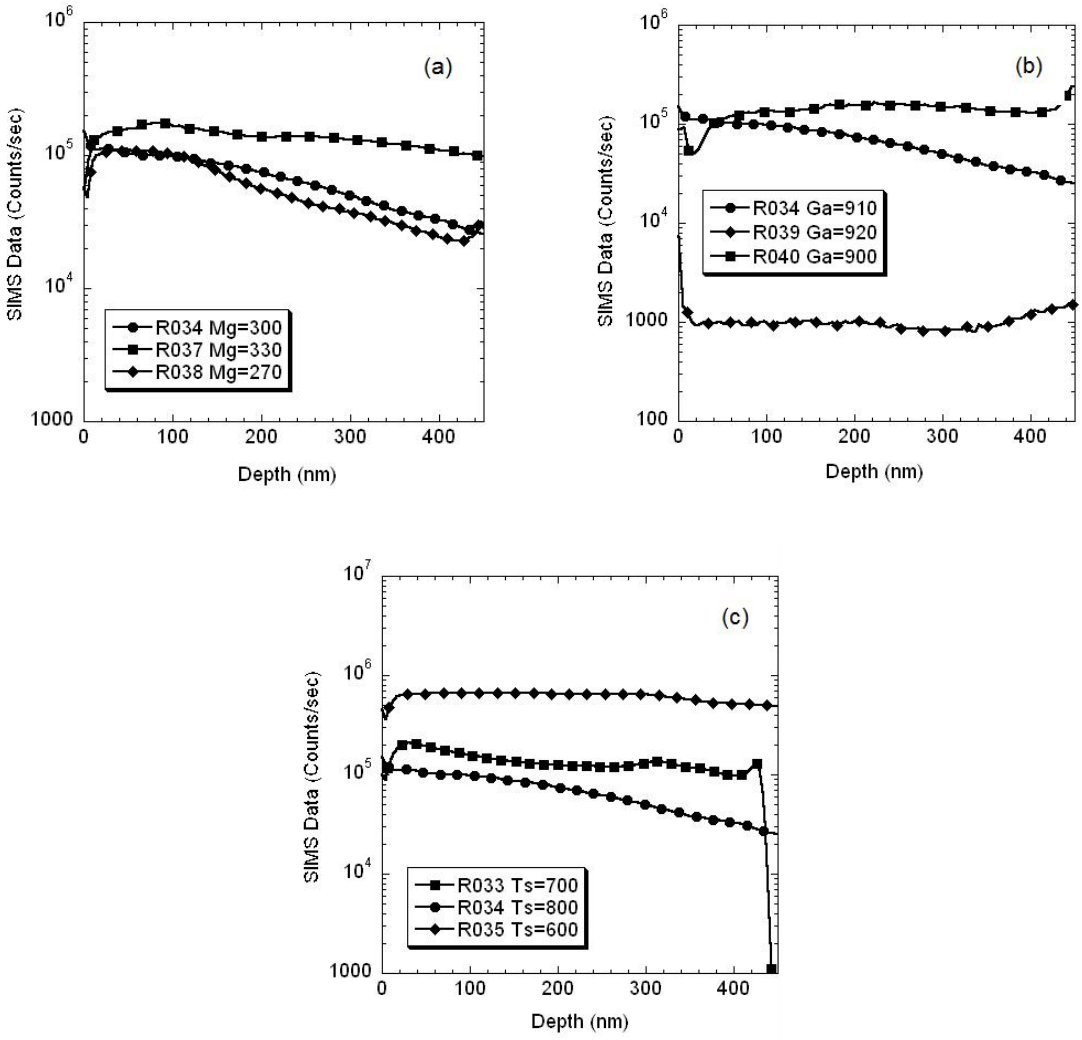

Fig 3.12 Mg doping profile in GaN thin films

with different (a) Mg temperature, (b) Ga temperature and (c) growth temperature.

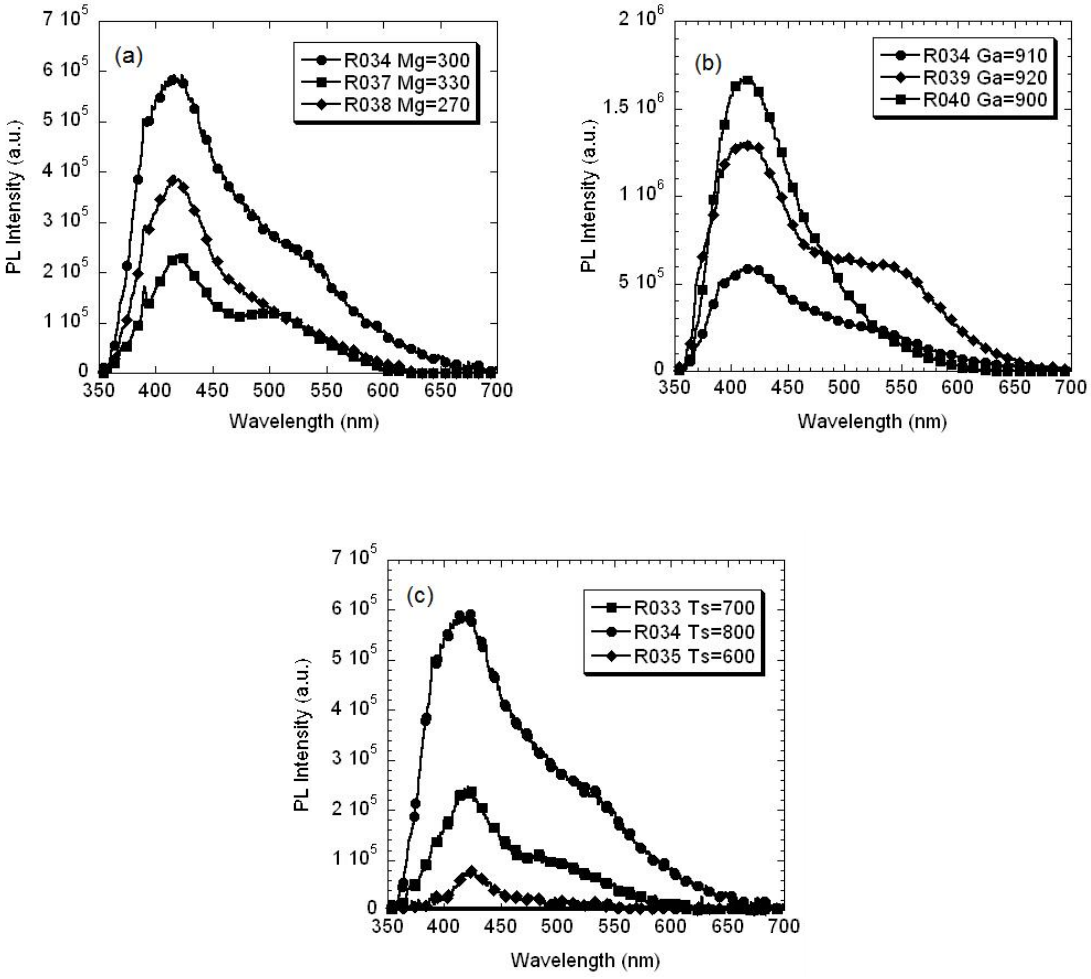

Fig 3.13 PL spectra from GaN:Mg thin films

with different (a) Mg temperature, (b) Ga temperature and (c) growth temperature.

References

[1] L. Dong-Seon, "Fabrication ...." in *Electrical & Computer Engineering and Computer Science*. vol. PhD Cincinnati: University of Cincinnati, 2001.

[2] M. Francisco, L. Zhi, S. Yun, P. Pianetta, W. E. Spicer, and R. F. W. Pease, "Simple method for cleaning gallium nitride (0001)," *J. Vac. Sci. Technol. A*, vol. 20, pp. 1784-1786, 2002.

[3] N. Grandjean, J. Massies, and M. Leroux, "Nitridation of sapphire. Effect on the optical properties of GaN epitaxial overlayers," *Appl. Phys. Lett.*, vol. 69, pp. 2071-2073, 1996.

[4] T. S. Ko, T. C. Wang, H. M. Huang, J. R. Chen, H. G. Chen, C. P. Chu, T. C. Lu, H. C. Kuo, and S. C. Wang, "Characteristics of a-plane GaN with the SiN_x insertion layer grown by metal-organic chemical vapor deposition," *J. Cry. Growth*, 2008.

[5] H. Amano, N. Sawaki, I. Akasaki, and Y. Toyoda, "Metalorganic vapor phase epitaxial growth of a high quality GaN film using an AlN buffer layer," *Appl. Phys. Lett.*, vol. 48, p. 353, 1986.

[6] S. Nakamura, T. Mukai, M. Senoh, and N. Iwasa, "Thermal annealing effects on p-type Mg-doped GaN films," *Jpn. J. Appl. Phy.*, vol. 31, pp. L139-L142, 1992.

[7] A. Bhattacharyya, W. Li, J. Cabalu, T. D. Moustakas, D. J. Smith, and R. L. Hervig, "Efficient p-type doping of GaN films by plasma-assisted molecular beam epitaxy," *Appl. Phys. Lett.*, vol. 85, p. 4956, 2004.

[8] H. Obloh, K. H. Bachem, U. Kaufmann, M. Kunzer, M. Maier, A. Ramakrishnan, and P. Schlotter, "Self-compensation in Mg doped p-type GaN grown by MOCVD," *J. Cry. Grow.*, vol. 195, pp. 270-273, 1998.

[9] L. K. Li, M. J. Jurkovic, W. I. Wang, J. M. Van Hove, and P. P. Chow, "Surface polarity dependence of Mg doping in GaN grown by molecular-beam epitaxy," *Appl. Phys. Lett.*, vol. 76, pp. 1740-1742, 2000.

4. Optimization Growth of Eu Doped GaN

Rare earth (RE) elements such as Eu and Er were *in situ* doped in GaN thin film by MBE technique. Eu^{3+} red (~622nm) and Er^{3+} Green (~537nm & 558nm) and IR (~1540nm) emissions were observed from all GaN:RE thin films. However, the RE^{3+} ions luminescence intensity and efficiency are highly dependent on GaN thin film growth conditions[1-3]. In order to get the strongest luminescence from RE^{3+} ions, it is necessary and important to optimize the growth of GaN:RE thin films.

In this chapter I studied the effect of growth conditions on Eu^{3+} luminescence intensity and efficiency from GaN thin films. All Eu doped GaN thin films were grown on C(0001) sapphire substrates by Riber 32 MBE system. The sapphire substrates were firstly nitridated in nitrogen plasma at 850ºC for 10mins prior to the growth. A 20nm GaN buffer layer was grown at 500ºC, followed by Eu doped GaN layer growth for 1hr. The growth conditions of Eu doped GaN layers were adjusted to get the strongest Eu^{3+} red luminescence. It was found that GaN thin film quality and Eu atomic concentration have great effect on Eu^{3+} PL emissions. Other factors such as the substrate and nitride hosts were also discussed.

4.1. Effect of III/V Ratio

Since Ga and N are introduced independently in MBE growth, III/V (Ga/N) ratio plays an important role for the growth quality. In RF plasma assisted SSMBE system, the N_2 plasma typically consists of ~5% N atoms and ~95% N_2 molecules with a base pressure of ~10^{-5}Torr. Because the plasma is related to the gas flow, RF power and base pressure, it is not easy to precisely control N flux. On the other hand, Ga flux can be measured as beam

equivalent pressure (BEP) by manipulator ion gauge and is exponentially proportional to Ga cell temperature, shown in Fig. 4.1. Therefore, we varied Ga cell temperature to get different III/V ratio growth condition.

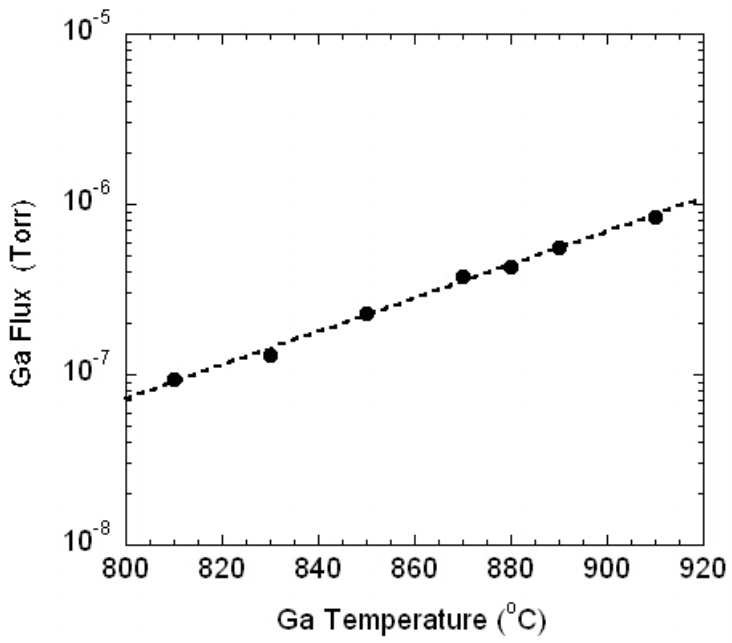

Fig 4.1 Ga flux (BEP) measured at different Ga cell temperature.

A set of Eu doped GaN samples were grown on sapphire substrates with different III/V ratio condition. N_2 gas was introduced at a flat flow rate of 2.2sccm and the plasma was generated under 400W RF power in the chamber with the base pressure of ~5.5×10^{-5}Torr. The growth temperature was kept at 800ºC and Eu cell temperature was kept at 450ºC. Ga cell temperature was varied from 810ºC to 910ºC with a step of 20ºC, corresponding to Ga flux from 0.9×10^{-7}Torr to 8.4×10^{-7}Torr. The growth rate of GaN:Eu thin films is plotted versus Ga flux and Ga cell temperature in Fig. 4.2. Initially the growth rate increases monotonically with Ga flux, but after ~$(3.5\text{-}4.0)\times10^{-7}$Torr it keeps constant at ~500nm/hr.

It is clearly shown that the growth rate on the left side is limited by Ga flux. When Ga flux increased to a level, the growth rate is saturated due to the limitation of N flux. The shaded column is considered as the stoichiometric growth condition, where III/V ratio equals ~1.0.

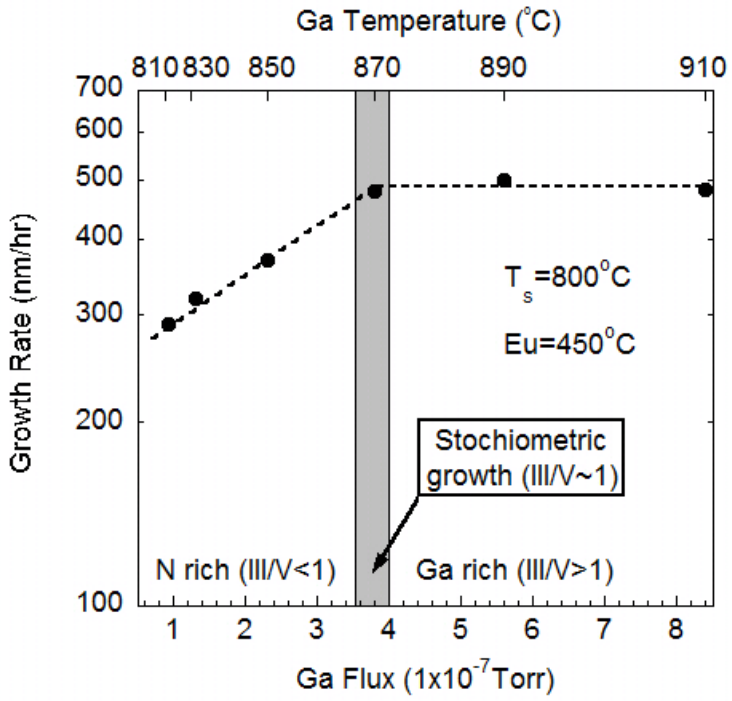

Fig 4.2 Growth rate of GaN:Eu thin films at different III/V ratio condition.

The crystallographic quality of GaN:Eu thin films was checked by XRD measurements and the results are plotted in Fig. 4.3. The shaded column acts as a very clear border between “good” and “bad” quality of GaN:Eu thin films. Apparently high quality GaN thin films were grown under III/V≧1 (Ga rich) growth condition.

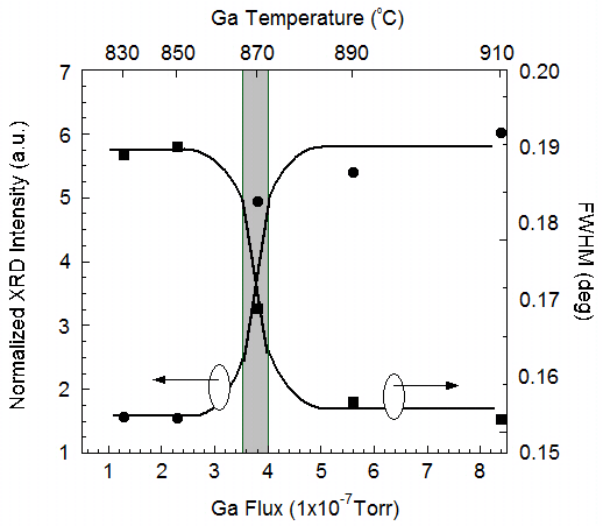

Fig 4.3 XRD measurements on GaN:Eu thin films grown at different III/V ratio.

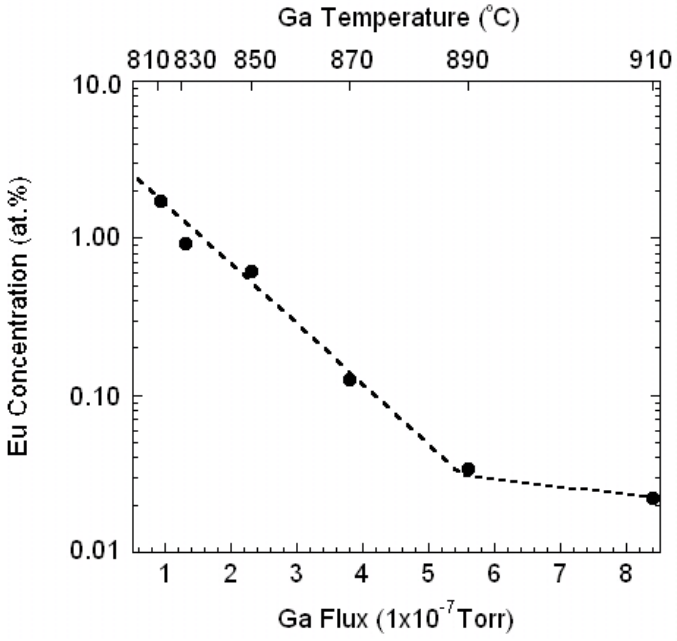

Fig 4.4 Eu atomic concentration in GaN:Eu thin films grown at different III/V ratio.

Eu doping profile was measured by SIMS system and the Eu atomic concentrations were calculated and plotted in Fig. 4.4. With Ga flux increasing, the Eu atomic concentration decreased from ~2.0 at.% down to ~0.02 at.%. It is believed that most of Eu^{3+} ions were incorporated in Ga^{3+} subsitutional sites during the growth. At lower Ga flux, a large numbers of Eu atoms could be incorporated due to the lower growth rate of GaN:Eu thin films. At higher Ga flux, the site competition between Ga and Eu atoms decreased the Eu concentration.

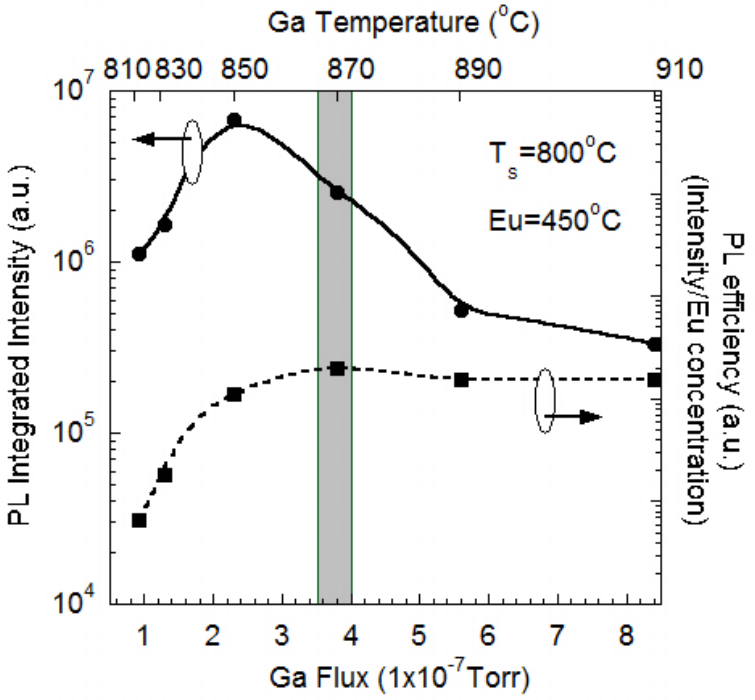

Fig 4.5 Eu^{3+} PL intensity and efficiency at different III/V ratio condition.

Eu^{3+} luminescence was investigated by "above-bandgap" PL measurement. In order to study the effect of III/V ratio, the PL intensity was integrated over the main peak (~622nm) and plotted as the solid curve in Fig. 4.5. The strongest PL emission are from "bad" quality

GaN:Eu thin films under III/V<1 region (slightly N-rich condition). Since Eu atomic concentration in GaN thin films decreased with Ga flux (shown in Fig. 4.4), it would be very interesting to calculate the Eu^{3+} PL efficiency (normalize raw PL intensity by Eu atomic concentration) and the results are plotted as the dashed curve in Fig. 4.5. The PL efficiency increases with Ga flux from N rich condition to the stoichiometric condition and becomes almost constant in III/V>1 region. We can draw the conclusion that the strongest Eu^{3+} PL occurs at slightly N rich condition (III/V<1), where GaN thin film quality is not optimum; but good quality of GaN:Eu grown under Ga rich and stoichimetric condition (III/V≥1) has better emission efficiency.

4.2. Optimization of Eu doping concentration

It is well known that RE luminescence has concentration quenching effect[4] in the host, that is, energy migration or cross relaxation process occurs between two neighboring RE ions, resulting in the increase of nonradiative relaxation. Therefore, it is important to optimize Eu doping concentration. Since both Eu flux and Ga flux mutually affected the Eu incorporation, three sets of samples were grown with different Eu cell temperature under different III/V ratio condition, including slightly N rich condition (III/V<1), stochiometric condition (III/V~1) and slightly Ga rich condition (III/V>1). Growth temperature was kept at 800ºC and nitrogen gas flow was kept 2.2sccm. Eu cell temperature was varied from 430ºC to 490ºC for each set.

Eu atomic concentration of all samples was calculated based on SIMS measurements and the results are plotted in Fig. 4.6. Clearly Eu concentration increases almost exponentially with Eu cell temperature for all three sets, while higher Ga flux results in lower Eu

incorporation in GaN thin films. XRD measurement results are consistent with the above results, as III/V≥1 ratio produces high quality GaN:Eu thin films.

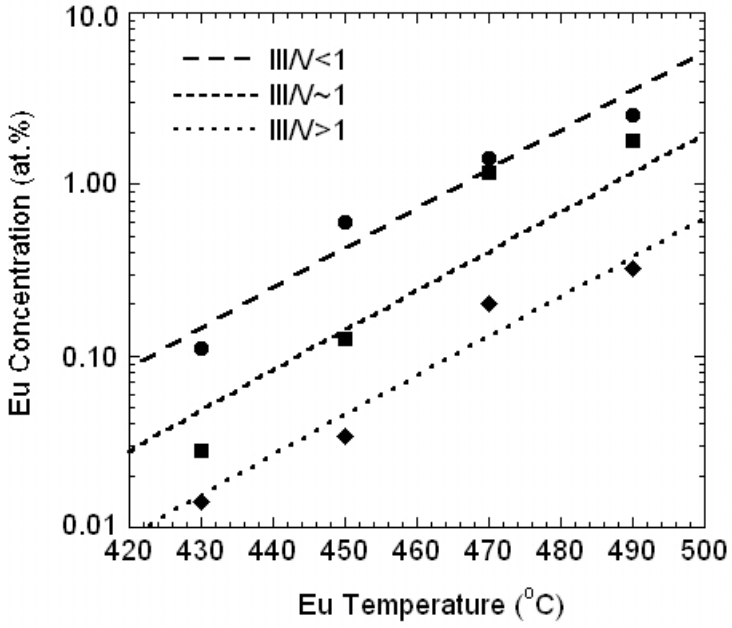

Fig 4.6 Eu atomic concentration in GaN:Eu thin films grown with different Eu temperature.

PL spectra were acquired by the spectrometer and the integrated PL intensity versus Eu cell temperature and Eu atomic concentration is plotted in Fig. 4.7. It clearly shows that the strongest PL intensity occurs at different Eu concentration for different III/V ratio condition. We can divide the Eu atomic concentration in four ranges and list them in Table 4.1. For Eu atomic concentration below ~0.034 at.%, Eu^{3+} PL intensity is very low. When Eu concentration is in the range of ~(0.034-0.2) at.%, GaN:Eu thin films grown under stoichiometric condition (III/V~1) have the highest Eu^{3+} PL intensity and good GaN:Eu quality, which is promising for the application of GaN:Eu LEDs and lasers. With Eu concentration increasing from ~0.2 at.% to 2.5 at.%, Eu^{3+} PL from "bad" quality of

GaN:Eu thin films have the strongest PL intensity. After Eu concentration reaches over 2.5 at.%, Eu^{3+} PL sharply decreases.

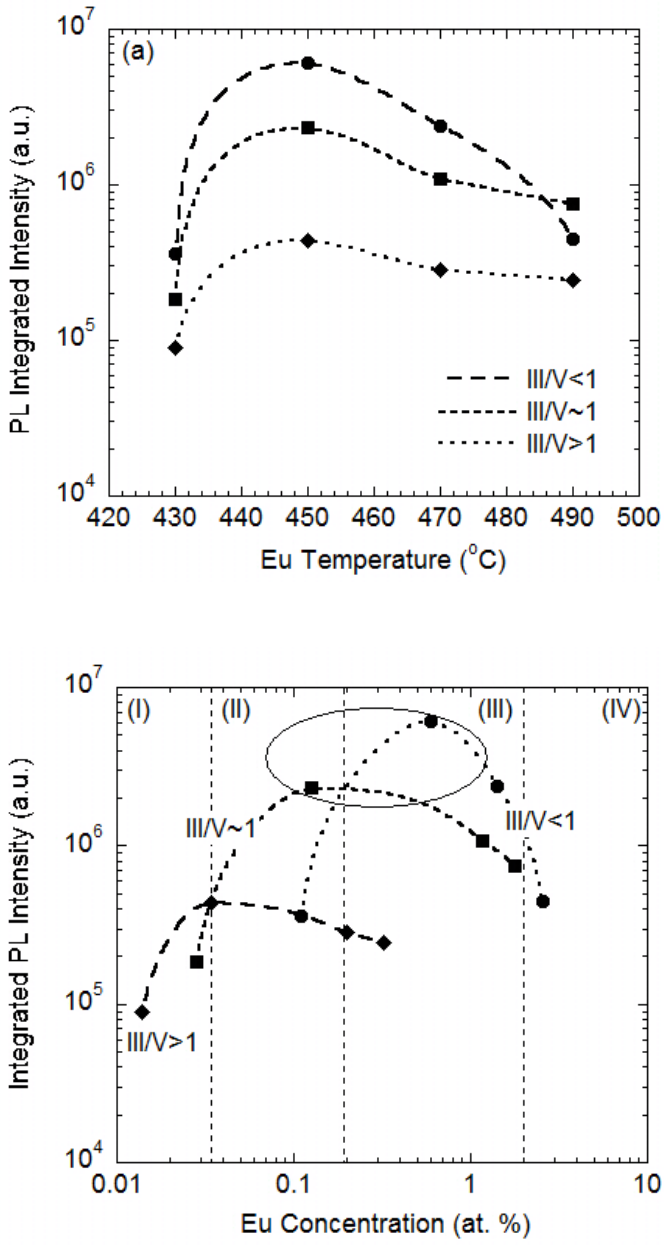

Fig 4.7 Eu^{3+} PL intensity from GaN:Eu thin films grown plotted vs (a) Eu cell temperature, (b) Eu doping concentrations.

Table 4.1 Effect of III/V ratio on Eu^{3+} PL at different Eu atomic concentration.

Eu concentration (at.%)	III/V<1	IIIV~1	III/V>1
<0.034(I)	Very low	Low	Low
0.034~0.2(II)	Low	**High**	Low
0.2~2.0(III)	**High**	Low	Very low
>2.0(IV)	Low	Low	Very low

In range I, Eu concentration is very low and high quality GaN:Eu thin films shows the highest Eu^{3+} emission intensity, probably due to higher Eu^{3+} ions emission efficiency. With Eu concentration increased to range II & III, Eu^{3+} PL intensity increased fast with increasing Eu concentration and then decreases slowly possibly due to concentration quenching. However, because of defect-mediated mechanism, Eu^{3+} PL intensity from "bad" quality of GaN:Eu grown under slightly N rich condition rapidly increased and became the strongest in the range III. After Eu concentration reached over ~2.0 at.% in range IV, sharp decrease of Eu^{3+} PL intensity happened probably due to large concentration quenching effect.

4.3. Growth Temperature Dependence

It was also found[5] that RE luminescence highly depends on the growth temperature. Therefore, a set of GaN:Eu samples were grown on sapphire at the growth temperature from 600ºC to 900ºC. N_2 plasma was generated under 400W RF power at a flow rate of 2.2 sccm. Ga and Eu cell temperature were kept constant for all samples. Since the range of

growth temperature is not very large, all growths are still around stochiometric condition, as all GaN:Eu thin films show good crystal quality seen from XRD measurements.

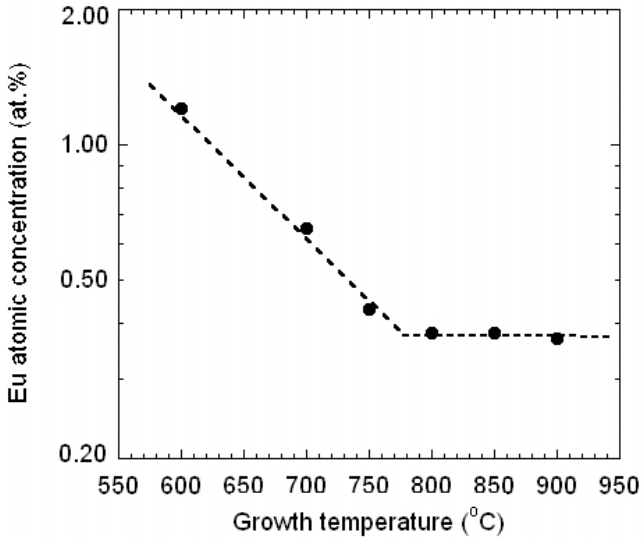

Fig 4.8 Eu atomic concentration from GaN:Eu thin films at different growth temperature.

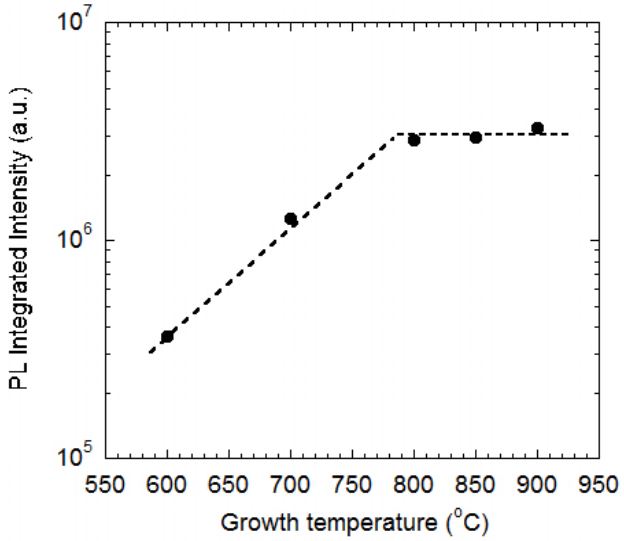

Fig 4.9 Eu^{3+} PL intensity from GaN:Eu thin films at different growth temperature.

Eu atomic concentration was calculated from SIMS measurements and shown in Fig. 4.8. The Eu concentration is ~1.2 at.% at lower growth temperature, and reached the saturation ~0.37at.% after ~750ºC. PL measurements were performed and the results are shown in Fig. 4.9. With growth temperature increasing, Eu^{3+} PL intensity increases till reaching the saturation after ~750ºC, inversely with trend of the Eu doping concentration. It is clearly that higher growth temperature enhanced Eu^{3+} PL intensity ~10×, while reducing the Eu atomic concentration ~3×. Therefore, the Eu^{3+} PL efficiency was enhanced ~30× by higher growth temperature.

4.4. Substrate Comparison

As discussed in chapter 3, device-quality GaN substrates is not yet available. High quality GaN thin films can be grown on sapphire and SiC substrates, but big lattice mismatch still exists. It is even more difficult to grow good quality of GaN thin films on Si substrates. In Nanolab, we used GaN template from Nitronex corporation, which has multiple $Al_xGa_{1-x}N$ buffer layers grown by MOCVD on p-Si(111).

Eu doped $Al_{0.04}Ga_{0.96}N$ thin films were grown on p-Si(100), p-Si(111), sapphire and Nitronex substrates at different growth temperature from 600ºC to 800ºC. Ga and Al temperature was kept 875ºC and 960ºC, so that the growth condition was slightly N rich condition. Eu temperature was kept 470ºC. The results from XRD measurements are shown in Fig 4.10. The crystal quality of AlGaN:Eu thin films grown on Nitronex substrates are much better than those grown on Si and sapphire substrates. Room temperature PL measurements were also performed and the results are shown in Fig 4.11.

Eu^{3+} PL intensities from AlGaN grown on Nitronex are stronger than those on other substrates at lower temperature, but have a big reduciton at high growth temperature.

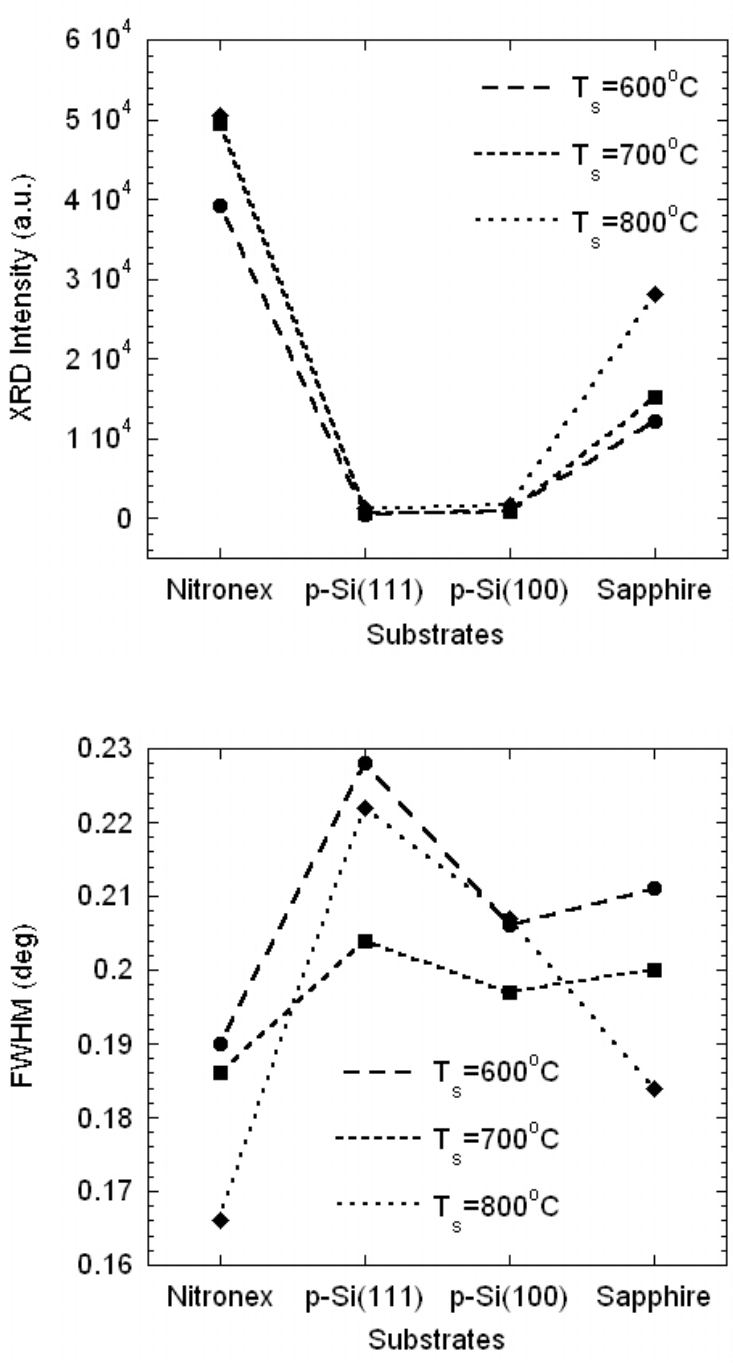

Fig 4.10 XRD measurements on AlGaN:Eu thin films grown on different substrates.

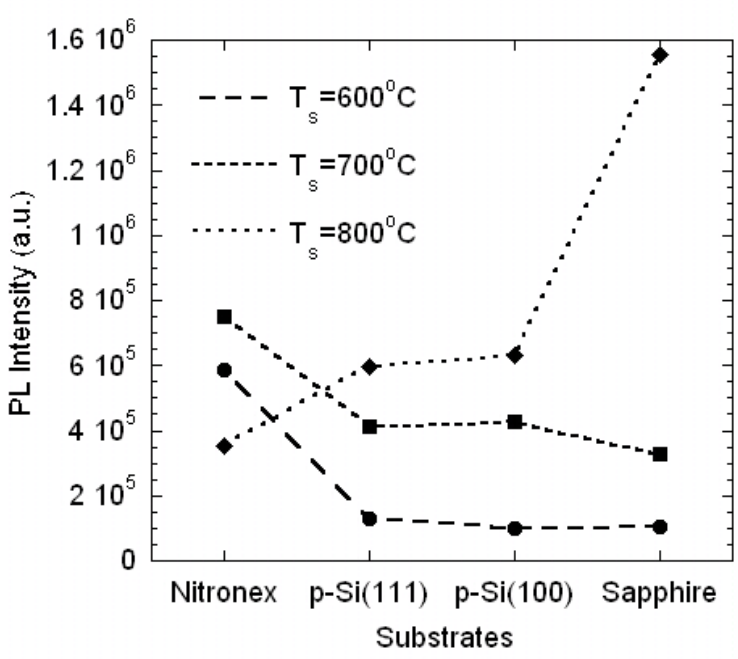

Fig 4.11 Eu^{3+} PL intensity from AlGaN:Eu thin films grown on different substrates.

4.5. Bandgap Engineering: AlGaN Host

Eu doped $Al_xGa_{1-x}N$ thin films with different Al composition were grown on p-Si(111) by MBE system. A 30nm low temperature AlN buffer layer was followed by 1 hour Eu doped $Al_xGa_{1-x}N$ layer growth at 650ºC. A very thin AlN layer was deposited as the capping layer. Ga and Al cell temperatures were relatively varied to grow different composition of $Al_xGa_{1-x}N$ thin films from 0% to 100%. Eu temperature was kept 450 ºC for all samples. The growth rate is ~0.6μm/hr.

XRD measurements were used to investigate the thin film quality and estimated the Al composition. Fig 4.12 shows the normalized XRD results of all $Al_xGa_{1-x}N$ thin films. The peaks of GaN(0002) and AlN (0002) in XRD spectra are 34.63º and 36.07º, respectively. With the Al composition increasing, the peak angle of AlGaN (0002) right-shifts within

this range. The Bragg's equation $d_{hkl} = n\lambda / 2\sin 2\theta$ can be used to calculate the main crystal c axis lattice constants. We obtained the lattice constant value of 5.178Å for GaN and 4.978Å for AlN based on our XRD results. According to the Vegard's law, the estimated Al composition can be calculated based on the following equation: $c\left(Al_x Ga_{1-x} N\right) = xc(AlN) + (1-x)c(GaN)$.

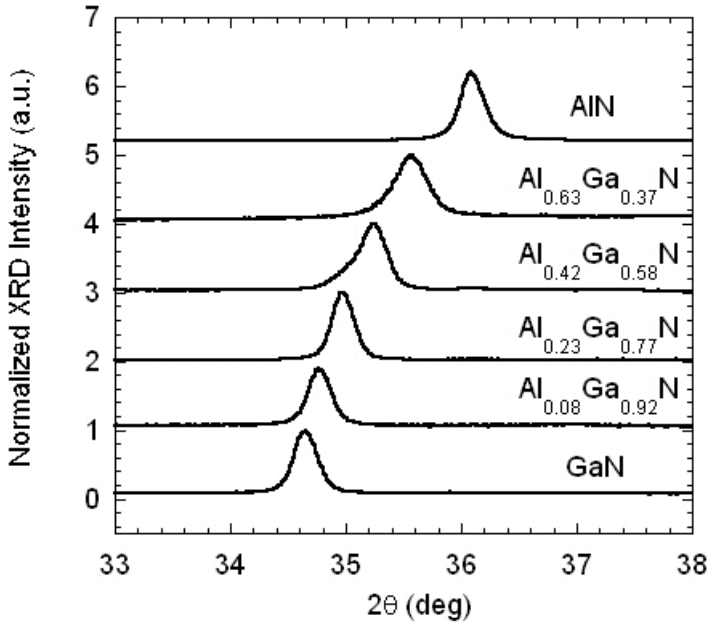

Fig 4.12 XRD spectra from AlGaN:Eu thin films with different Al composition.

Eu^{3+} PL from $Al_xGa_{1-x}N$:Eu was excited by 325nm He-Cd lasers and all thin films showed very strong red emissions. The PL intensities was found to be dependent on the Al composition, shown in Fig 4.13. The maximum PL peak occurs at x=0.2, that is $Al_{0.2}Ga_{0.8}N$. The peak wavelength of Eu^{3+} red emission also shifts from 622.4nm in GaN to 624nm in AlN. However, since the bandgap of AlN is as high as 6.2eV, "above-bandgap" PL measurements should be excited by 197nm Ti:Sapphire laser or 193nm ArF laser.

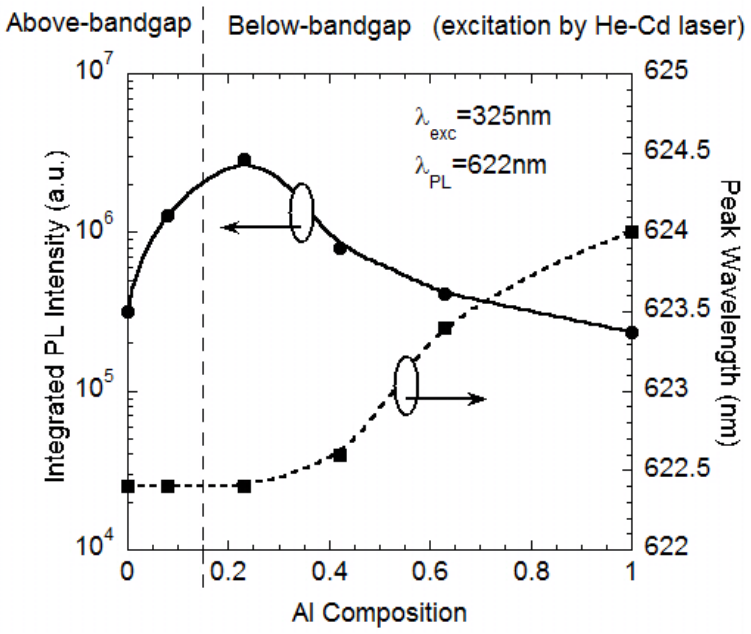

Fig 4.13 Eu^{3+} PL intensity and peak wavelength dependence on Al composition.

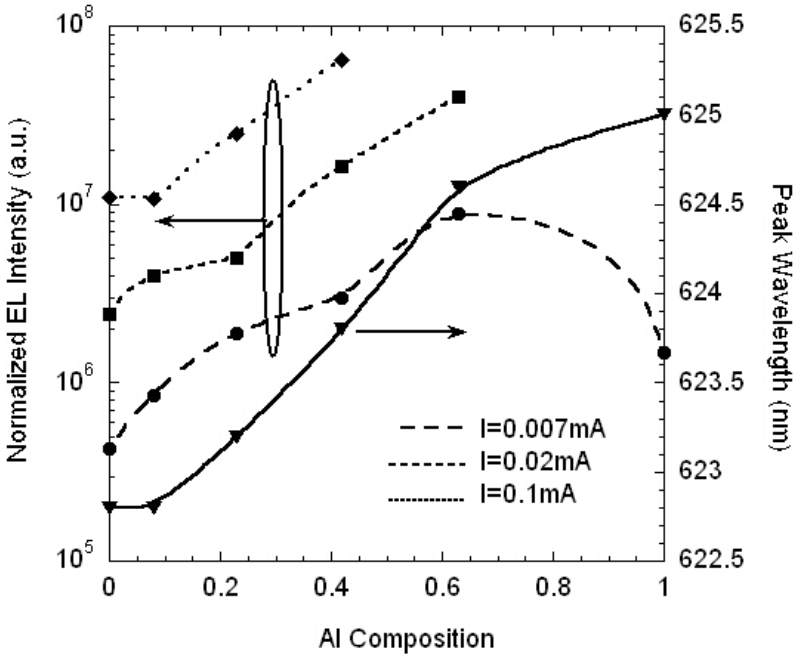

Fig 4.14 Eu^{3+} EL intensity and peak wavelength dependence on Al composition.

EL measurements were also performed on all $Al_xGa_{1-x}N$:Eu thin films. Since the resistance becomes larger and larger with Al composition increasing, the current flow under same voltage is smaller for higher Al composition. Because RE^{3+} EL emission is mainly related to the number of electrons, it is better to compare the EL brightness normalized by the current flow[6] (defined as BIV) instead of the raw brightness. The results from EL measurements are shown in Fig 4.14. The maximum EL intensity occurs during x=0.6-0.8 range. The peak wavelength also shifted from 622.8nm in GaN to 625nm in AlN, similar to the trend of PL peak.

References

[1] D. S. Lee, J. Heikenfeld, and A. J. Steckl, "Optimum Er concentration for in situ doped GaN visible and infrared luminescence," *Appl. Phys. Lett.*, vol. 79, p. 719, 2001.

[2] D. S. Lee, J. Heikenfeld, and A. J. Steckl, "Growth-temperature dependence of Er-doped GaN luminescent thin films," *Appl. Phys. Lett.*, vol. 80, p. 344, 2002.

[3] D. S. Lee and A. J. Steckl, "Ga flux dependence of Er-doped GaN luminescent thin films," *Appl. Phys. Lett.*, vol. 80, p. 728, 2002.

[4] R. Mach and G. O. Muller, "Physical Concepts of High-Field, Thin-Film Electroluminescence Devices," *physica status solidi (a)*, vol. 69, pp. 11-66, 1982.

[5] D. S. Lee, J. Heikenfeld, and A. J. Steckl, "Growth-temperature dependence of Er-doped GaN luminescent thin films," *Applied Physics Letters*, vol. 80, pp. 344-346, 2002.

[6] D. S. Lee, J. Heikenfeld, A. J. Steckl, U. Hommerich, J. T. Seo, A. Braud, and J. Zavada, "Optimum Er concentration for in situ doped GaN visible and infrared luminescence," *Appl. Phys. Lett.*, vol. 79, pp. 719-721, 2001.

5. Co-doping of Si in Rare Earth Doped GaN

5.1. Motivation of Si and Rare Earth Co-doping

The quality of GaN:RE thin films and RE doped profile were demonstrated the great effect on RE^{3+} luminescence in Chapter 4. The structural or chemical defects introduced during the growth process was found[1-3] to have an important role in the energy transfer process from the host to RE^{3+} sites. Therefore, the incorporation of co-dopants along with RE elements in the host could also mediate the energy transfer and have significant influence on RE luminescence. Several papers have reported that oxygen enhances Er^{3+} IR luminescence when co-doped in host materials such as Si[4], AlGaAs[5] and GaN[6]. The co-doping of C in GaN:Er was also reported[7] to result in an enhancement of Er^{3+} IR luminescence at a certain concentration. Er implanted into Mg-doped GaN was reported[8] to exhibit enhancement of minor IR Er^{3+} emission peaks compared to Mg-free GaN:Er. Other papers have also reported[9-11] on the enhancement of Eu luminescence with impurity co-doping in glasses.

In this chapter, we report on the strong effect on RE^{3+} luminescence of Si co-doping in GaN thin films. Si was chosen to co-doped in GaN:RE thin films because of several reasons. Firstly, most of Si atoms would replace Ga sites substitutionally like RE atoms so that there is small effect on host lattice and GaN:RE thin film quality would not be degraded too much. Secondly, as a shallow donor in GaN bandgap, Si could introduce energy level and defects below conduction band to provide more channels for energy transfer from GaN to RE^{3+} ions levels. Thirdly, Si co-doping in GaN:RE could change the electrical properties of GaN:RE thin films. More electrons could possibly increase electro-hole recombination process, resulting in RE^{3+} luminescence enhancement.

Additionally, Si is available in our MBE system and easily to *in situ* co-doped in GaN:RE thin films.

5.2. Effect of Si Co-doping in Eu Doped GaN

Si and Eu co-doped GaN thin films (GaN:Eu,Si) were *in situ* grown on c-plane (0001) sapphire wafers by MBE technique. The sapphire wafers was first cleaned by a standard wet clean procedure and then degassed at 850ºC under ~10^{-10}Torr vacuum. A N_2 gas flow rate of 2.2sccm was used in conjunction with a plasma RF power of 400W. The sapphire wafers were nitridated in N_2 flow only at 850ºC for 10min prior to growth. A 20nm low temperature GaN buffer layer was followed by 1 hour growth of Eu and Si co-doped GaN at 800ºC. The beam equivalent pressure (BEP) of Ga flux was measured as ~2.5×10^{-7}Torr, where the growth condition is lightly N rich condition (III/V ratio <1). The Eu cell temperature was maintained at 450 ºC for all samples discussed. Si cell temperatures from 950ºC to 1200 ºC were used to obtain different Si doping concentrations. The growth rate was ~0.45μm/hr. For comparison, GaN samples doped only with Eu were also grown under the same conditions.

(1) Eu and Si doping concentration

The Eu atomic concentration in GaN thin films is typically ~0.10-1.00at.%. The incorporation of Si atoms in the thin films competes with Eu atoms incorporation since both are mostly located on substitutional Ga sites. Therefore, heavy Si doping is likely to affect the Eu concentration. The doping depth profiles in GaN:(Eu, Si) and GaN:Eu films were investigated by SIMS. The estimated Eu and Si atomic concentrations based on SIMS measurements are shown in Fig 5.1 as a function of Si cell temperature.

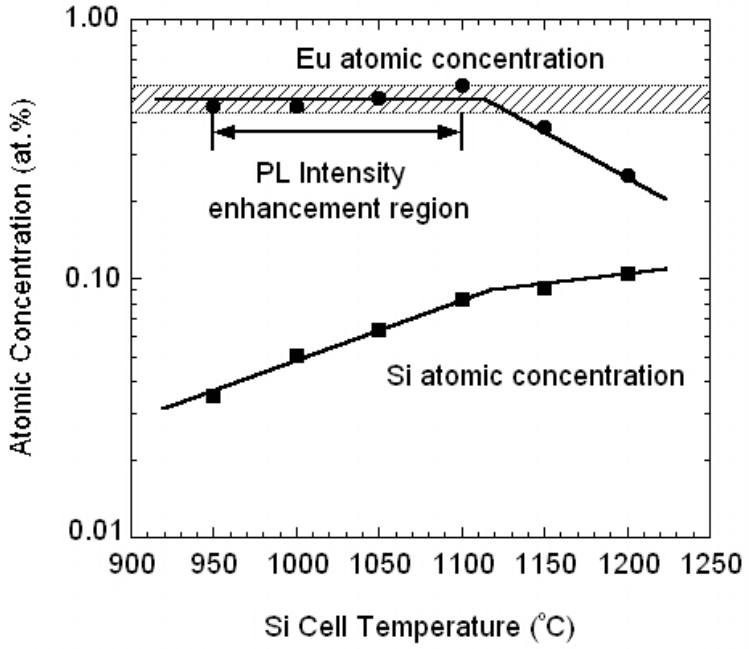

Fig 5.1 Eu and Si doping concentration dependence on Si cell temperature.

The hashed region shows the range of typical Eu concentration (~0.50at.%) from GaN:Eu thin films on sapphire substrates under the same growth condition. As seen in Fig 5.1, at low Si concentrations the Eu level in co-doped GaN thin films is constant and similar to that of Eu-only GaN thin films. As the Si cell temperature reaches levels (~1100°C) that produce Si concentrations of ~0.1at.%, the Eu concentration incorporated into the GaN film begins a steady and significant decrease, reaching almost one half of its initial value when Si cell temperature is 1200 ºC. On the other hand, the Si concentration increases monotonically with the Si cell temperature. The rate at which the Si concentration increases is reduced at approximately the same Si cell temperature (~1100°C) at which the Eu concentration begins to decrease.

(2) Enhancement of Eu^{3+} luminescence

The effect of Si co-doping on Eu^{3+} red luminescence was first studied by "above-bandgap" PL excitation, using a 325nm He-Cd UV laser. Normalized PL spectra of the co-doped GaN:(Si, Eu) thin films with different Si doping concentrations is shown in Fig 5.2, having very strong red emission at ~622nm from $^5D_0$-$^7F_2$ transitions of Eu^{3+} ions. Several weaker emission lines at ~600nm, ~663nm and ~546nm are also present. Only at the highest Si temperature (1200°C), there is a broad blue band (~420nm) possibly from the defects introduced by Si incorporation.

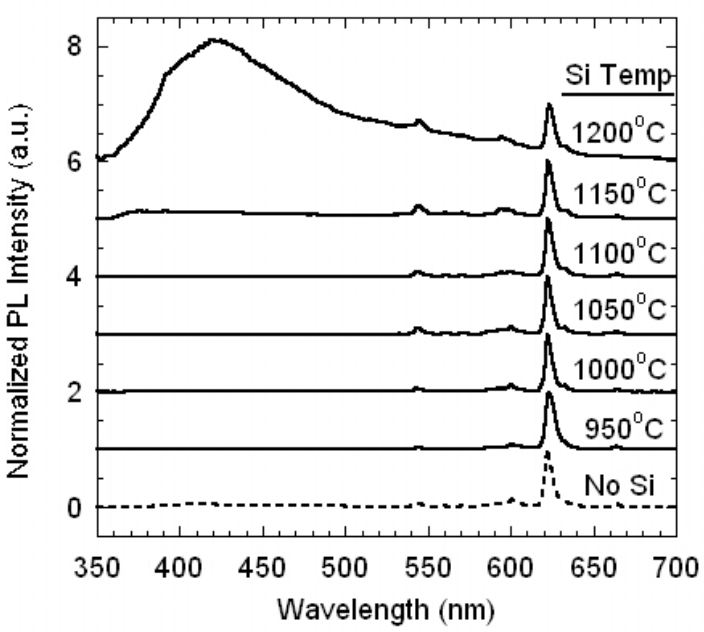

Fig 5.2 Normalized PL spectra from GaN:(Si, Eu) thin films with different Si doping.

Fig 5.3 shows the strong effect of Si co-doping on the Eu^{3+} red luminescence, where PL intensity (integrated over the ~622nm red emission range) is plotted as a function of Si concentration and corresponding cell temperature. For comparison, the PL intensity range of GaN:Eu thin films is shown as the hashed bar on the left side.

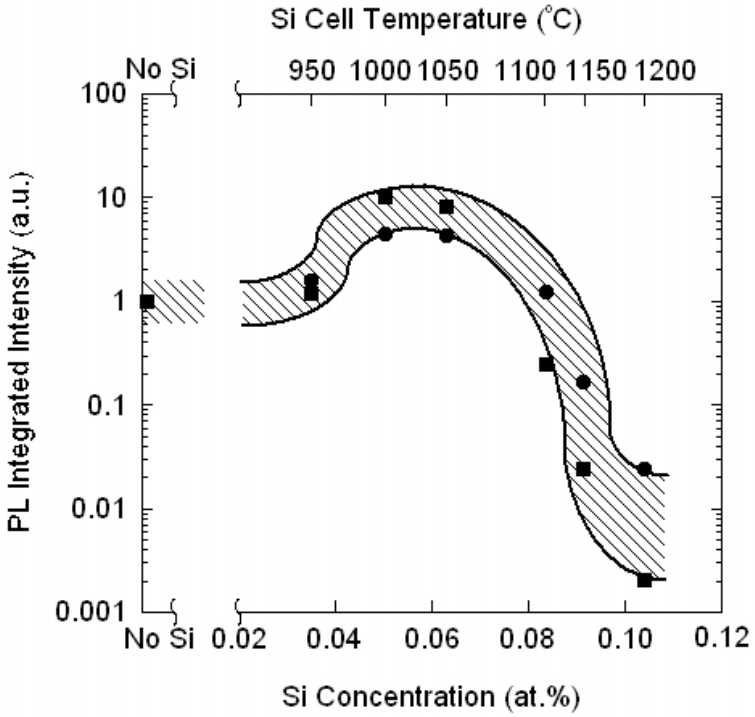

Fig 5.3 Integrated PL intensity at ~622nm as a function of Si concentration.

At sufficiently low Si concentration (~0.04at.%), the PL intensity from GaN:Eu and GaN:(Si, Eu) films are very similar. As the Si cell temperature is increased and more Si atoms are incorporated into GaN thin films, the Eu^{3+} emission intensity increases significantly. A ~5-10× PL increase was obtained for a Si concentration of ~ 0.05at.% (Si cell temperature between 1000ºC and 1050ºC). However, for Si concentrations higher than ~0.07at.%, the PL emission starts to decrease rapidly. When the Si cell temperature is ~1200ºC (resulting in a Si concentration of ~0.1at.%), the PL emission is ~1000× lower than its peak value. Clearly, the reduction in Eu emission is much stronger than the decrease of Eu concentration (~2×) over the entire Si concentration range.

In order to study more clearly the effect of Si co-doping, time resolved PL experiments were performed. PL decay transients were recorded using an optical parametric oscillator system (repetition rate: 10 Hz, pulse width: 5-10 ns) operating at 471 nm for below-gap (resonant) pumping. The fourth harmonic output of a Nd: YAG laser at 266nm was employed for above-gap pumping. Emission at ~622nm was dispersed using a 0.3m monochromator equipped with a photomultiplier tube for detection. Fig 5.4 shows PL decay transients from GaN:(Si, Eu) thin films pumped at 266nm. At moderate Si doping, the PL intensity shows a slower decay process than the PL from GaN:Eu thin films.

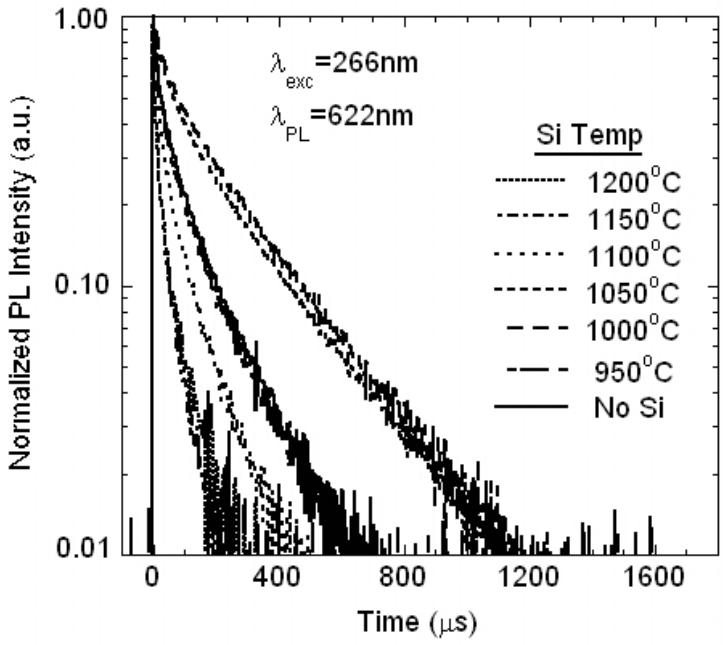

Fig 5.4 Normalized time resolved PL spectra at ~622nm pumped by 266nm laser.

PL lifetimes can be calculated by the following equation

$$\tau = \frac{\int tI(\lambda)d\lambda}{\int I(\lambda)d\lambda}, \qquad (1)$$

Fig 5.5 shows the calculated PL lifetime dependence on Si doping concentration. The trend of PL lifetime dependence on Si doping concentration is similar but not identical to that of red PL intensity shown in Fig 5.3. Insert in Fig 5.5 shows that the PL intensity does not have a simple linear dependence on the lifetime.

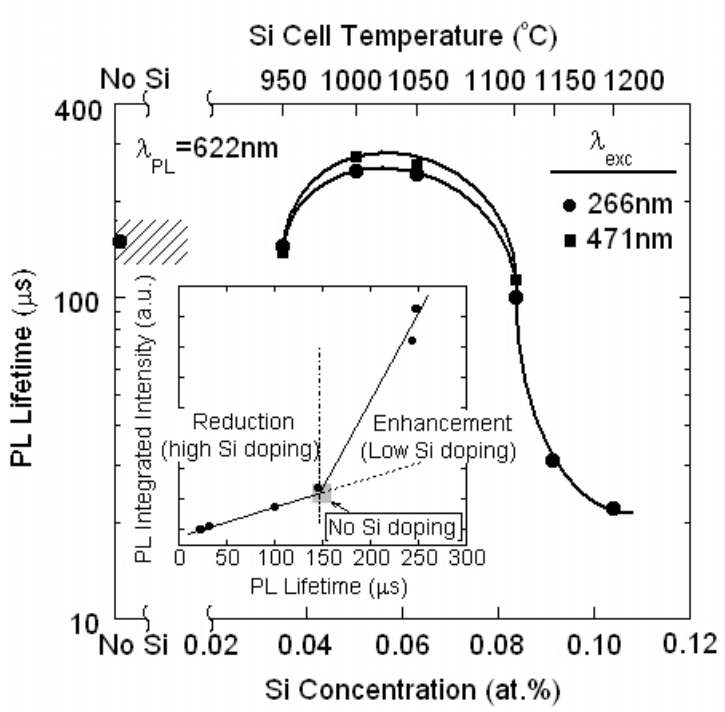

Fig 5.5 PL lifetime vs Si concentration (insert shows PL intensity vs lifetime).

PL excitation (PLE) of the luminescence at ~622nm was investigated primarily covering the $^5D_0$-$^7F_0$ transition region. The PLE spectra were recorded using the tunable laser output (~565nm-595nm) from the narrow-band OPO system (linewidth: ~0.2cm^{-1}) mentioned before, and processed using a boxcar averaging system. Fig 5.6 shows PLE spectra from GaN:(Si, Eu) co-doped thin films with different Si concentrations. Several Eu sites were inferred based on excitation peaks at 585nm, 588.3nm and 591nm in the $^5D_0$-$^7F_0$ region[12, 13]. In the moderate Si doping range, corresponding to the red emission enhancement

region, a satellite peak at 587.5nm appears next to the 588.3nm peak. This additional peak could be due to some of the Eu^{3+} ions being in displaced lattice locations. The PLE wavelength difference between the main and satellite peaks is 0.8nm. This is quite similar to the reported[14] 0.7nm difference in the PL emission from the $^5D_0$-$^7F_2$ between normal and displaced Eu sites in GaN thin films. The strong excitation peak at 571nm is probably an additional line from Eu^{3+} ions at Ga substitutional sites[12].

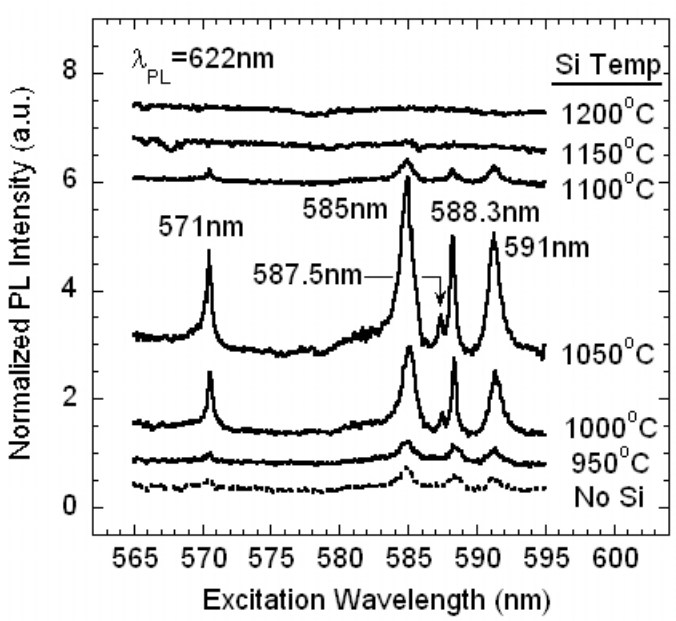

Fig 5.6 PLE spectra for $^5D_0$-$^7F_0$ region from co-doped GaN:(Si, Eu) thin films.

As seen from the PLE spectra, Eu^{3+} luminescence under resonant excitation was enhanced by Si co-doping, with the maximum enhancement occurring at a Si cell temperature ~1050°C. This trend corresponds very well to the enhancement of Eu^{3+} luminescence excited by above-bandgap pumping. Non-resonant (below bandgap) excitation did not result in any red emission for all samples.

The effect of Si co-doping on Eu^{3+} red emission for steady state excitation under small pump power can be explained by the following equations[15]:

$$I_{PL} \propto \frac{N_{Eu}^{*}}{\tau_{rad}} = \sigma_{eh}\phi N_{Eu}\frac{\tau}{\tau_{rad}}, \quad (2)$$

$$\frac{1}{\tau} = \frac{1}{\tau_{rad}} + \frac{1}{\tau_{nrad}}, \quad (3)$$

where the PL intensity is proportional to the Eu^{3+} ions concentration N_{Eu}, the lifetime τ, the excitation cross section through electron-hole recombination σ_{eh}, the carrier flux ϕ, and inversely dependent on the radiative lifetime τ_{rad}. We can draw some preliminary conclusions regarding to the mechanism responsible for the Eu^{3+} PL intensity dependence on Si concentration by considering the trend shown in the Fig 5.5 insert. High Si doping levels result in a decrease in PL lifetime (with additional non-radiative decay processes produced by defects surrounding Eu^{3+} ions such as Si-Si complexes and Si related defects). Combined with the simultaneous decrease in Eu concentration (as seen in Fig 5.1), this can certainly explain the reduction in PL intensity. It is more difficult to identify the mechanism responsible for PL enhancement. In the enhancement region, the Si doping is at "moderate" levels. The observed increase in PL lifetime (could be due to a more highly spaced Eu^{3+} distribution). However, this is not sufficient to explain the sharp increase in PL intensity in this region. Another possible factor is an increase in excitation cross-section due to the formation of Eu-Si complex sites. Moreover, the shallow energy levels introduced by moderate Si doping could provide another efficient energy transfer channel, resulting in Eu^{3+} PL emission enhancement.

(3) Change of electrical properties of GaN:Eu thin films

Undoped GaN films generally display n-type conductivity due to nitrogen vacancies. Undoped GaN thin films grown in our MBE system typically have electron concentrations of ~$10^{17}cm^{-3}$. However, Eu-doped GaN films are highly resistive. It is thought that the free electrons are trapped by deep level centers introduced by the Eu doping. On the other hand, Si is commonly used as the n-type dopant in GaN, with electron concentration from 10^{18}-$10^{20}cm^{-3}$. We have expected that the co-doping of Si in GaN:Eu thin films would affect the electrical properties. Hall effect measurement was used to obtain the resistivity and electrical concentration of co-doped GaN thin films, shown in Fig 5.7. For low Si doping, co-doped GaN thin films are still high resistive. However, with increasing Si concentration GaN:(Si, Eu) thin films became increasingly n-type conductive, reaching the electron concentrations of ~$10^{19}cm^{-3}$. By comparison (also shown in Fig 5.7), GaN thin films heavily doped with Si only (no Eu) at Si cell temperature from 1100ºC to 1200ºC have electron concentrations up to 10^{20}~$10^{21}cm^{-3}$, with electron mobility in the range of 10~20cm^2/V-s. The electron mobility of co-doped GaN thin films was significantly lower (~0.2 cm^2/V-s) than that of Si-only films. It is likely that in co-doped films many electrons produced by Si doping are trapped by deep Eu centers, resulting in the low mobility observed. These electrons could increase the hot carrier capture cross-section and provide an increased probability for the impact excitation process, which would be very useful in enhancing the efficiency of Eu^{3+} EL in devices with co-doped GaN layers.

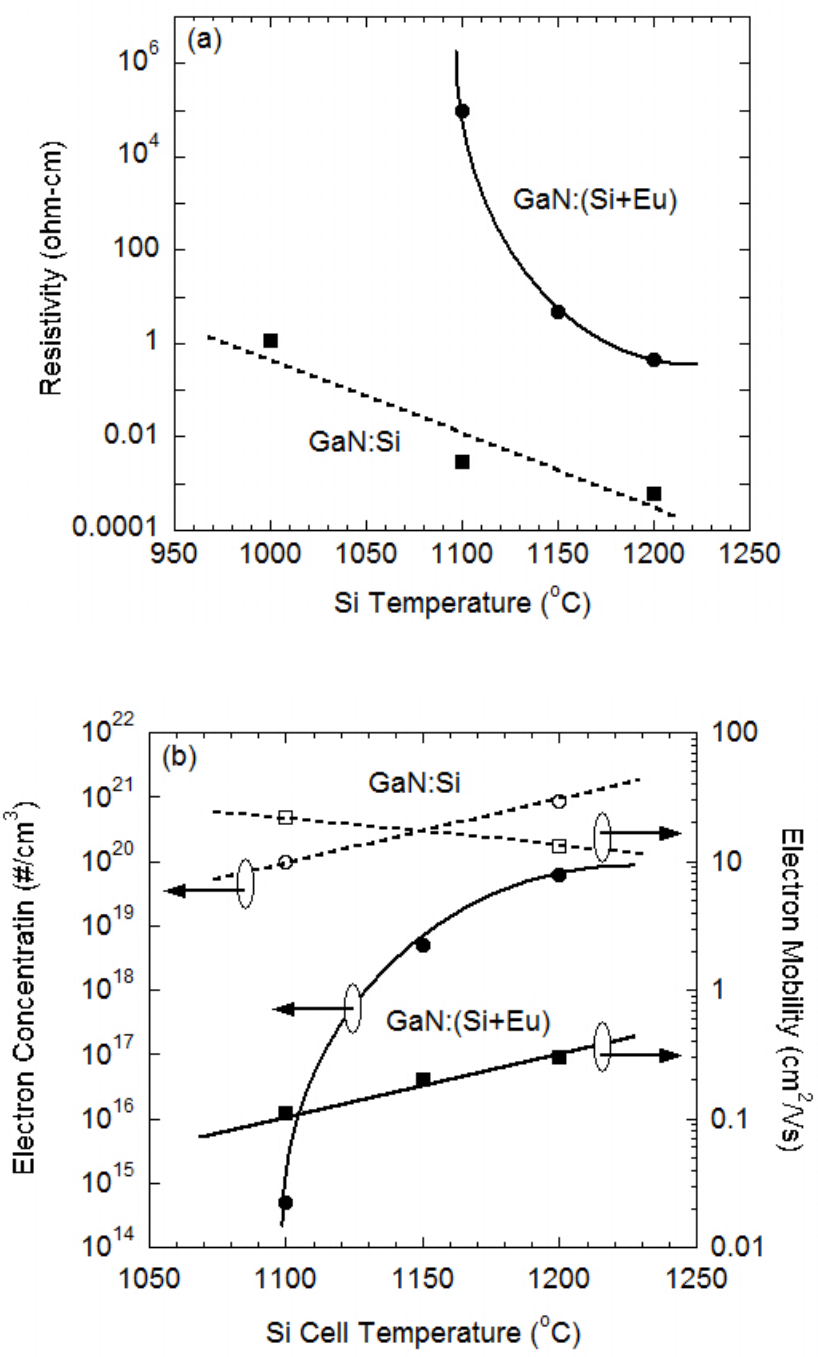

Fig 5.7 (a) Resistivity and (b) conductivity of co-doped GaN:(Si, Eu) thin films.

5.3. Effect of Si Co-doping in Er Doped GaN

Er and Si co-doped GaN thin films were also grown on sapphire substrates. The growth process is similar to that of GaN:(Eu, Si) thin films. A 20nm AlN buffer layer was followed by 1 hour growth of Er and Si co-doped GaN at 800ºC. The beam equivalent pressure (BEP) of Ga flux was measured as ~3.5×10^{-7}Torr, where the growth condition is almost stoichiometric condition (III/V~1). The Er cell temperature was maintained at 860ºC. Si cell temperatures from 1000ºC to 1150ºC were used to obtain different Si doping concentrations. GaN samples doped only with Er were also grown under the same conditions.

(1) Effect of Si co-doping on Er^{3+} luminescence

Room temperature PL measurements were performed on GaN:(Er, Si) thin films. Visible PL was excited by "above-bandgap" pumping with 325nm He-Cd laser and the spectra are shown in Fig 5.8a. With Si temperature increasing, the "yellow band" became bigger and bigger so that two green peaks from Er^{3+} ions were covered after Si temperature reaches 1150ºC. In order to study the effect of Si co-doping, the "yellow band" background was subtracted and the Er^{3+} PL intensity integrated on two green peaks are plotted versus Si temperature in Fig 5.8b. No enhancement by Si co-doping on Er^{3+} green emission was found, but the PL intensity decreases slowly with Si temperature. There is a big reduction after 1100 ºC, which is similar to the effect of high Si co-doping on Eu^{3+} red emission.

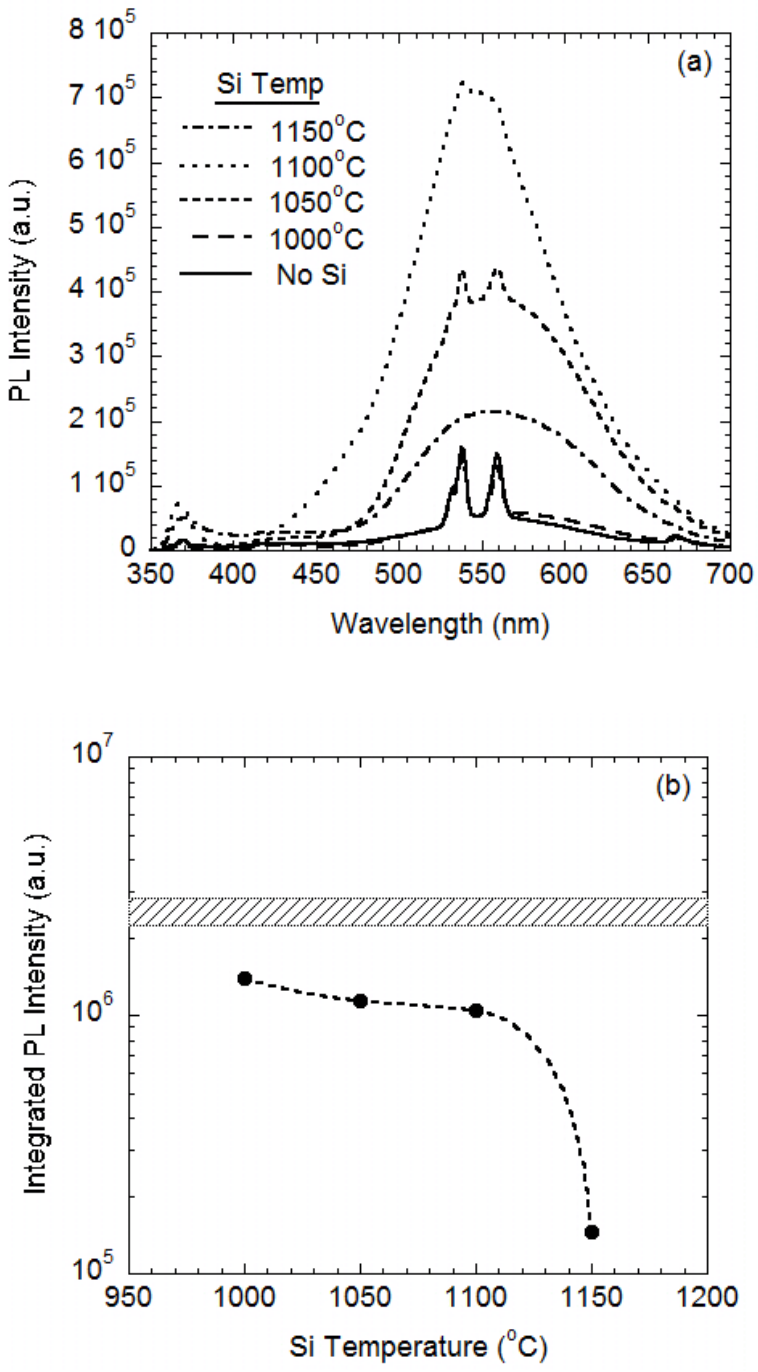

Fig 5.8 (a) Visible PL spectra from GaN:(Si, Er);(b) PL intensity vs Si temperature.

Er^{3+} ions PL emission in IR range (1.54μm) was also pumped by a 496nm Nd:YAG laser and the spectra are shown in Fig 5.9a. Similar to visible emission, the Er^{3+} IR emission intensity decreases with Si temperature increasing. PLE measurements for 1.54μm emission were also performed and the results are shown in Fig 5.9b. There is no big difference between GaN:(Er, Si) thin films. Time resolved PL measurements were also performed on 1.54μm Er^{3+} emissions by Nd:YAG laser.. Fig 5.10 shows time resolved PL spectra by 538nm resonant wavelength pumping. The estimated IR PL lifetimes are around ~1-2ms for all GaN:(Er, Si) thin films.

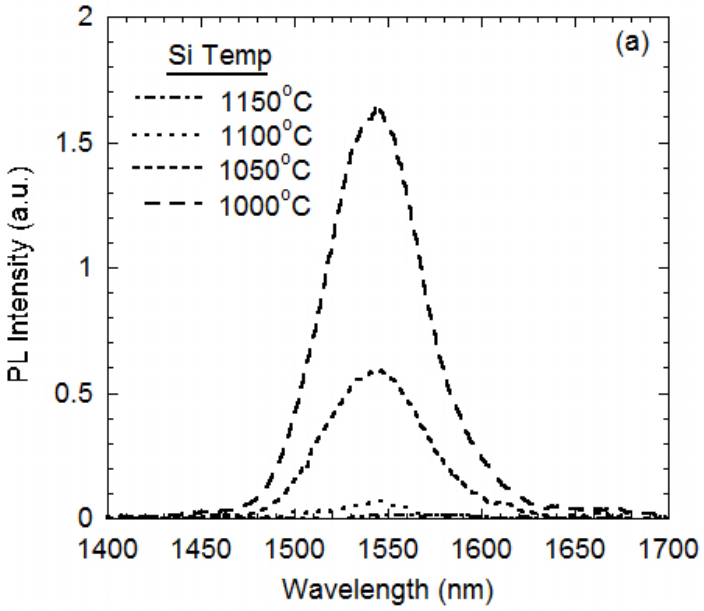

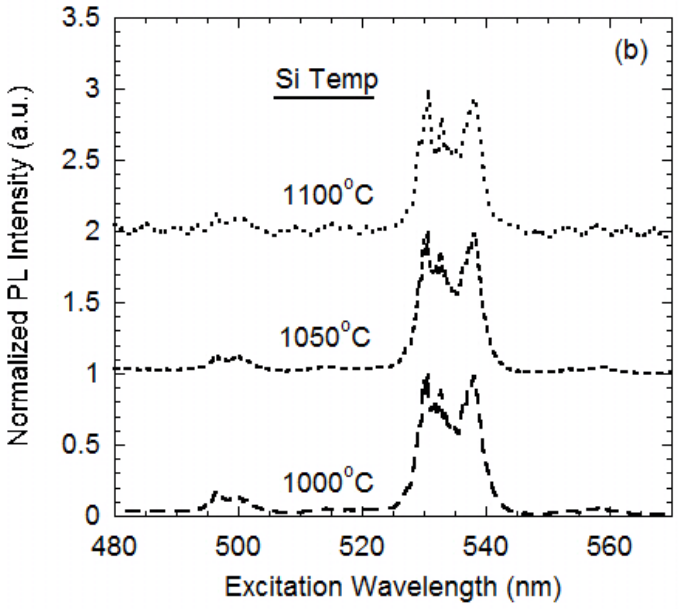

Fig 5.9 (a) IR PL spectra from GaN:(Si, Er) thin films; (b) PLE spectra for 1.54μm emission.

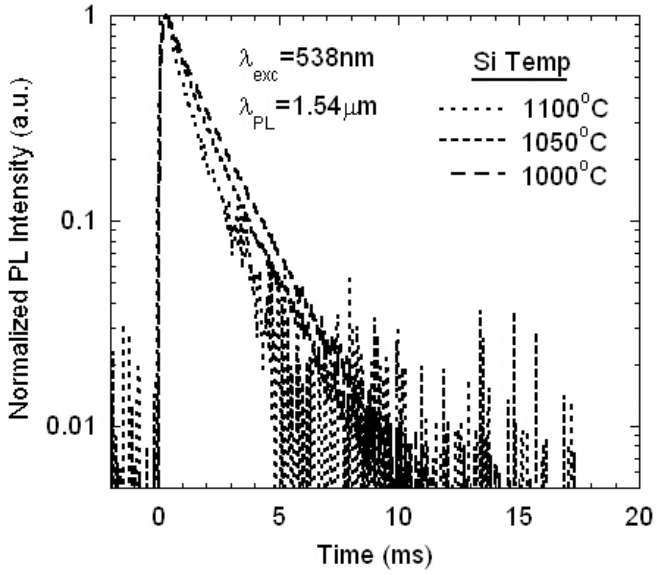

Fig 5.10 Time resolved PL spectra from GaN:(Si, Er) thin films by 538nm pumping.

(2) Change of electrical properties of GaN:Er thin films

Hall effect measurements were performed on all GaN:(Si, Er) thin films and the results were shown in Fig 5.11. Similar to GaN:(Si, Eu) thin films, at high Si temperature (>1050ºC) GaN:(Si, Er) thin films became increasingly n-type conductive, reaching the electron concentrations of ~$10^{19}$$cm^{-3}$. The electron mobility of GaN:(Si, Er) is lower (~10cm^2/Vs) than that of Si-only GaN films. Compared to GaN:(Si, Eu) thin films, the mobility is much higher, which shows that there are fewer Er trap centers so that there are still a lots of free electrons. It probably could explain why there is no enhancement on Er^{3+} luminescence.

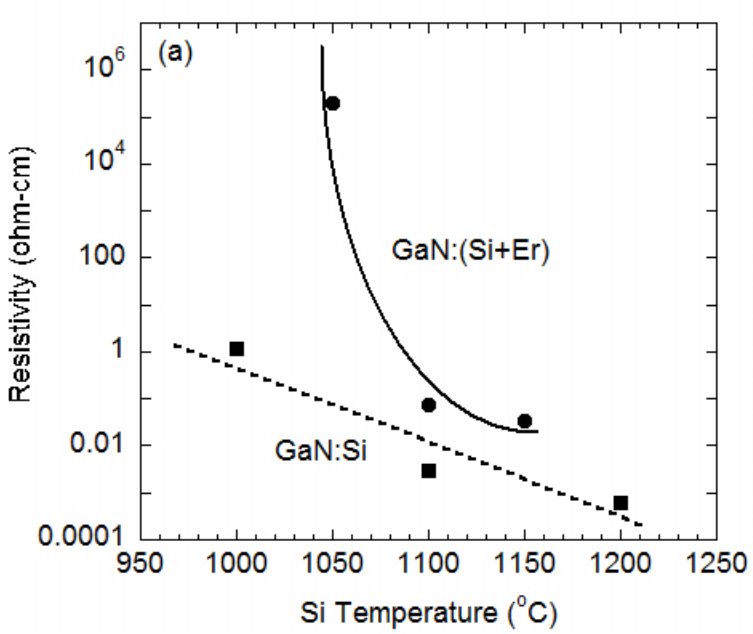

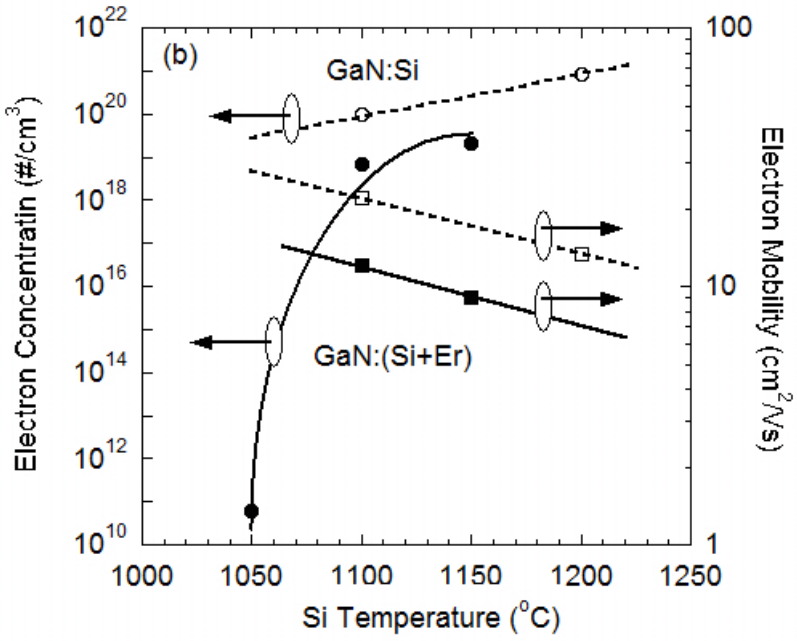

Fig 5.11 (a) Resistivity and (b) conductivity of co-doped GaN:(Si, Er) thin films.

References

[1] Z. Li, H. Bang, G. Piao, J. Sawahata, and K. Akimoto, "Growth of Eu-doped GaN by gas source molecular beam epitaxy and its optical properties," *J. Crystal Growth*, vol. 240, pp. 382-388, 2002.

[2] E. E. Nyein, U. Hommerich, J. Heikenfeld, D. S. Lee, A. J. Steckl, and J. M. Zavada, "Spectral and time-resolved photoluminescence studies of Eu-doped GaN," *Appl. Phys. Lett.*, vol. 82, pp. 1655-1657, 2003.

[3] H. Y. Peng, C. W. Lee, H. O. Everitt, D. S. Lee, A. J. Steckl, and J. M. Zavada, "Effect of optical excitation energy on the red luminescence of Eu^{3+} in GaN," *Appl. Phys. Lett.*, vol. 86, p. 051110, 2005.

[4] P. N. Favennec, H. L'Haridon, D. Moutonnet, M. Salvi, and M. Gauneau, "Optical Activation of Er^{3+} Implanted in Silicon by Oxygen Impurities," *Jpn. J. Appl. Phys.*, vol. 29, pp. L524-L526, 1990.

[5] J. E. Colon, D. W. Elsaesser, Y. K. Yeo, R. L. Hengehold, and G. S. Pomrenke, "Enhancement of the Er^{3+} emissions from AlGaAs:Er codoped with oxygen," *Appl. Phys. Lett.*, vol. 63, pp. 216-218, 1993.

[6] J. T. Torvik, C. H. Qiu, R. J. Feuerstein, J. I. Pankove, and F. Namavar, "Photo-, cathodo-, and electroluminescence from erbium and oxygen co-implanted GaN," *J. Appl. Phys.*, vol. 81, pp. 6343-6350, 1997.

[7] M. Overberg, C. R. Abernathy, J. D. MacKenzie, S. J. Pearton, R. G. Wilson, and J. M. Zavada, "Effect of carbon doping on GaN:Er," *Mat. Sci. and Eng. B*, vol. 81, pp. 121-126, 2001.

[8] S. Kim, S. J. Rhee, X. Li, J. J. Coleman, and S. G. Bishop, "Selective enhancement of 1540 nm Er^{3+} emission centers in Er-implanted GaN by Mg codoping," *Appl. Phys. Lett.*, vol. 76, pp. 2403-2405, 2000.

[9] B. N. Mahalley, S. J. Dhoble, R. B. Pode, and G. Alexander, "Photoluminescence in $GdVO_4:Bi^{3+}$, Eu^{3+} red phosphor," *Appl. Phys. A*, vol. 70, pp. 39-45, 2000.

[10] M. K. Chong, K. Pita, and C. H. Kam, "Photoluminescence of sol–gel-derived $Y_2O_3:Eu^{3+}$ thin-film phosphors with Mg^{2+} and Al^{3+} co-doping," *Appl. Phys. A,* vol. 79, pp. 433-437, 2004.

[11] B. Liu, M. Gu, X. Liu, C. Ni, D. Wang, L. Xiao, and R. Zhang, "Effect of Zn^{2+} and Li^{+} codoping ions on nanosized $Gd_2O_3:Eu^{3+}$ phosphor," *J. Alloys Compounds,* vol. 440, pp. 341-345, 2007.

[12] U. Hommerich, E. E. Nyein, D. S. Lee, J. Heikenfeld, A. J. Steckl, and J. M. Zavada, "Photoluminescence studies of rare earth (Er, Eu, Tm) in situ doped GaN," *Mat. Sci. and Eng. B,* vol. 105, pp. 91-96, 2003.

[13] H. Y. Peng, C. W. Lee, H. O. Everitt, C. Munasinghe, D. S. Lee, and A. J. Steckl, "Spectroscopic and energy transfer studies of Eu^{3+} centers in GaN," *J. Appl. Phys.,* vol. 102, p. 073520, 2007.

[14] J. H. Park and A. J. Steckl, "Site specific Eu^{3+} stimulated emission in GaN host," *Appl. Phys. Lett.,* vol. 88, p. 011111, 2006.

[15] F. Priolo, G. Franz, S. Coffa, and A. Carnera, "Excitation and nonradiative deexcitation processes of Er^{3+} in crystalline Si," *Phys. Rev. B,* vol. 57, p. 4443, 1998.

6. Rare Earth Doped GaN Electroluminescent Devices

6.1. Design of GaN:RE Electroluminescent Devices

In order to investigate the device application of RE doped GaN, electroluminescent devices (ELDs) were investigated, as shown in Fig. 6. A simple Schottky diode structure, shown in Fig 6.1a, was designed[1] in Nanolab before. Patterned ring ITO contact was deposited on the top of GaN layer and a metal-semiconductor schottky diode was formed. External voltage was biased between outer and inner rings and RE^{3+} emission was emitted out from inner ring.

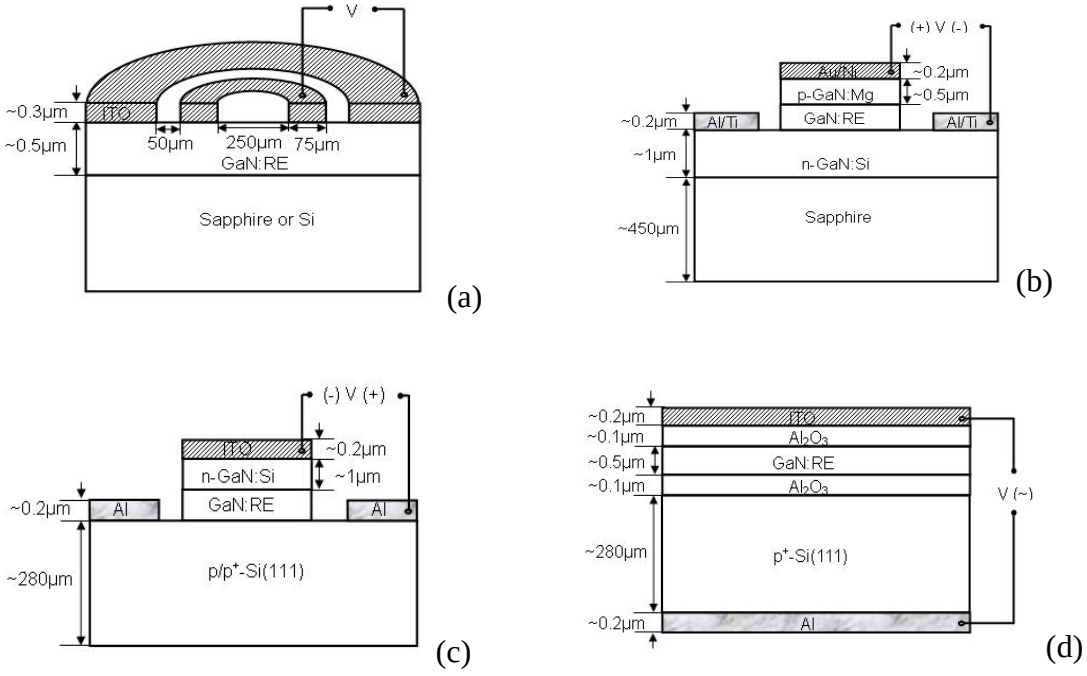

Fig 6.1 Diagram of various GaN:RE optoelectronic device structures.

P type-intrinsic-n type (PIN) structure is usually used to make light emitting diodes (LED) and lasers. Fig 6.1b shows the prototype of a GaN:RE homo-junction PIN LEDs.

Mesa structure was fabricated by dry etching on GaN layers. Au/Ni and Al/Ti metals were deposited for p-type and n-type layer contacts, respectively.

A hetero-junction PIN LED structure was also designed and fabricated, employing Si substrates as p-type conducting layer. The device diagram was shown in Fig 6.1c. Al was deposited on Si substrates as metal contact. ITO was patterned on the top of GaN layer as n-type contact since ITO is high transparent for visible and IR emissions. P^+-Si substrates were also used to improve the p-type layer conductivity.

Except the DC devices, AC GaN:RE devices were also investgitaed. A simple thin film electroluminescent devices (TFEL) was shown in Fig 6.1d. Dielectric layers such as Al_2O_3 were deposited on both sides of GaN:RE layer. ITO and Al were deposited as the metal contacts.

6.2. Device Fabrication and Characterization Techniques

(1) Photolithography

Photolithography is used to make pattern for etching and metallization in semiconductor microfabrication process. Light-sensitive photoresists are spin-coated on the samples and exposed through a photomask under UV light. For positive photoresist, the exposed part becomes soluble in the developer. While for negative photoresist, the exposed part becomes insoluble to the solvent, but the unexposed part can be removed by the developer.

A Karl Suss mask aligner MJB3 was used to make the pattern. Positive photoresist Shipley 1818 was spin-coated on the samples at 4000RPM for 30 seconds. The thickness of photoresist was measured ~2.2μm. After pre-baked in the conventional oven at 95ºC for 30mins, the samples were exposed under a UV mercury lamp with G line (435nm)

emission at 12mW/cm^2 for 10 seconds. The exposed photoresist was removed by the developer (351:DI water=1:5). Another positive photoresist AZ4620 was also used because the thickness of AZ4620 can be ~6.5μm even at very high rotation speed (5000RPM). Such thick photoresist layer is beneficial for the mask in dry etching of GaN thin films.

(2) Inductively Coupled Plasma Etching

Mesa structure is widely designed in multilayer semiconductor devices for metal contact deposition. So the etching of GaN layer is an important step in ELD fabrication processes. Anisotropic dry etching techniques such as reactive ion etching (RIE) can be used. These techniques use plasma at low pressure to generate high-energy ions to attack the wafer surface and chemically react with the atoms to form the volatile compounds, which can be desorbed from the surface. In Nanolab, GaN thin films were dry-etched by inductively coupled plasma (ICP) etching technique for better selectivity and high aspect ratio. Compared to conventional RIE system, ICP system is equipped with a low frequency inductive RF coil, which can transform power into a low pressure gas and generate a high-density plasma discharge. Typical processing pressures are at or below 10mTorr, where plasma can quickly diffuse from the generation region to uniformly fill the plasma vessel and drift to the substrate. Additionally, high density plasma sources allow the bias voltage to be controlled by a second RF power supply, independent of ion current and plasma density.

Nanolab has one Plasma Therm 790 ICP etching system with chloride etchant, consisting of a dielectric chamber vessel, an inductive RF coil, a standard RF power supply and automatic impedance matching network. A turbo pump is used to pump down the chamber

till 10^{-6}Torr. The substrate is cooled at room temperature during the process by a heat exchanger. Cl_2 and Ar gas molecules were used to etch GaN layers. Etch rate of GaN thin films is highly dependent on the quality, the conductivity and doping of GaN thin film. Typical etch rate of undoped and conductively doped GaN is ~250nm/min and that of RE doped GaN is ~150nm/min. Fig 6.2 shows a SEM picture of mesa GaN structure after ICP dry etching.

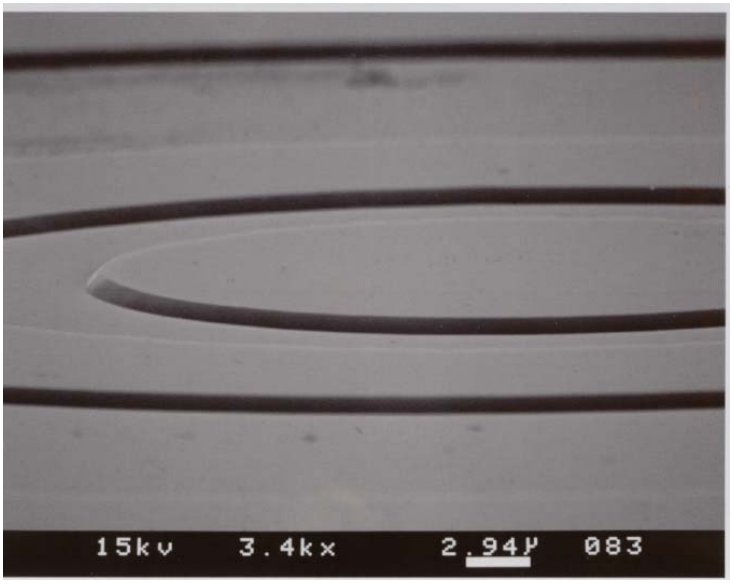

Fig 6.2 SEM image of mesa structure on GaN:Eu/Si sample after ICP dry etching.

(3) Sputtering

Dielectric and metal layers were deposited on the samples by sputtering technique. High energy ions generated by plasma bombarded into the target and ejected the atoms out. The ejected atoms were deposited on the samples. Compared to evaporation technique, the quality of sputtering film and the adhesion to the substrate is better, but there is also damage from plasma and not good for photoresist “lift-off” technology.

Nanolab has a Denton Vacuum sputtering system with ITO, Al and Si_3N_4 targets. ITO and Al targets are biased by DC power with 100W and 150W, respectively. The deposition rate of ITO and Al is ~600nm/hr. Si_3N_4 target is biased by RF power at 150W and the deposition rate is ~200nm/hr.

(4) Rapid Thermal Annealing

The metal contact layers after the deposition were generally annealed at high temperature to increase the adhesion and conductivity. Rapid thermal annealing (RTA) technique is often used for this purpose. The samples are placed in nitrogen ambient chamber and heated by high intensity lamps to high temperature for several minutes so that the electrical properties can be changed. The heating process can activate dopants, change film-to-film or film-to-wafer substrate interfaces, densify deposited films, change states of grown films, repair damage from ion implantation move dopants or drive dopants from one film into another or from a film into the wafer substrate.

An AG associate Heatplus was used to do the RTA process for ITO and Al contact layer. The sheet resistance of as-deposited ITO film is ~120Ω/□. After 450ºC annealing for 3mins, it decreases to ~30Ω/□. The RTA recipe for Al metal layer is 650ºC for 5mins.

(5) Atomic Layer Deposition

The dielectric layer in AC device can be fabricated by sputtering technique, but the thin film quality is not good. Another technique, atomic layer deposition (ALD), is used to deposit good dielectric layer. ALD is similar to chemical vapor deposition (CVD) technique, but the chemical reaction process is different. The ALD reaction typically involves two chemicals, called precursors. Both precursors are separated and react with the surface alternatively in a sequential manner. Therefore, the film growth is self-limited and

only based on surface reactions, so that the atomic scale deposition control is possible, which can be obtained as fine as ~ 0.1Å per monolayer.

Nanolab has an ALD system from Cambridge Technologies. TMAl, $Zn(C_2H_5)_2$, and H_2O (water vapor) are installed in the system for the deposition of Al_2O_3 and ZnO. Good dielectric layer of Al_2O_3 can be grown at the growth rate as low as ~20nm/hr. The breakdown voltage of 100nm Al_2O_3 can achieve as high as ~10^7V/cm.

(6) I-V Characteristics

The electrical properties of GaN:RE ELDS were investigated by the current-voltage (I-V) characteristics. A Labview controlled HP 6634B DC power supply can apply the bias till 100V on the devices and the current data are automatically recorded into the computer. Fig 6.3 shows typical IV characteristics from RE doped GaN Schottky diode ELDs.

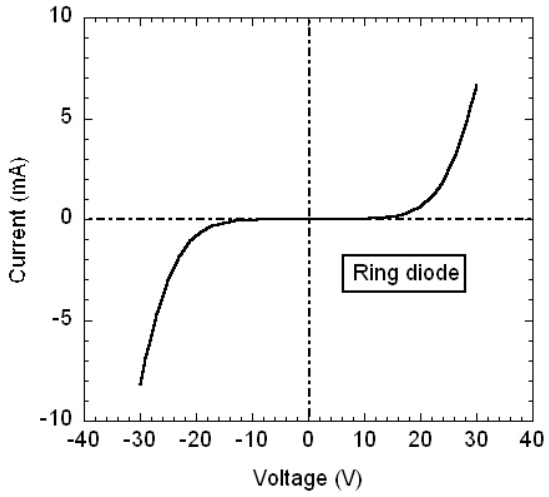

Fig 6.3 IV Characteristics from GaN:RE Shottky diode ELDs.

(7) Electroluminescence

Electroluminescence (EL) measurements were performed to study the optical properties of GaN:RE ELDs. Two major RE^{3+} ions emission mechanisms were in EL process:

electron-hole recombination and impact excitation. The first one is similar to that in PL process, except that the electrons and holes are injected from external source. It is dominant for forward biased PIN LEDs. The other emission mechanism, impact excitation, is dominant in reverse biased PIN LEDs or schottky diodes. Hot carriers (electrons) were injected into GaN:RE layer under high voltage. There are two major ways for the energy of hot electrons to be transferred to the 4*f* electrons of RE ions: (1) hot electrons directly collided with RE^{3+} ions and transferred energy; (2) hot electrons transferred the energy to impurity states surrounding the RE^{3+} ions with subsequent energy transfer to 4*f* electrons. Finally, radiative relaxation occurred between RE^{3+} energy levels and the photons were emitted out.

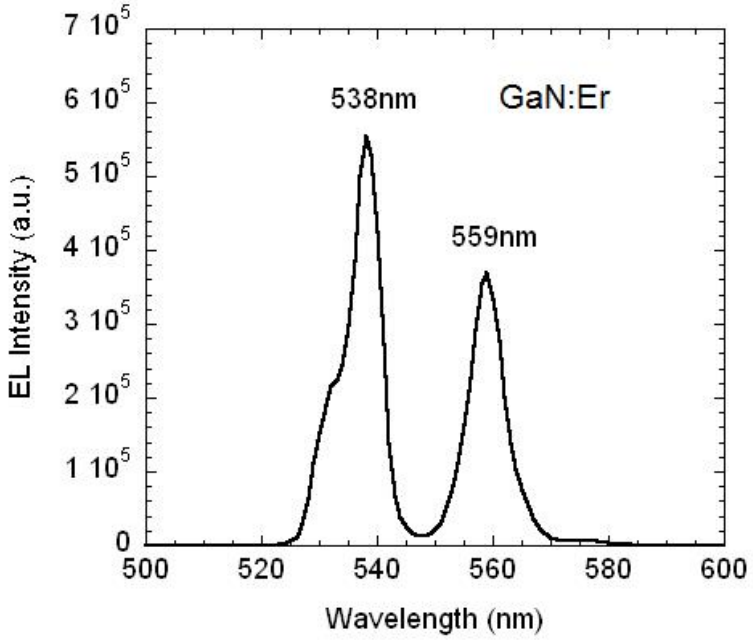

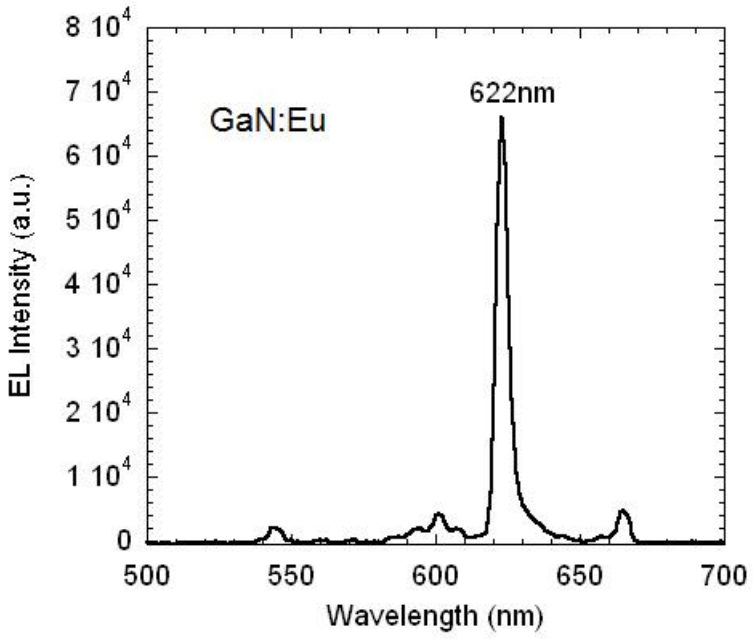

Fig 6.4 Typical EL spectra from GaN:Er and GaN:Eu ELDs.

EL spectra from GaN:RE ELDs were recorded by Princeton Instruments/Acton Research SP2550i spectrometer system equipped with a PMT and InGaAs detector. Fig 6.4 shows typical EL spectra from Er and Eu doped GaN ELDs. Notice that the EL spectra from GaN:Eu are similar to the PL spectra shown in Fig 3.9b. The main peak is at ~622nm from the radiative transitions $^5D_0$-$^7F_2$. Some weaker emission lines at ~600nm, ~663nm and ~546nm were also present in the spectra.

6.3. Homo-junction Devices on Sapphire Substrate

PIN sandwich structure is widely used in light emitting devices because of high level carrier injection. The intrinsic layer is a wide, light-doped or undoped layer while the p type and n type layer are typically heavily doped for ohmic contact. Under forward bias, the electrons from n-type layer and the holes from p-type layer were injected into the

intrinsic layer. Because of the wide intrinsic layer, the current doesn't go through until the injected electrons and holes reach the equilibrium, where the amount of electrons is equal to that of holes. The injected carrier concentration is typically several orders higher than the intrinsic level carrier concentration. Moreover, wide intrinsic region provides a long path for the electrons and holes to meet each other before they reach the p/n type region. The electron-hole recombination rate increases, resulting in high radiative relaxation probability so that more photons could be emitted out. Under reverse bias, the depletion region exists almost completely in the wide intrinsic region. This depletion region is much larger than in a reversed PN diode, and almost constant-size, independent of the reverse bias applied to the diode. The electrons and holes were blocked outside of intrinsic region so that there is no current flow. Only at high reverse voltage, the "hot" electrons with enough energy could be injected the intrinsic region and few of them could tunnel the region.

PIN GaN:RE LED structure was shown in Fig 6.1b. Intrinsic region is RE doped GaN layer, which is usually highly resistive. The growth conditions of RE doped GaN thin film were optimized in Chapter 4 for the best RE luminescence intensity and efficiency. Si doped n-type GaN thin films were also successfully grown by MBE technique. However, it is very difficult to grow high quality Mg doped p-type GaN thin films. Therefore, a MIN structures without p-type layer were fabricated. All LEDs were designed as the circular structure with different diameter from 0.2mm to 2mm. A ~1μm thick Si doped GaN layer was grown on sapphire wafer, followed by ~0.5μm RE doped GaN layer. Mesa structure was fabricated by photolithography and ICP etching. Al metal film around 300nm was

deposited on GaN:Si layer for n-type contact. ITO thin film was deposited directly on GaN:RE layer as the metal contact.

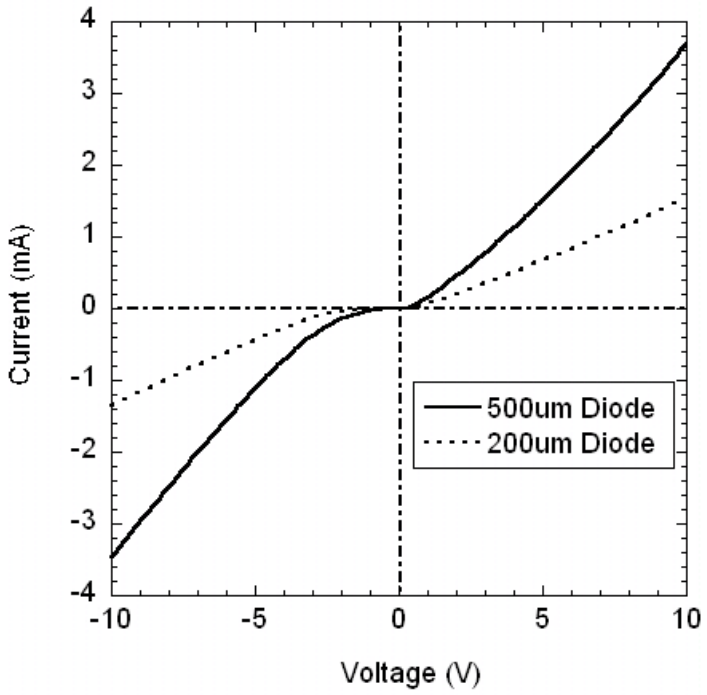

Fig 6.5 Typical I-V characteristics from Er doped GaN MIN LEDs.

Er doped GaN MIN LEDs were fabricated. The results from I-V measurements are plotted in Fig 6.5. Rectifying characteristics are clearly shown in the figure. Visible EL spectra are shown in Fig 6.6, two green peaks at 536nm and 557nm from Er^{3+} ions. The applied voltage on 200um diode is 70V and the current flow is ~40mA. However, the emission is very weak compared to Schottky diodes.

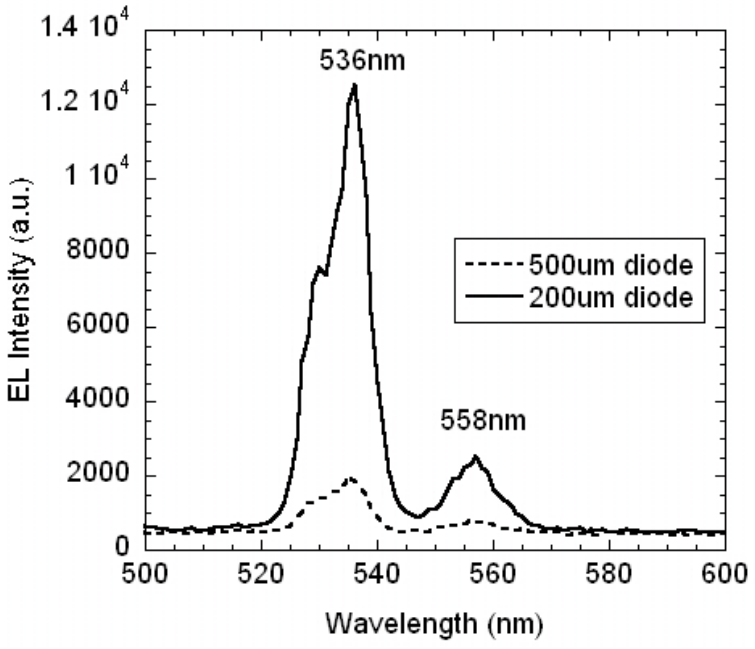

Fig 6.6 Typical EL spectra from Er doped GaN MIN LEDs.

6.4. Hetero-junction Devices on Si Substrate

RE doped GaN devices on Si substrate are very attractive because of integration with Si microelectronics industry. GaN:RE thin film growth on Si wafers has been previously investigated in Nanolab and Schottky diodes based on GaN:RE/Si were also fabricated and tested.

Since it is not easy to get good p-type GaN thin film, we employed p-Si substrate as p-type conducting layer as shown in Fig 6.1c. Mesa structure was also fabricated by photolithography and ICP etching. Al thin films were deposited on p-type Si substrates as metal contact. Since Si substrates is not transparent for visible and IR light, 200nm ITO

thin film was deposited on top of GaN:RE layer as metal contact. ITO layer is heavily n-type doped layer with sheet resistance of ~40 ohm/□, and Si wafer is moderately doped p-type doped layer with resistivity of 1-10 ohm-cm. GaN:RE active layers were high insulative, so the device is essentially a PIN hetero-junction structure.

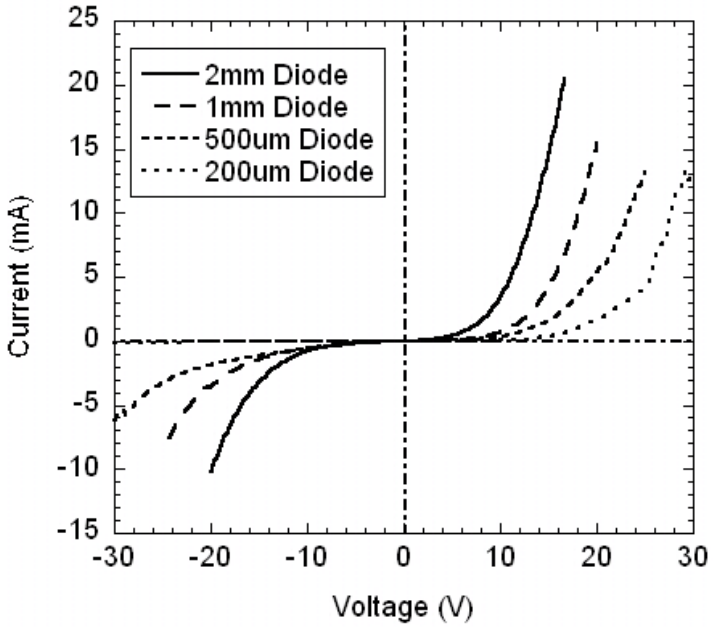

Fig 6.7 Typical IV spectra from GaN:Er/p-Si(111) PIN LEDs.

Fig 6.7 shows IV characteristic curves of different diameters of diodes fabricated on GaN:Er/p-Si(111) samples. Compared to ring diode EL devices (shown in Fig 6.1a), the current flows vertically through the GaN:RE layer instead of horizontally. The IV curves show more rectifying characterization than those of ring diode devices (shown in Fig 6.3).

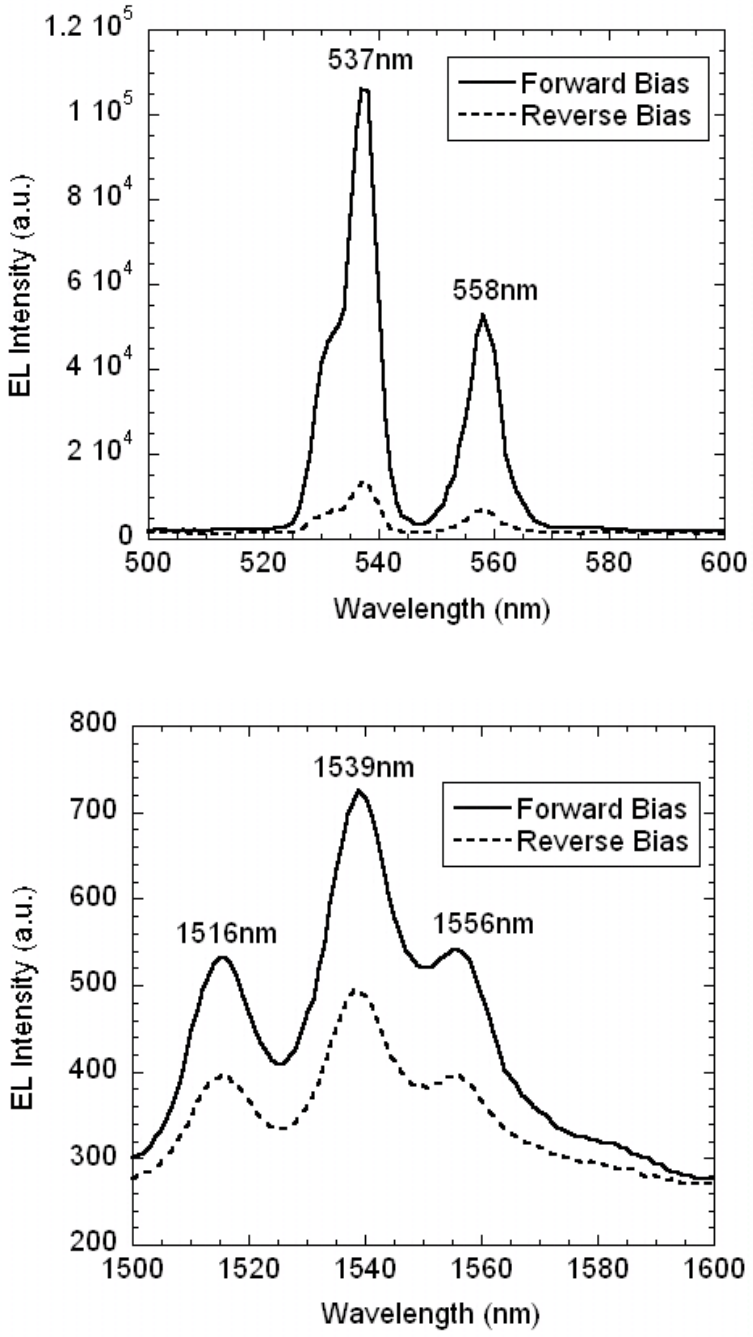

Fig 6.8 Typical (a) visible and (b) IR EL spectra from GaN:Er/p-Si(111) PIN ELDs.

Visible and IR EL emission spectra of GaN:Er devices are shown in Fig 6.8. As seen from the figure, EL intensity under forward bias is more than 5 times stronger than that under reverse bias for 536nm & 557nm green emission and twice for 1540nm IR emission. Visible luminescence dependence on voltage measurement was performed and the results are plotted in Fig 6.9. It is apparent that Er^{3+} emission under forward bias has a lower threshold voltage.

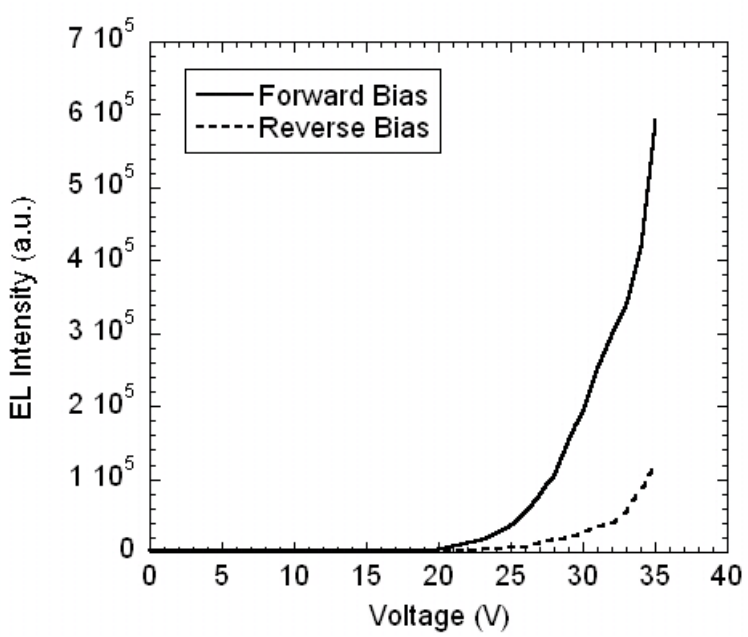

Fig 6.9 Visible (537nm) luminescence dependence on voltage measurement.

References

[1] A. J. Steckl, J. C. Heikenfeld, L. Dong-Seon, M. J. Garter, C. C. Baker, W. Yongqiang, and R. Jones, "Rare-earth-doped GaN: growth, properties, and fabrication of electroluminescent devices," *IEEE J. Selected Topics in Quantum Electronics,* , vol. 8, pp. 749-766, 2002.

7. Electroluminescent Devices Based on Si Co-doped GaN:RE

The Si co-doping in GaN:RE changed the electrical properties of GaN:RE thin films and had a great effect on RE^{3+} luminescence by optical pumping. So it is very interesting to study the effect of Si co-doping on the performance of GaN:RE ELDs and RE^{3+} luminescence by electrical pumping. In this chapter, GaN ELDs were fabricated on GaN:(RE,Si) thin films grown on Si substrates and the results were discussed.

7.1. Si Co-doped GaN:RE DC ELDs

Er and Si co-doped GaN thin films were grown on p-type Si(111) substrates. A 20nm AlN buffer layer was first grown at 500ºC, followed by 1hr growth of co-doped GaN layer at 600ºC. The Ga effusion cell temperature was kept at 875ºC (III/V~1), while the Si and Er cell temperatures were kept at 1050ºC and 860ºC. The thickness of GaN thin films was approximately 500nm. GaN doped with Er only were also grown under the same conditions for comparison.

PL spectra from GaN:(Si, Er) and GaN:Er samples are plotted in Fig 7.1. Both samples show green peaks of 538nm and 559nm from Er^{3+} ions, corresponding to radiative transitions from Er^{3+} ions energy levels $^2H_{11}$-$^4I_{15/2}$ and $^4S_{3/2}$-$^4I_{15/2}$. The peak intensities are similar if we subtract yellow band background from the spectra. There is also a small peak around 369nm corresponding to free exciton emission from GaN bandgap for both samples. No Si-related peak was observed in the PL spectra of (Er, Si) co-doped GaN thin films.

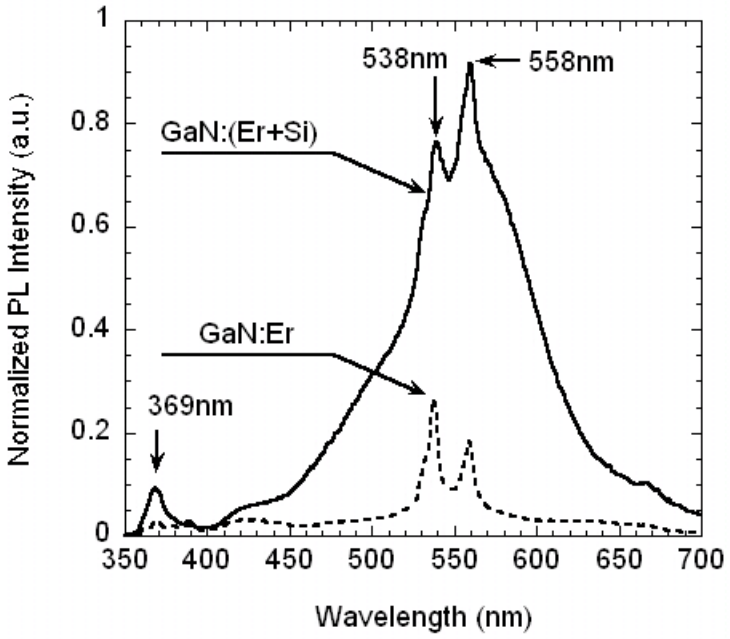

Fig 7.1 Visible PL spectra from GaN:(Si, Er)/p-Si and GaN:Er/p-Si samples.

Schottky diodes and PIN hetero-junciton LEDs (structure shown in Fig 5.1) were fabricated both on GaN:(Si, Er) and GaN:Er thin films. For schottky diode structure, ring-pattern electrodes were deposited on top of GaN thin films. To fabricate PIN hetero-junction LED, mesa structure was patterned by photolithography and etched by ICP dry etching. ITO and Al thin films were deposited by sputtering and rapid thermally annealed.

The current-voltage measurements were performed for all GaN ELDs and typical results are plotted in Fig 7.2. Er doped GaN ELDs have similar I-V under forward and reverse bias, while co-doped GaN ELDs exhibit strong I-V rectifying characteristics.

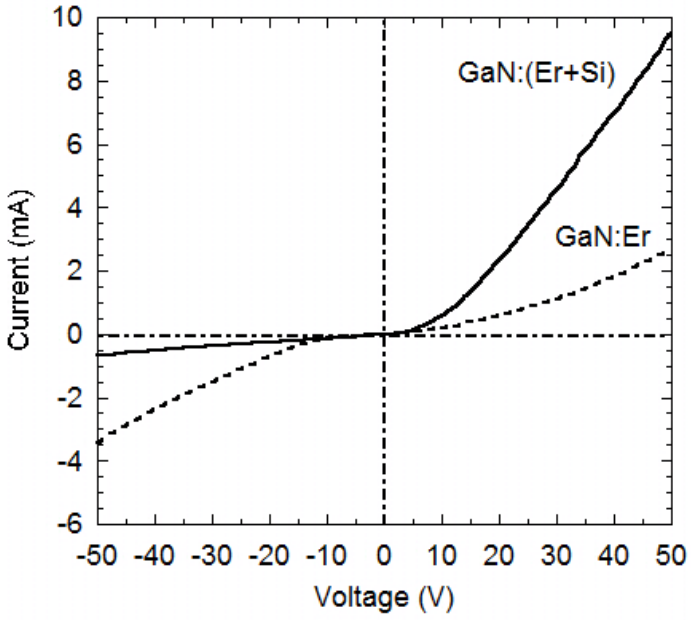

Fig 7.2 Typical I-V characteristics from GaN:(Si, Er)/p-Si and GaN:Er/p-Si ELDs.

EL measurements were performed on (Si, Er) co-doped and Er only GaN ELDs. Visible and IR EL spectra are shown in Fig 7.3 and Fig 7.4 at different bias levels. Green and IR emissions from Er doped GaN ELDs are similar to the results shown in chapter 6, stronger under forward bias than under reverse bias. For (Si, Er) co-doped GaN ELDs, green and IR EL emission is clearly strong under forward bias, with the intensity proportional to the current. But under reverse bias as high as 100V, little or no emission was observed. It is first time that GaN:RE ELDs were observed to have strong emission under forward bias with no emission under reverse bias. However, Er^{3+} visible and IR emission intensity from (Si, Er) co-doped GaN ELDs is weaker than Er doped GaN ELDs. The visible and IR luminescence dependence on voltage and current was also obtained for both GaN:(Si, Er) and GaN:Er ELDs, and the results are shown in Fig 7.5-7.8.

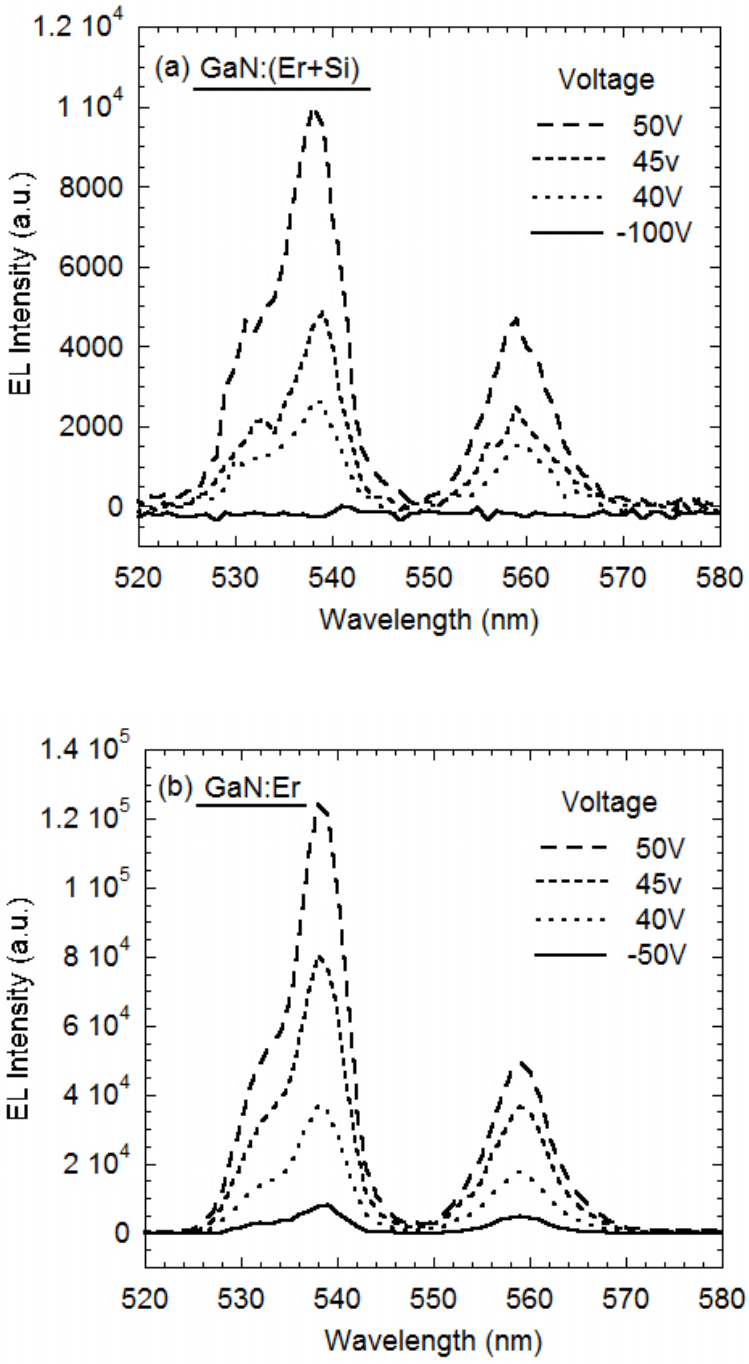

Fig 7.3 Visible EL spectra from (a) GaN:(Si, Er)/p-Si and (b) GaN:Er/p-Si ELDs.

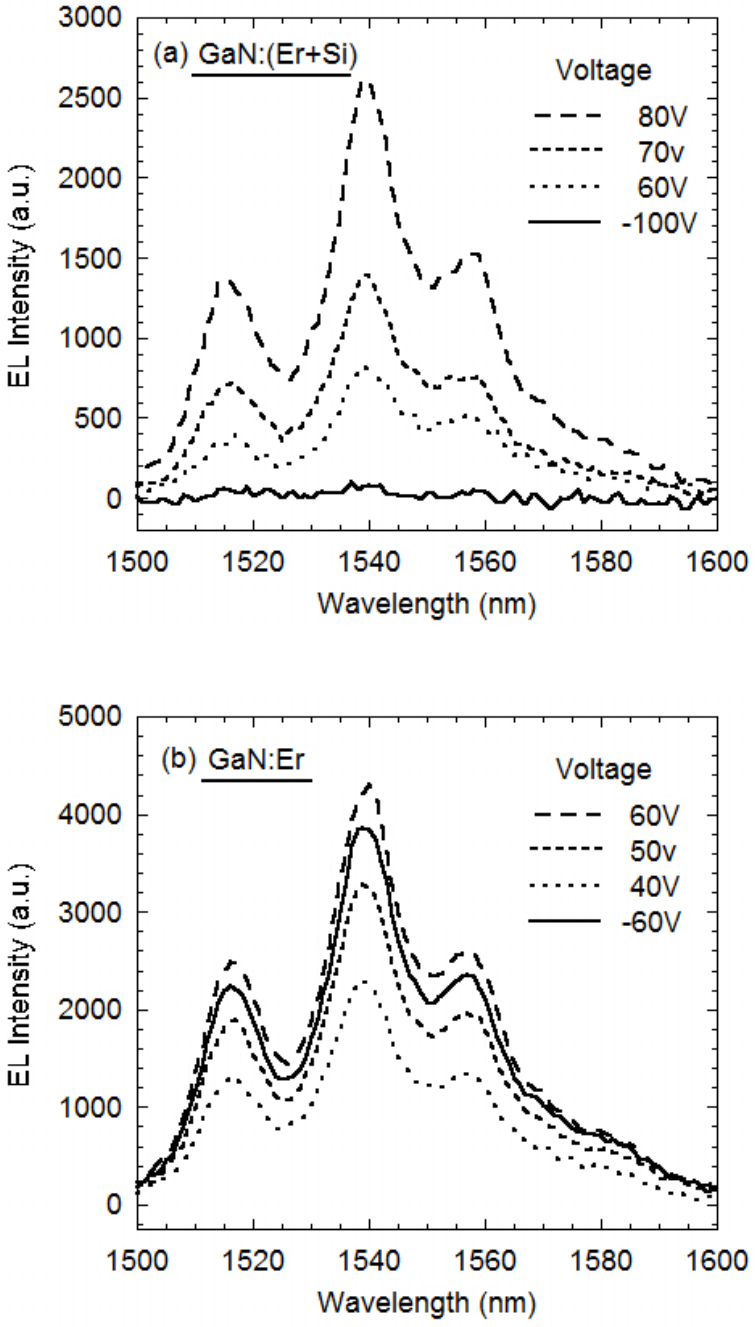

Fig 7.4 IR EL spectra from (a) GaN:(Si, Er)/p-Si and (b) GaN:Er/p-Si ELDs.

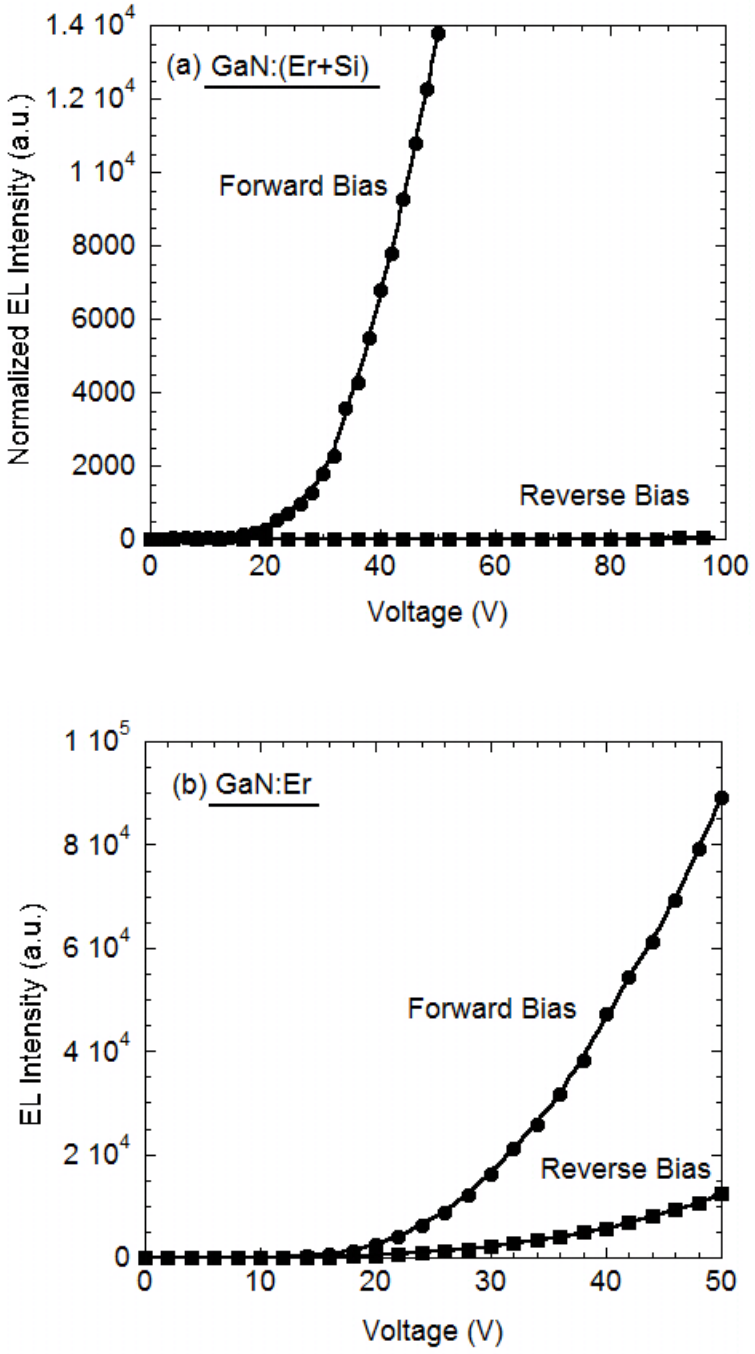

Fig 7.5 Er^{3+} visible (538nm) luminescence dependence on voltage measurements from (a) GaN:(Si, Er)/p-Si ELDs and (b) GaN:Er/p-Si ELDs.

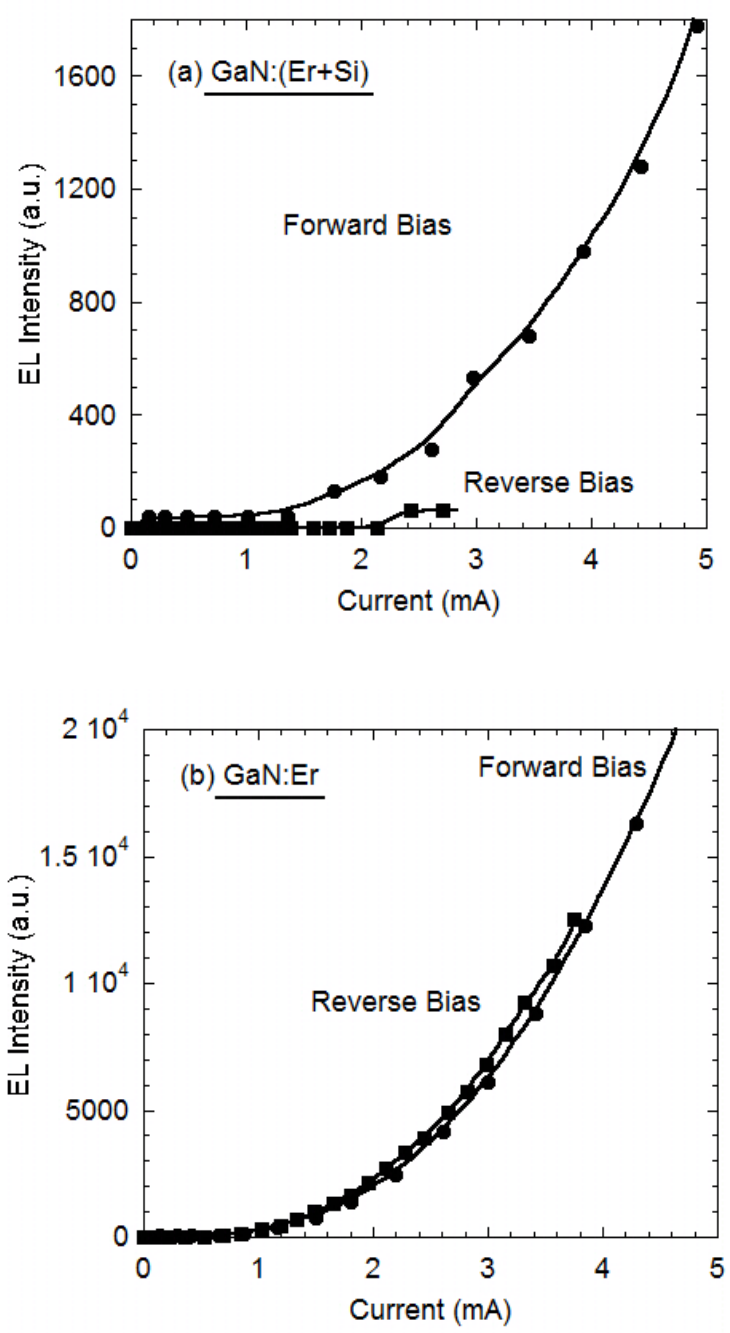

Fig 7.6 Er^{3+} visible (538nm) luminescence dependence on current measurements from (a) GaN:(Si, Er)/p-Si ELDs and (b) GaN:Er/p-Si ELDs .

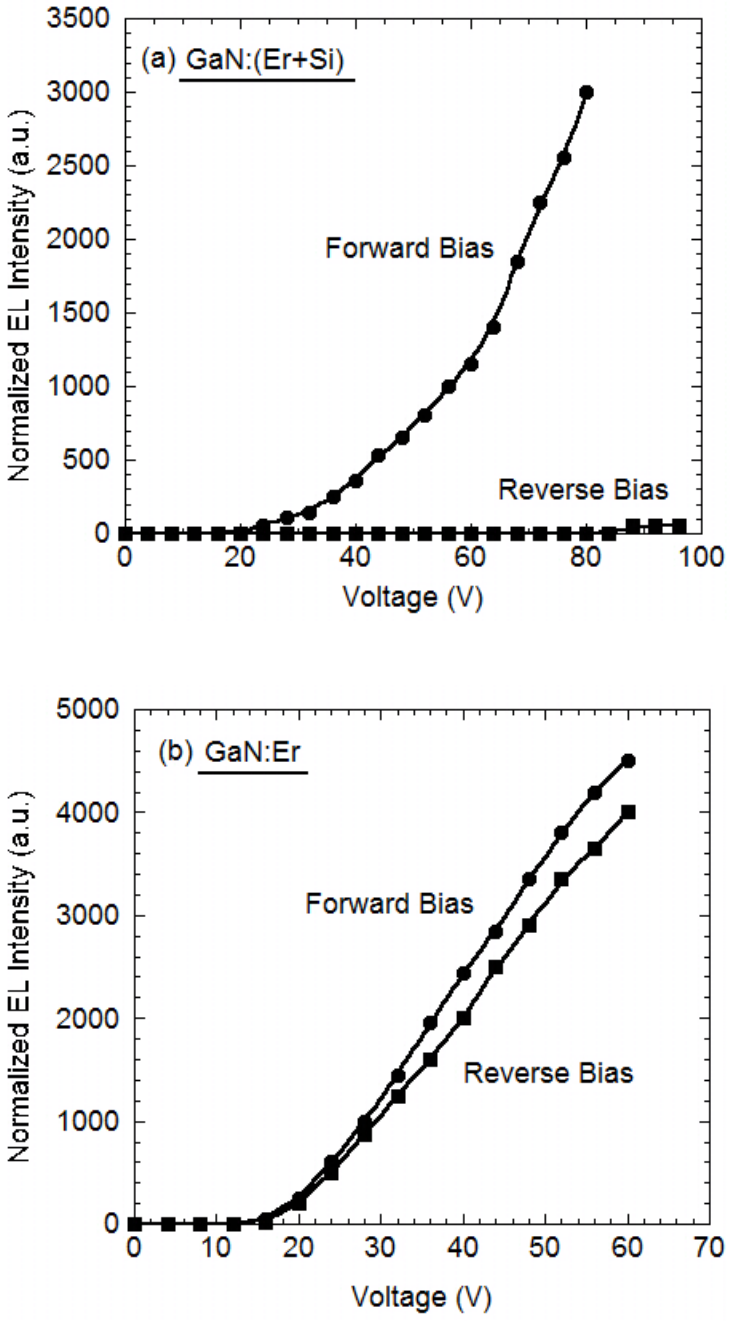

Fig 7.7 Er^{3+} IR (1.54μm) luminescence dependence on voltage measurements from (a) GaN:(Si, Er)/p-Si ELDs and (b) GaN:Er/p-Si ELDs .

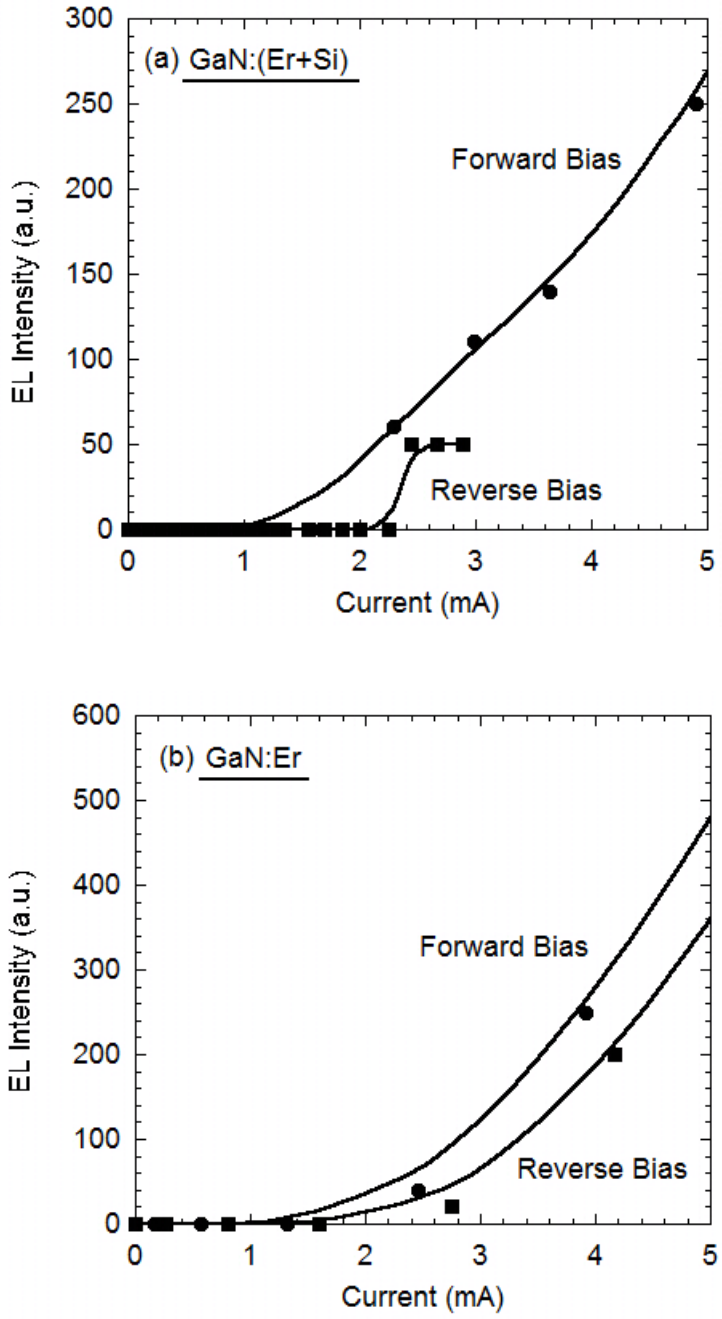

Fig 7.8 Er^{3+} IR (1.54μm) luminescence dependence on current measurements from (a) GaN:(Si, Er)/p-Si ELDs and (b) GaN:Er/p-Si ELDs .

With Si co-doping in GaN:RE thin films, Si atoms act as donors and provide a significant source of electrons. The electrical properties of GaN:Er thin films have been modified from highly resistive to weakly n-type. The sheet resistance of (Si, Er) co-doped GaN thin films was measured as $1.15x10^5$ Ω/□ by four point probe meter, whereas the Er-doped-only GaN has a resistance too large to be measured (>10^{10} Ω/□). Combined with the p-type Si(111) substrate, a pn^- heterojunction is formed at the interface between the GaN layer and the Si layer. The electrical properties of the pn hetero-structure strongly affect the I-V characteristics of GaN:Er ELDs under different DC bias.

As we introduced before, there are two major mechanisms for RE^{3+} EL emission: electron-hole recombination and hot carriers impact excitation. As electrons and holes are injected into the active GaN layer under forward bias, they recombine and transfer their energy to neighboring RE^{3+} ions. Some of the excited RE^{3+} ions relax radiatively, resulting in EL emission. Under reverse bias, hot electrons injected into the GaN layers collide with RE^{3+} ions and directly transfer their energy to RE^{3+} ions. For Si co-doped GaN:Er ELDs, the pn^- hetero-junction acts as a barrier for electrons under reverse bias. Even a few "hot" electrons can tunnel through the GaN:(Si, Er) layer, their energy probably is not sufficient to excite Er^{3+} emission. So the impact excitation mechanism was quenched.

7.2. Si Co-doped GaN:RE AC ELDs

AC devices were also fabricated on GaN:(Si, Eu) thin films with the structure shown in Fig 6.1d. Dielectric layers Al_2O_3 (~100nm) were grown at 250ºC by ALD technique. Active layer GaN:(Si, Eu) was grown at 700ºC for 1hr. The Ga cell temperature was kept

for III/V ratio~1. The Eu and Si temperature was kept 450ºC and 1100ºC. GaN:Eu thin films were also grown at same condition.

The PL spectra from GaN:(Si, Eu) and GaN:Eu samples are shown in Fig 7.9. The intensity from (Si, Eu) co-doped GaN sample is higher than Eu doped only GaN sample, which is consistent with the results in Chapter 6. EL measurements were also performed with 1kHz sine wave AC bias and the results are shown in Fig 7.10. It is clearly seen that (Si, Eu) co-doped GaN TFELs have higher emission intensity and efficiency than Eu doped only GaN TFELs.

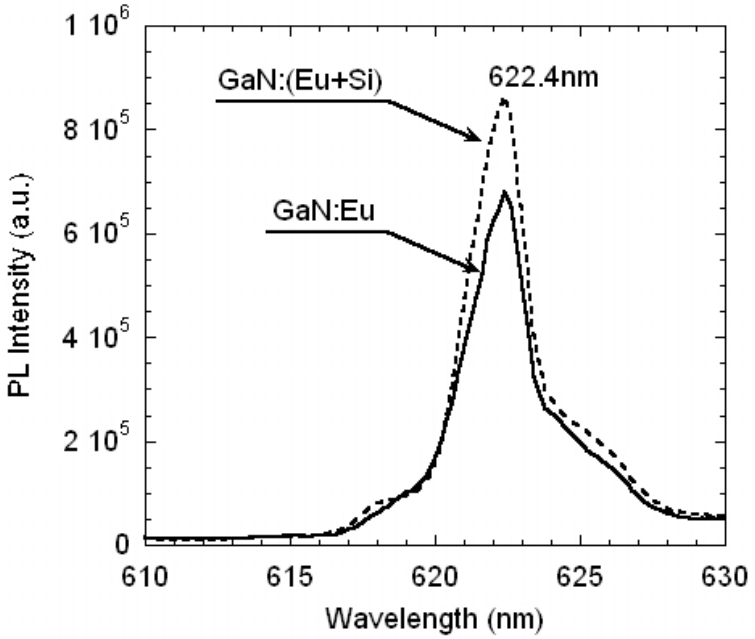

Fig 7.9 PL spectra from GaN:(Si, Eu) and GaN:Eu samples.

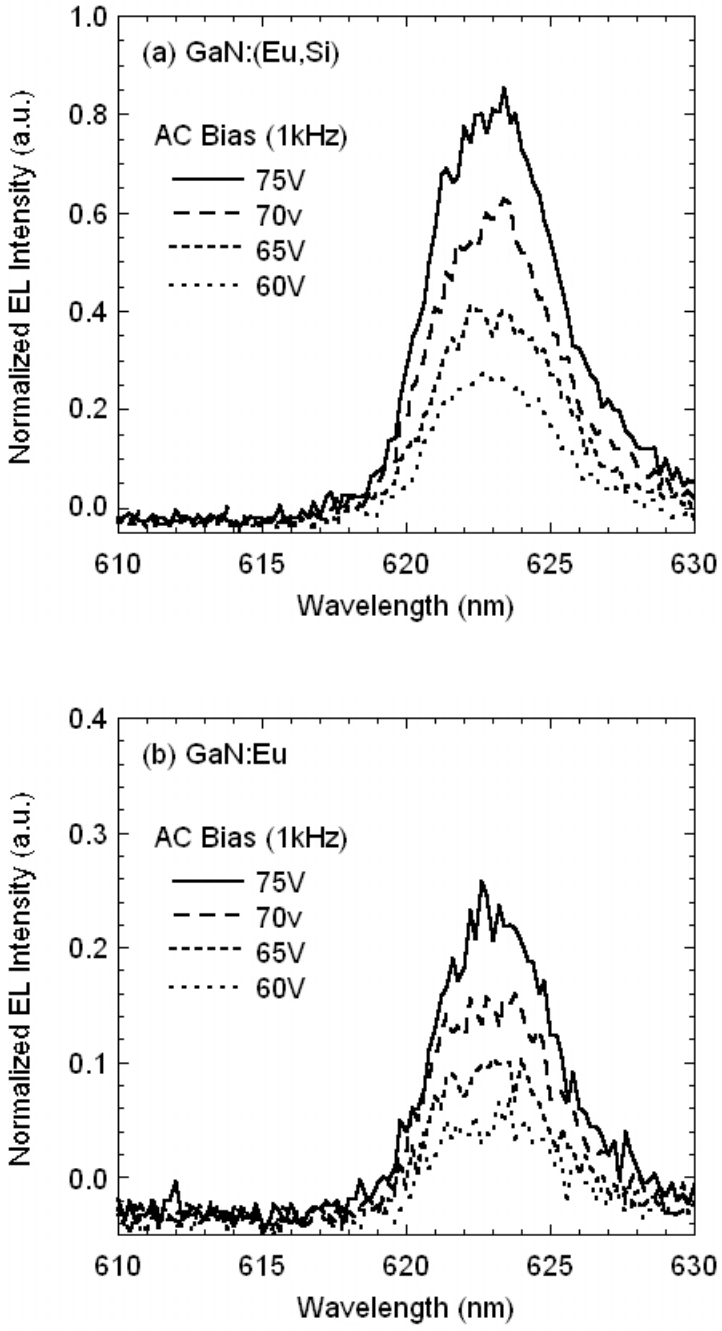

Fig 7.10 EL spectra from (a) GaN:(Si, Eu) and

(b) GaN:Eu samples under different AC bias.

8. Conclusions and Future Work

8.1. Conclusions

Following on the path of RE doped GaN research in UC Nanolab, the research continues on GaN:RE thin film growth and GaN:RE ELDs application, focusing on the effect of co-doping of electronic impurities (Si) on RE^{3+} luminescence. In brief, the principal achievements include:

(4) Optimization of GaN:Eu thin films growth

The growth conditions of GaN:Eu thin films, such as III/V (Ga/N) ratio, Eu cell temperature and growth temperature, were optimized to obtain the strongest Eu^{3+} luminescence. It was found that high quality GaN:Eu thin films were grown under Ga rich condition (III/V>1), but the strongest Eu^{3+} luminescence was obtained under slightly N rich condition (III/V<1). The optimum Eu doping concentration for luminescence is ~0.1-1.0at.%, depending on the GaN:Eu thin film quality. In particular, for Eu doping concentrations in the range of ~0.034-0.2at.%, GaN:Eu thin film grown under the stoichiometric growth condition (III/V~1) has both the highest Eu^{3+} emission and good GaN quality, which is very promising for the fabrication of GaN:Eu LED and laser. Higher growth temperature (>750ºC) was also found to enhance Eu^{3+} luminescence intensity (~10×) and efficiency (~30×).

(5) Effect of co-dopant (Si) on RE^{3+} luminescence

The co-dopant (Si) was *in situ* doped with RE elements in GaN thin films by MBE technique. The effect of Si co-doping on optical and electrical properties of GaN:RE thin films was studied. It was found that a moderate Si co-doping (~0.05-0.07at. %) enhances

Eu^{3+} red PL intensity ~5-10×. Higher Si co-doping results in the quenching of the Eu^{3+} luminescence, but it changes GaN:Eu thin films from highly resistive to n-type conductive. Possible mechanisms for the effects of Si co-doping were investigated by detailed PL measurements including time resolved PL and PLE. An increase of Eu^{3+} PL lifetime at low-moderate concentration possibly due to the incorporation of Si shielding Eu-Eu interactions (by uniformly distributing Eu ions), combined with an increase in excitation cross section due to Eu-Si complex formation, results in a significant enhancement on Eu^{3+} PL intensity.

(6) Fabrication and characterization of GaN:(RE, Si) ELDs

Advanced GaN:RE ELD structure, including PIN LEDs and AC TFELs, were designed and fabricated to study RE^{3+} EL emission mechanisms. A hetero-junction PIN GaN:Er ELD employing p-Si substrate as p-type conductive layer was fabricated and tested. Er^{3+} ions had strong visible and IR emissions with the emission intensity higher (~5× for visible and ~2× for IR) under forward bias than under reverse bias.

GaN:(RE, Si)-based ELDs were also fabricated and an improvement in device performance was found. Hetero-junction PIN ELDs were fabricated on GaN:(Er, Si) thin films, and for the first time it was found that strong EL emission was obtained under forward bias while there was no or little emission under reverse bias. AC TFELs were also fabricated on GaN:(Si, Eu) thin films, which showed that Si co-doping increases Eu^{3+} EL emission intensity and efficiency.

8.2. Future work

Several important future tasks for achieving the goal of electrically pumped GaN:RE lasersare outline here.

The growth of GaN:Er and GaN:Eu was optimized[1-4] for green and red emission, so the final step is to optimize the GaN:Tm growth for blue Tm^{3+} emission, which is important for the realization of RGB color integration. Additionally, GaN template can be used to improve thin film quality and RE^{3+} luminescence. AlGaN hosts were found[5] to improve RE^{3+} PL and EL emission, but the bandgap engineering should be studied more clearly.

The Si co-doping in GaN:Eu was demonstrated to significantly enhance Eu^{3+} luminescence and increase GaN:Eu thin film conductivity. Moreover, the Si co-doping was also proved to enhance room temperature ferromagnetisim from Gd[6] and Eu[7] doped GaN. Therefore, it is important and necessary to study the effect of co-doping in GaN:RE. Different RE elements (Eu, Er, etc) and different co-doping elements (Mg) can be investigated. Moreover, the co-doped GaN devices with the application of optical/electrical control of magnetism can be investigated.

With the study of highly conductive p-type GaN:Mg growth by MBE technique, PIN GaN:RE LEDs and lasers can be fabricated using the structure shown in Fig 6.1b. Better quality of GaN thin films can be grown on GaN templates, which is believed to improve device performance, such as decreasing threshold voltage and increasing luminescence efficiency. Meantime, the growth of high quality GaN:RE thin films on Si substrates should be also studied so that the integration of red (Eu), green (Er) and blue (Tm) doped GaN lasers in one single Si wafer may be possible[8].

Novel device structures can be also studied on RE doped GaN thin films. For example, microdisk laser structure can be fabricated on GaN:RE/Si. GaN:RE layer is patterned by photolithography and etched by anisotropic ICP dry etching technique. After isotropic wet

etching of Si substrates, GaN:RE microdisks are fabricated, sitting on the Si columns. Such GaN:RE microdisk lasers can have whispering gallery mode so that they can realize lasing at very low threshold.

References

[1] D. S. Lee, J. Heikenfeld, and A. J. Steckl, "Optimum Er concentration for in situ doped GaN visible and infrared luminescence," *Appl. Phys. Lett.*, vol. 79, p. 719, 2001.

[2] D. S. Lee, J. Heikenfeld, and A. J. Steckl, "Growth-temperature dependence of Er-doped GaN luminescent thin films," *Appl. Phys. Lett.*, vol. 80, p. 344, 2002.

[3] D. S. Lee and A. J. Steckl, "Ga flux dependence of Er-doped GaN luminescent thin films," *Appl. Phys. Lett.*, vol. 80, p. 728, 2002.

[4] R. Wang and A. J. Steckl, "Effect of Growth Condition on Eu^{3+} Luminescence from GaN:Eu Thin Films Grown by RF plasma Molecular Beam Epitaxy," *In preparation*, 2009.

[5] R. Wang and A. J. Steckl, "Luminescence Properties of Eu doped $Al_xGa_{1-x}N$," *In preparation*, 2009.

[6] J. K. Hite, R. M. Frazier, R. P. Davies, G. T. Thaler, C. R. Abernathy, S. J. Pearton, J. M. Zavada, E. Brown, and U. Hömmerich, "Effect of Si Co Doping on Ferromagnetic Properties of GaGdN," *Journal of Electronic Materials*, vol. 36, pp. 391-396, 2007.

[7] N. Nepal, J. M. Zavada, R. Wang, and A. J. Steckl, "Electrical and Magnetic Properties of GaN Co-doped with Si and Eu," *In preparation*, 2009.

[8] A. J. Steckl, J. H. Park, and J. M. Zavada, "Prospects for rare earth doped GaN lasers on Si," *Materials Today*, vol. 10, pp. 20-27, 2007.